COUPLED ADVANCED OXIDATION AND BIOLOGICAL PROCESSES FOR WASTEWATER TREATMENT

THÈSE N^O 2785 (2003)

PRÉSENTÉE À LA FACULTÉ ENVIRONNEMENT NATUREL, ARCHITECTURAL ET CONSTRUIT

Institut des sciences et technologies de l'environnement

SECTION DES SCIENCES ET INGÉNIERIE DE L'ENVIRONNEMENT

ÉCOLE POLYTECHNIQUE FÉDÉRALE DE LAUSANNE

POUR L'OBTENTION DU GRADE DE DOCTEUR ÈS SCIENCES TECHNIQUES

PAR

Victor-Manuel SARRIA MUÑOZ

chimiste, Université del Valle, Cali, Colombie
et de nationalité colombienne

acceptée sur proposition du jury:

Dr C. Pulgarin, directeur de thèse
Dr M. Bolte, rapporteur
Prof. S. Esplugas, rapporteur
M. J. Kiwi, rapporteur
Prof. D. Ollis, rapporteur
Prof. P. Péringer, rapporteur

Lausanne, EPFL
2003

To Erica Lorena, my wife
the water that I drink
the sun that warms me up
my life.

SUMMARY

The incapability of conventional biological wastewater treatment to remove effectively biorecalcitrant and/or toxic pollutants, as well as the shortage of world water resources have promoted the research of more efficient and ecologically friendly water treatment technologies.

This thesis contributes to the development of a new hybrid technology combining advanced oxidation processes (AOP) and biological processes for the treatment of wastewater containing biorecalcitrant and toxic pollutants.

In the proposed coupled system, AOP is applied exclusively as pre-treatment with the aim to modify the chemical structure of the pollutants to transform them into biodegradable intermediates. During this step partial mineralization of pollutant take place, and the subsequent biological treatment is applied to complete mineralization. This approach is viable from the economic and environmental point of view, and appears as an alternative to the drastic and/or inefficient single-step processes actually applied for the treatment of biorecalcitrant wastewater.

This thesis is organized in 6 chapters and focuses on the degradation of a model biorecalcitrant pollutant: 5-amino-6-methyl-2-benzimidazolone (AMBI) an important precursor in the industrial production of dyes. In the first chapter, AOP and the concept of coupling AOP-biological process are introduced. An overview of studies which used a combination of photoassisted and biological degradation of organic contaminants in water was performed.

Chapter 2 focuses on an exploratory study with some of the most representative AOP. Thus sonochemical, electrochemical and photochemical oxidation processes were applied to degrade AMBI. The comparison of these AOP revealed that the iron photo-assisted processes are the most advantageous, and have an application potential in sunny regions.

Chapter 3 focuses on the degradation of AMBI by means of the $h\nu/Fe(III)/O_{2(air)}$ and $h\nu/Fe(III)/H_2O_2$ systems using an artificial irradiation source. The transformation of AMBI photoinduced by the Fe(III) in presence of both $O_{2(from\ air)}$ and H_2O_2 electron acceptors is studied. The effect of AMBI, Fe^{3+} and H_2O_2 concentration for the degradation of AMBI wastewater in the photo-Fenton process was discussed and optimal conditions were found.

Chapter 4 focuses on coupling iron photoassisted process with a biological system at lab scale. Here a general strategy to develop combined photochemical and biological systems for biorecalcitrant wastewater treatment is proposed. Following this strategy, two kinds of combined systems were developed and tested using for the photocatalytic pretreatment $h\nu/Fe^{3+}/O_{2(air)}$ or $h\nu/Fe^{3+}/H_2O_2$ and in both cases fixed bed with activated sludge culture for the biological step.

To replace relatively expensive artificial irradiation in photoassisted processes, the solar irradiation was applied. Chapter 5 illustrates the development and optimization at pilot scale, of a coupled solar-biological system for water treatment. The following points were taking into account: (i) the choice of the most appropriate solar collector and the most efficient photocatalytic system, (ii) the optimization of the photocatalytic system, (iii) the monitoring of the chemical and biological characteristics of photo-treated solution and (iv) the evaluation of the performances of the coupled solar-biological system for the treatment of real industrial wastewater containing AMBI. Results indicate that coupling solar-biological processes at pilot scale is an effective method to the treatment of non-biodegradable industrial pollutants such as AMBI.

To overcome the problem of electricity supply for pumps used for the recirculation of wastewater in a coupled water detoxification process, chapter 6 proposes a new Hybrid Photocatalytic-Photovoltaic System (HPPS). HPPS is a device which allows simultaneously decontaminate water and convert solar energy into electricity. This ecological equipment (**which is actually following a patent procedure at the EPFL**) was designed, installed, and tested. The results show that the HPPS represents an autonomous and environmentally friendly method for this strategy of polluted water remediation.

RÉSUMÉ

L'incapacité de procédés de traitement biologiques conventionnels des eaux usées à dégrader les polluants biorécalcitrants et/ou toxiques, ainsi que la disponibilité décroissante de ressources hydriques ont favorisé le développement des projets et programmes de recherche sur des technologies plus efficaces et plus écologiques pour la détoxication de l'eau.

La présente thèse contribue au développement d'une nouvelle technologie hybride combinant des procédés d'oxydation avancés (POA) et des procédés biologiques pour le traitement des eaux contenant des contaminants biorécalcitrants et toxiques.

Dans le système couplé proposé, le POA est appliqué exclusivement comme pré-traitement dans le but de modifier la structure chimique des contaminants pour les transformer en substances intermédiaires biodégradables. Au cours de cette étape, la minéralisation partielle du polluant a lieu et le traitement biologique subséquent est appliqué pour compléter la minéralisation. Cette approche apparaît comme une alternative plus ciblée, moins coûteuse et environnementalement moins controversée que les procédés drastiques appliqués actuellement pour le traitement de tels contaminants dans l'eau.

Organisée en 6 chapitres, cette thèse s'intéresse en particulier à la dégradation d'un contaminant biorecalcitrant modèle, le 5-amino-6-methyl-2-benzimidazolone (AMBI) qui est un précurseur utilisé dans la fabrication industrielle des colorants. Le premier chapitre décrit les POA et le concept du processus couplé POA-biologique. Il donne également une vue d'ensemble des études utilisant une combinaison de procédés photochimiques et biologiques pour la dégradation des contaminants organiques dans l'eau.

Le chapitre 2 porte sur une étude exploratoire de trois POA parmi les plus représentatifs. Ainsi, pour dégrader l'AMBI les processus d'oxydation sonochimique, électrochimique et photochimique ont été appliqués. La comparaison de ces procédés a indiqué que les processus

photochimiques utilisant le fer comme catalyseur sont les plus avantageux et offrent des possibilités intéressantes d'application dans les régions ensoleillées.

Le chapitre 3 se concentre sur la dégradation de l'AMBI au moyen des systèmes $h\nu/Fe(III)/O_{2(air)}$ et $h\nu/Fe(III)/H_2O_2$ en utilisant une source artificielle d'irradiation. La transformation de l'AMBI photo-induite par le Fe(III) en présence des accepteurs d'électrons $O_{2(air)}$ et H_2O_2 est étudiée. L'effet de la concentration de l'AMBI, de Fe^{3+} et du H_2O_2 pour la dégradation de l'AMBI dans le processus de photo-Fenton est discuté et les conditions optimales trouvées sont présentées.

Le chapitre 4 porte sur le couplage des processus photochimiques et biologiques à l'échelle de laboratoire. Une stratégie générale est présentée pour développer les systèmes couplés photochimiques et biologiques pour le traitement des eaux résiduaires biorécalcitrants. Suivant cette stratégie, deux systèmes couplés ont été développés et testés en utilisant pour le pré-traitement photocatalytique les systèmes $h\nu/Fe^{3+}/O_{2(air)}$ ou $h\nu/Fe^{3+}/H_2O_2$ et dans les deux cas pour le traitement biologique un système à biomasse immobilisée.

Le chapitre 5 illustre le développement et l'optimisation à l'échelle pilote, d'un système couplé solaire-biologique pour le traitement de l'eau. Les points suivants sont abordés: (i) le choix du capteur solaire le plus approprié et du système photocatalytique le plus efficace, (ii) l'optimisation du système photocatalytique, (iii) le suivi des caractéristiques chimiques et biologiques de la solution photo-traitée et (iv) l'évaluation des performances du système solaire-biologique couplé pour le traitement d'une eau usée industrielle réelle contenant AMBI. Les résultats indiquent que le couplage des processus solaire-biologique est une méthode efficace pour le traitement des polluants industriels non-biodégradables tels que l'AMBI.

Pour surmonter le problème de l'alimentation en électricité des pompes utilisées pour faire récirculer l'eau usée dans ce procédé couplé de désintoxication de l'eau, le chapitre 6 propose un nouveau Système Hybride Photocatalytique-Photovoltaïque (HPPS). Le HPPS est un dispositif qui permet simultanément de décontaminer l'eau et de convertir l'énergie solaire en électricité. Cet équipement écologique (**dont une procédure de brevet est actuellement en cours à l'EPFL**) a été conçu, installé et testé. Les résultats expérimentaux montrent que le HPPS représente une méthode autonome et écologique pour cette stratégie de traitement de l'eau.

Mots clés: traitement des eaux, procédés d'oxydation avancées, photocatalysis, photo-Fenton, procédés couplés, oxydation biologique, oxydation électrochimique, oxydation sonochimique, application de l'énergie solaire, photovoltaïque, réacteur à l'échelle pilot, méthodologie de surface de réponse.

ACKNOWLEDGMENTS

This thesis has been carried out at the Laboratory for Environmental Biotechnology (LBE) at the EPFL within the framework of "project environnement EPFL-UNIVALLE".

While I alone am responsible for this thesis, it is nonetheless at least as much a product of years of interaction with, and inspiration by, a large number of friends and colleagues as it is my own work. For this reason, I wish to express my warmest gratitude to all those persons whose comments, questions, criticism, support and encouragement, personal and academic, have left a mark on this work. Regrettably, but inevitably, the following list of names will be incomplete, and I hope that those who are missing will forgive me, and will still accept my sincere appreciation of their influence on my work. Very special tanks go to:

César Pulgarin, my supervisor and friend. For his enthusiasm and inspiration. He was always there when I needed him. He manages to strike the perfect balance between providing direction and encouraging independence.

Professor Paul Péringer for receiving me in his laboratory (LBE) and for the support and confidence that he has given to César and his research group.

Rhoner AG, a Basel to have provided to the product 5-amino-6-methyl-2-benzimidazolone and wastewaters for our study.

the reviewers of this thesis, Prof. M. Bolte, Prof. S. Esplugas, Dr. J. Kiwi, Prof. D. Ollis and Prof. P. Péringer for accepting to read and evaluate my work and for providing valuable suggestions and comments.

my colleagues of the LBE, especially to Sandra Parra, Guiovana Rincon, Ricardo Torres and Siméon Kenfack, for their assistance in the daily work, their support, help and friendship.

Finally, to my parents Daniel and Magdalena, my wife Erica Lorena and all my family for their guidance, support, love and enthusiasm. Without these things this thesis could not have been possible.

LIST OF SYMBOLS

AMBI	5-Amino-6-methyl-2-benzimidazolone
AOP	Advanced Oxidation Processes
AOS	Average Oxidation State
APO	Advanced Photoassisted Oxidation Processes
BOD	Biological Oxygen Demand
c	Light speed
$\mathbf{C_i}$	Initial concentration
COD	Chemical Oxygen Demand
CPC	Compound Parabolic Collector
CR	Concentration Ratio
DOC	Dissolved Organic Carbon
$\mathbf{E_{bg}}$	Semiconductor band-gap energy
$\mathbf{EC_{50}}$	Effective Concentration at which 50% of light is lost
HM	Helioman collector
HPLC	High Performance Liquid Chromatography
k	First-order rate constant
l	Litre
LBE	Laboratory of Environmental Engineering
λ	Wavelength
pKa	Acid dissociation constant
PSA	Plataforma Solar de Almería
PTC	Parabolic Trough Collector
$\mathbf{t_r}$	Residence time

V	Volume
v_o	Initial degradation rate
V_{TOT}	Total volume
UV_D	Direct ultraviolet light
UV_G	Global ultraviolet light
VB	Valence Band

TABLE OF CONTENTS

CHAPTER 4
COUPLED PHOTOCATALYTIC-BIOLOGICAL PROCESS AT LAB SCALE   81

CHAPTER 5
COUPLED SOLAR-BIOLOGICAL SYSTEM AT FIELD PILOT SCALE   99

CHAPTER 6
HYBRID PHOTOCATALYTIC-PHOTOVOLTAIC SYSTEM   127

LIST OF FIGURES

LIST OF TABLES

INTRODUCTION AND BACKGROUND OF THE THESIS

1.1   Water pollution and conventional treatments

World water consumption per year is about 9×10^3 km^3 and at present, the quantity of available potential drinking water per year is between 10 and 30×10^3 km^3 [UNESCO report 2003]. This numbers clearly illustrates how even a small shortage of water could become a threat to mankind. Besides, the world suffers from growing health and hygienic problems and a high percentage of diseases in developing countries is caused by a deficient drinking water supply.

The drinking water is not only rare and limited, but also the central element of all the vital, social, and economic processes in the frame of the closed water cycle. This cycle is in crisis because of the development of a consumer society that entails the augmentation of industrial or agro-industrial activities. These activities generate an enormous diversity of commercialized chemical substances (~200.000) that arrive in huge quantities to the water cycle by different ways, endangering the fragile natural equilibrium of which all animals, including humans, are tributary.

One of the most alarming phenomena is the growing accumulation of hardly- biodegradable anthropogenic substances under the saturated auto-depurative conditions of such perturbed and overloaded cycle. The situation worsens by the lack, or insufficiency, of adequate water treatment systems capable of diminishing the concentration of toxic substances that represent a chronic chemical risk. It can be said that badly-treated wastewaters lead inevitably to a deterioration of water sources quality and consequently, of drinking water.

Two strategies of water treatment have to be forced in order to counterbalance these growing environmental problems:

- the development of appropriate treatment processes for contaminated drinking, ground, and surface water treatment, and particularly

- the development of appropriate treatment processes for wastewaters containing toxic or non-biodegradable compounds.

The processes and technologies available at present are very diverse. In general, the conventional processes, are often classified as preliminary, primary, secondary and tertiary treatment [Horan 1990].

- Preliminary treatment is designed to remove the debris and sandy materials from the wastewater.

- Primary treatment is the second step in treatment and separates suspended solids and greases from wastewater. Wastewater is held in a quiet tank for several hours allowing the particles to settle to the bottom and the greases to float to the top. The solids drawn off the bottom and skimmed off the top receive further treatment as sludge. The clarified wastewater flows on to the next stage of wastewater treatment. Clarifiers and septic tanks are usually used to provide primary treatment.

- Secondary treatment is a biological treatment process to remove dissolved organic matter from wastewater. The microorganisms absorb organic matter from sewage as their food supply. Two approaches are used to accomplish secondary treatment by aerobic means: fixed biomass and suspended biomass systems.

- **Fixed biomass systems** grow microorganisms on solid supports such as rocks, sand or plastic. The wastewater is spread over the supports, allowing the wastewater to flow past the film of microorganisms fixed to the solid supports. As organic matter and nutrients are absorbed from the wastewater, the film of microorganisms grows and thickens. Trickling filters, rotating biological contactors, and sand filters are examples of suspended biomass systems.

- **Suspended biomass systems** stir and suspend microorganisms in wastewater. As the microorganisms absorb organic matter and nutrients from the wastewater they grow in size and number. After the microorganisms have been suspended in the wastewater for several hours, they are settled out as a sludge. Some of the sludge is pumped back into the incoming wastewater to provide "seed" microorganisms. The remainder is wasted and sent on to a sludge treatment process. Activated sludge, extended aeration, oxidation ditch, and sequential batch reactor systems are all examples of suspended biomass systems.

- Tertiary treatment focuses on removal of disease-causing organisms from wastewater. Treated wastewater can be disinfected by adding chlorine or by using ultraviolet light. High levels of chlorine may be harmful to aquatic life in receiving streams. Treatment systems often add a chlorine-neutralizing chemical to the treated wastewater before stream discharge.

The incapability of conventional biological wastewater treatment to remove effectively many industrial biorecalcitrant and/or toxic pollutants, evidences that new efficient treatment systems are needed. For the last 25 years the water purification research has been extensively growing. Rigorous pollution control and legislation in many countries [EEC 1992; Suisse 1998] have resulted in an intensive search for new and more efficient water treatment technologies.

In the last decade a lot of research have been addressed to a special class of oxidation techniques defined as Advanced Oxidation Processes (AOP), pointing out its potential prominent role in the wastewater purification [Ollis and Ekabi 1993]. It was shown that AOP could successfully solve the problem of biorecalcitrant water pollutants working at or near ambient temperature and pressure.

These AOP are useful complements to well established techniques like flocculation, precipitation, adsorption on granular activated carbon, air stripping or reverse osmosis, combustion, and aerobic biological oxidation. Some of these latter techniques could transfer pollutants from the aqueous phase to a second one, but they do not destroy the pollutant. Others may be selective but slow to moderate in destruction rate, or rapid but not selective, thus generating appreciable reactor or energy costs. Aerobic biological oxidation is limited when the wastewater contains substances either recalcitrant to biodegradation, or inhibitory or toxic to the bioculture.

Other conversion processes can be limited by economic reasons, oxidative potential, effluent characteristics, or tendency to form harmful disinfection by-products as, for example, the case of formation of trihalomethanes (THMs) when a chlorination procedure is used for drinking water treatment.

Although AOP are cheaper than combustion or wet oxidation technologies, a serious drawback of AOP is their relatively high operational costs compared to those of biological treatments. However, their use as a pretreatment step for the enhancement of the biodegradability of wastewater containing recalcitrant or inhibitory compounds can be justified when the intermediates resulting from the reaction can be readily degraded by microorganisms. Therefore, combinations of AOP as preliminary treatments with inexpensive biological processes, seem very promising from an economical point of view.

The conventional process treating domestic and industrial biodegradable wastewater as well as proposed system in this thesis for the treatment of biorecalcitrant industrial wastewater are presented in Fig. 1.1.
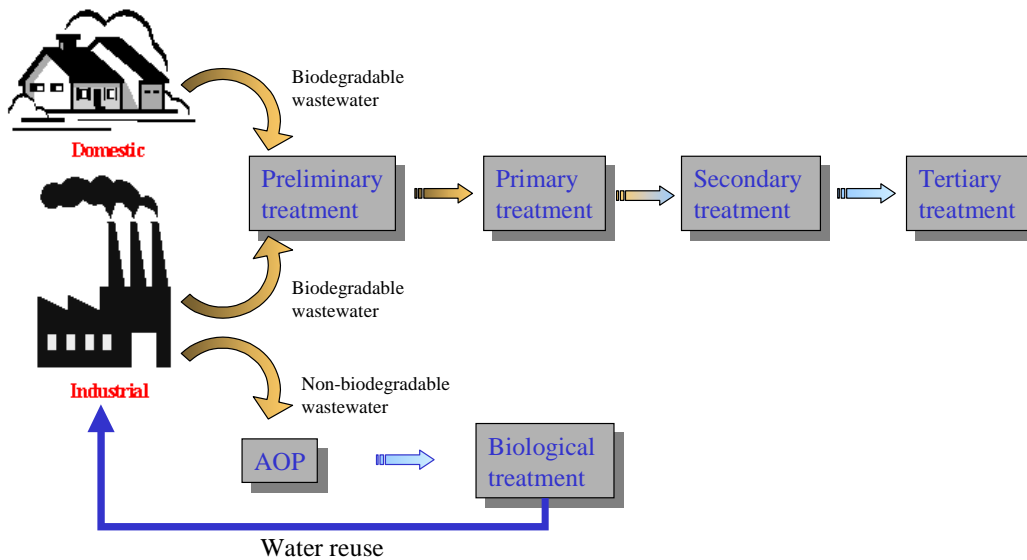
FIGURE 1.1   *Schematic representation of conventional and proposed wastewater treatment*

1.2 Aims of the thesis

The aim of this thesis is the development and optimization, at pilot scale, of a hybrid technology combining an AOP and a biological process for the treatment of biorecalcitrant wastewater. The emphasis will be on the oxidative pretreatment. This pretreatment have to modify the structure of the pollutants by transforming them into less toxic and more biodegradable intermediates. Biological treatment will then complete the degradation of the pollutant load. This approach should be viable from the economic and environmental point of view, as an alternative to the drastic and/or inefficient single-step processes actually applied in biorecalcitrant pollutant elimination. Fig. 1.2 presents the main existing wastewater treatment process and its inconveniences, as well as the approach proposed in this thesis and the expected benefits.

For the development of a AOP-biological system, the following scientific and technological objectives are foreseen:

- Evaluation of several AOP with the aim to choose the most appropriate AOP for the treatment of the wastewater containing the biorecalcitrant pollutant such as AMBI.

- Definition of the optimal conditions: pollutant, catalyst and oxidant concentrations for the most appropriate system chosen as pretreatment.

- Elucidation of the AMBI degradation mechanism by means of the chosen AOP.

- Evaluation of the bio-compatibility (toxicity, biodegradability) of the photochemically pretreated solution.

- Proposition of a general strategy to develop combined photochemical and biological system for the treatment of AMBI.

- Evaluation of the performances of coupled photocatalytic-biological system at lab scale for the degradation of AMBI.

- Application of solar photochemical-biological coupled system at pilot scale for the treatment of AMBI.
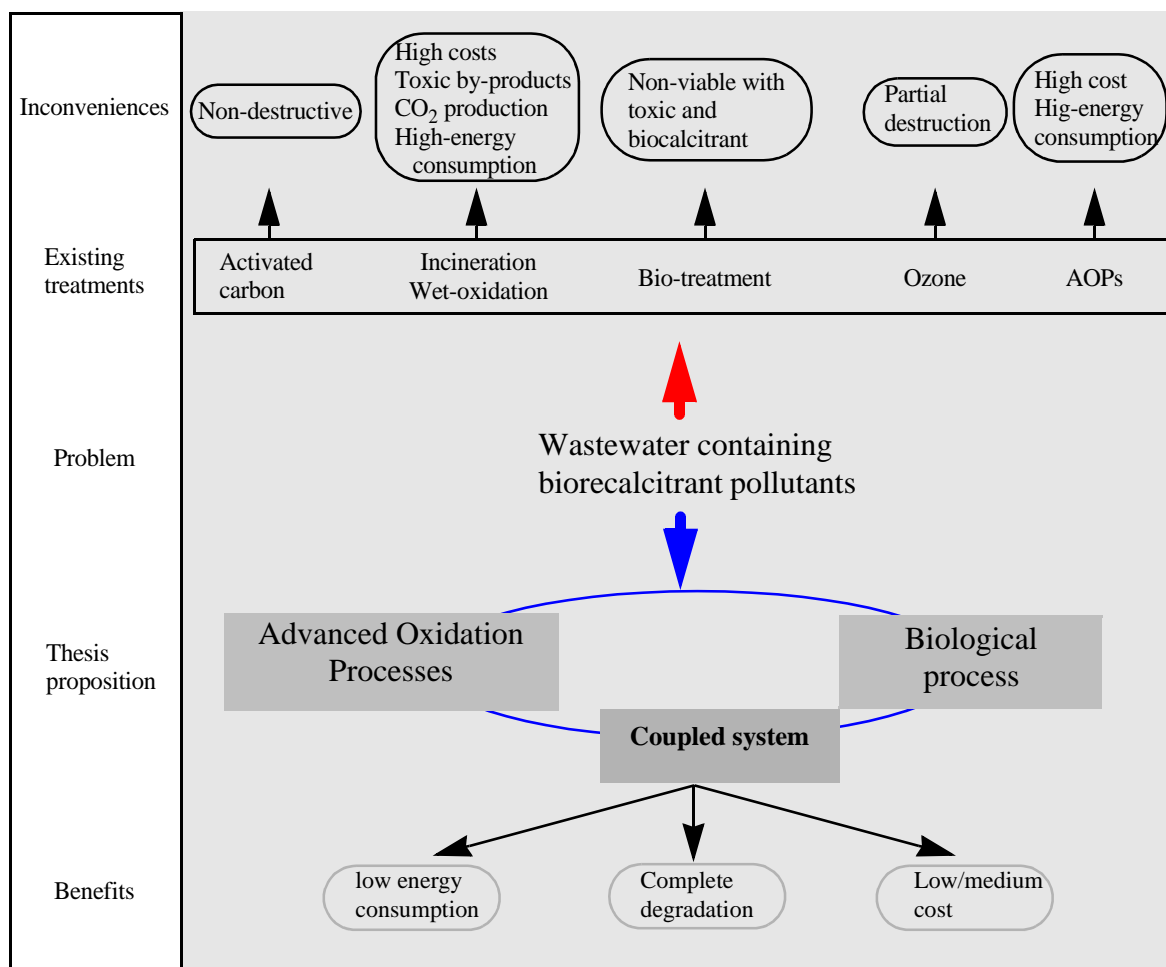
FIGURE 1.2   *Schematic representation of the state of the art of wastewater treatment and innovation aspects of this thesis.*

1.3   Outline of the thesis

This thesis is organized in 6 chapters, the fundamental an technological achievements of each chapter are represented in Fig 1.3. In the first chapter, AOP and the concept of coupling AOP-Biological process are introduced. Chapter 2 focuses on an exploratory study on sonochemical, electrochemical and photochemical oxidation processes degrading a model pollutant, 5-amino-6-methyl-2-benzimidazolone (AMBI). This chapter is organised around three major topics: (i) the

biodegradability enhancement of AMBI wastewater using ultrasounds, (ii) by the electrochemical oxidation, on Pt anodes and (iii) the comparison of some Advanced Photochemical Oxidation Processes in the same purpose. Chapter 3 focuses on the degradation of AMBI by means of the $h\nu/Fe(III)/O_{2(air)}$ and $h\nu/Fe(III)/H_2O_2$ systems using an artificial irradiation source. In chapter 4 a general strategy to develop combined photochemical and biological systems for biorecalcitrant wastewater treatment is proposed. For the choice of treatment, the following points were taken into account: the biodegradability of the initial pollutant, the chemical and biological characteristics of the phototreated solutions, the definition of the optimal pretreatment time, and the efficiency of the coupled reactor. Following this strategy, two kinds of combined systems were developed using in all cases immobilized activated sludge culture for the biological step and for the photocatalytic pretreatment $h\nu/Fe^{3+}/O_{2\ (air)}$ or $h\nu/Fe^{3+}/H_2O_2$. Both coupled systems were successfully employed for the treatment of AMBI. Chapter 5 illustrates the development and optimization, at pilot scale (60 l), of a coupled system for water treatment. In this chapter a coupled solar-biological system at field pilot scale was designed, builds and experimental results are presented. Finally in chapter 6, a Hybrid Photocatalytic-Photovoltaic System (HPPS) was designed, installed, and tests results are presented. The HPPS consist of an autonomous device with dual operation: (i) The photocatalytic system, which uses the UV radiation to promote the degradation of organic pollutants, and retained the IR radiation. (ii) The photovoltaic system converts the visible radiation into electricity, which is directly used by the recirculation pump or is stored in a battery for other purposes.

Fundamental achievements

Technological achievements

Ch.6
Development of a Hybrid Photocatalytic-
Photovoltaic system for water treatment

Ch.5
Development of a solar-biological
coupled system at field pilot scale

Ch.4
Development of a coupled
system at lab scale

Ch.3
Fundamental study of
$h\nu/Fe(III)/O_2$ and
$h\nu/Fe(III)/H_2O_2$ systems

Ch.2
Exploratory study of sono, electro and
photochemical degradation systems

Ch.1
Introduction of AOPs and OP-biological
coupled systems for water treatment
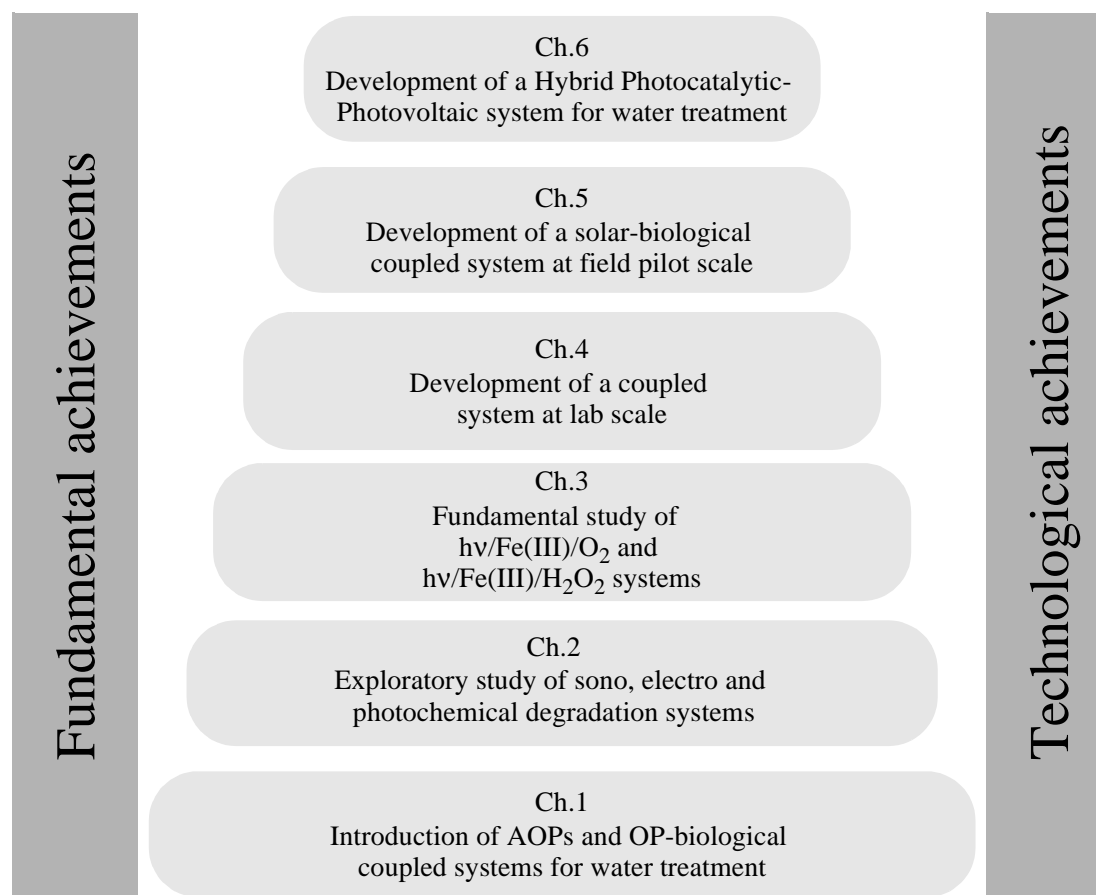
FIGURE 1.3   *Schematic representation of the outline of this thesis.*

1.4   Advanced Oxidation Process

Advanced Oxidation Processes (AOP) are an attractive alternative for the treatment of contaminated ground, surface, and waste waters containing hardly-biodegradable anthropogenic substances as well as for the purification and disinfection of drinking water [Legrini et al. 1993; Bahnemann et al. 1994; Bolton and Cater 1994; Hoffmann et al. 1995; Robertson 1996].

Although AOP use different reacting systems, all are characterized by the same chemical feature: production of $^\bullet OH$ radicals. This radicals are extraordinarily reactive species, they attack the most part of organic molecules with rate constants usually in the order of 10^6–10^9 M^{-1} s^{-1} [Hoigne 1997].

•OH radicals are also characterised by a low selectivity of attack which is a useful attribute for an oxidant used in wastewater treatment and to solve pollution problems. The versatility of AOP is also enhanced by the fact that they offer different possible ways for •OH radicals production thus allowing a better compliance with the specific treatment requirements.

Table 1.1 shows that •OH has the highest thermodynamic oxidation potential, which is perhaps why •OH-based oxidation processes have gained the attention of many advanced oxidation technology developers. In addition, most environmental contaminants react 1 million to 1 billion times faster with •OH than with O_3, a conventional oxidant [US.EPA 1998].

TABLE 1.1   *Oxidation potential of several oxidants in water*

Oxidant	Oxidation potential (eV)[a]
•OH	2.80*
$O(^1D)$	2.42
O_3	2.07
H_2O_2	1.77
Permanganate ion	1.67
Chlorine	1.36
O_2	1.23

Notes:

[a] Source: CRC Handbook 1995

* Nevertheless, calculations in aqueous solutions suggest that the oxidation potential •OH/OH⁻ is 1.91 and not 2.80. Source: Sulzberger et al. 1997.

The oxidation reactions involving hydroxyl radical and organic substrates (RH or PhX) in aqueous solutions, may be classified with respect to their character to [Bossmann et al. 1998]:

a) abstraction of hydrogen

$$•OH + RH \rightarrow R^• + H_2O \qquad \qquad \textbf{(1.1)}$$

b) addition reactions

$$\bullet OH + PhX \rightarrow HOPhX^{\bullet} \qquad\qquad\qquad (1.2)$$
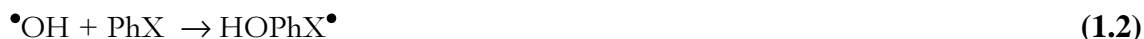
c) electron transfer

$$\bullet OH + RH \rightarrow [R\text{-}H]^{+\bullet} + HO^{-} \qquad\qquad\qquad (1.3)$$

Application of AOP depends on polluting load of wastes (see Fig. 1.4).
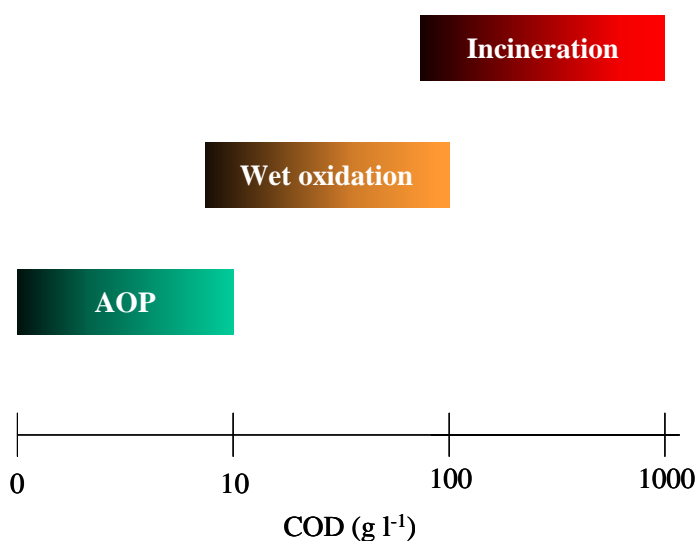
FIGURE 1.4   *Suitability of water treatment technologies according to COD contents (source [Andreozzi et al. 1999])*

Only wastes with relatively small Chemical Oxygen Demand (COD) contents ($\leq 5.0 \, g \, l^{-1}$) can be suitably treated by means of these techniques [Andreozzi et al. 1999] since higher COD contents would require the consumption of too large amounts of expensive reactants. Wastes with more massive pollutants contents can be more conveniently treated by means of wet oxidation or incineration [Mantzavinos et al. 1997; Luck 1999].

AOP are usually classified of different ways according to the reaction phase (homogeneous or heterogeneous) or to the $\bullet OH$ generation methods (chemical, electrochemical, sonochemical, or photochemical). The main used AOP are shown in Fig. 1.5 and are briefly described below to provide a brief knowledge of each one of them, that will be useful within the framework of this thesis.
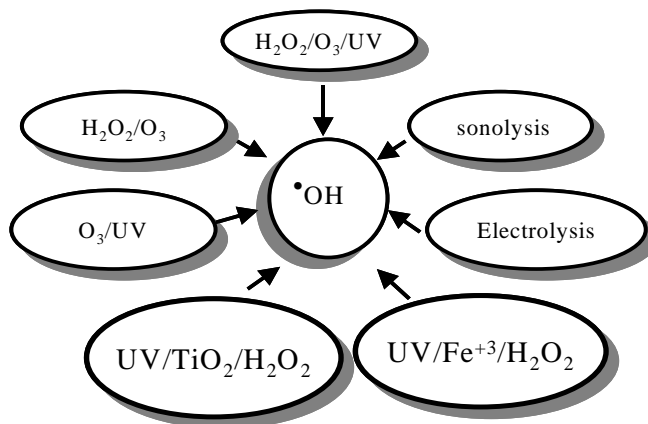
FIGURE 1.5 *Main Advanced Oxidation Process*

1.4.1 Sonochemical oxidation methods

Sonochemical Oxidation Techniques (SOT) have received considerable attention as AOP because they lead to rapid degradation of chemical contaminants in water [Francony and Petrier 1996; Theron et al. 2001]. SOT involve the use of ultrasonic waves to produce an oxidative environment via cavitation that yields localized microbubbles and supercritical regions in the aqueous phase.

Ultrasounds are waves at frequencies beyond human hearing, from 20KHz to about 10MHz. When liquids are exposed to these high frequency vibrations, both physical and chemical changes occur as a result of a physical phenomenon, known as cavitation. Cavitation is the formation, growth, and sudden collapse (implosion) of microscopic gas bubbles in liquids (Fig. 1.6).
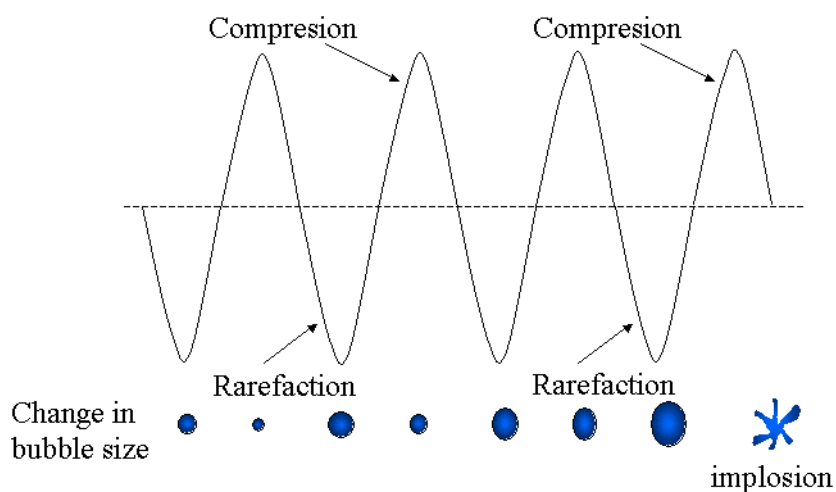
FIGURE 1.6   *Sound motion related to bubble growth and implosion*

The collapse of these bubbles leads to surprisingly high local temperatures (2000 to 5000 ^{o}C) and pressures (500 atmospheres) [Adewuyi 2001]. These extreme conditions, are very short-lived but have shown to result in the generation of highly reactive species. The water vapour and O_2 in the cavitation bubbles undergo thermal dissociation to yield •H, •OOH and •OH radicals as well as O atoms. H_2O_2 is formed as a consequence of hydroxyl and hydroperoxyl recombination outside the cavitation bubbles.

In the cavitation process, three regions for the occurrence of chemical degradation reactions are postulated [Adewuyi 2001] (Fig. 1.7): (1) a hot gaseous nucleus; (2) an interfacial region with radial gradient in temperature and local radical density: and (3) the bulk solution at ambient temperature.

It has been shown [Francony and Petrier 1996] that degradation depends of the physical and chemical properties of the organic pollutants as follow:

- Hydrophilic and non-volatile compounds, are oxidised by the highly reactive radicals (e.g., •OH, •OOH, etc. formed on sonolysis) in bulk solution and/or at the interface of liquid-bubbles depending on the substrate concentrations.

- Hydrophobic and volatile substrates, are destroyed predominantly by direct pyrolitic decomposition which takes place within the hot interfacial region or whitin the gas phase of collapsing bubbles.

BULK SOLUTION MEDIA : T~300K

Hydrophilic compounds

CAVITY INTERIOR

~5000 °K

~500 atm

$H_2O \rightarrow {}^*OH + H^*$

Hydrophobic compounds

GAS-LIQUID INTERFACE T ~2000 °K
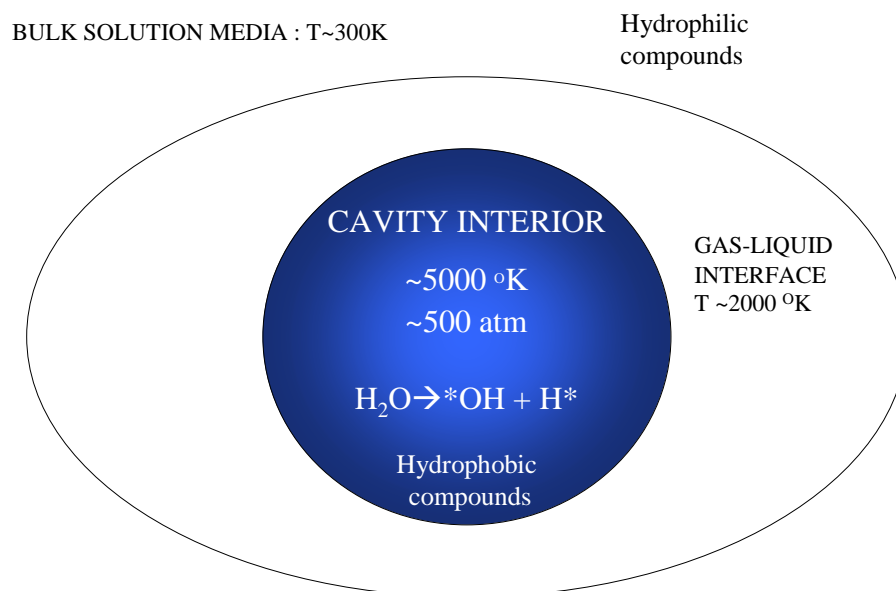
FIGURE 1.7   *Three reaction zones in the cavitation process (source: [Adewuyi 2001]).*

1.4.2   Electrochemical methods

In the last years, there is great interest in the development of effective electrochemical treatments for the destruction of toxic and biorefractory organics in waters [Pulgarin and Kiwi 1996; Enea and Pulgarin 2000]. Anodic oxidation and indirect electro-oxidation with H_2O_2 electrogeneration are the most usual techniques utilized to achieve the mineralization of such pollutants, i.e. their final conversion into CO_2, water and inorganic ions. In anodic oxidation, adsorbed hydroxyl radicals ($^\bullet$OH) are formed at the surface of a high-oxygen overvoltage anode from water oxidation:

$$H_2O \rightarrow {}^\bullet OH_{ads} + H^+ + e^- \tag{1.4}$$

This radical, as shown previously, is a powerful oxidizing agent, with ability to react with organics giving dehydrogenated or hydroxylated derivatives. Anodic oxidation [Comninellis and

Pulgarin 1991, 1993] is usually performed in the anodic compartment of a divided cell, where the contaminated solution is treated using an anode of Pt, undoped and doped PbO_2, doped SnO_2 or IrO_2. Under these conditions, however, most aromatic solutions are poorly mineralized, because of the generation of hardly oxidable carboxylic acids.

More potent indirect electro-oxidation methods for water remediation involve the continuous supply of a strong oxidant such as H_2O_2 to the treated solution from the two-electron reduction of oxygen on graphite [Do and Chen 1994], carbon [Ponce de Leon and Pletcher 1995], mercury pool [Oturan 2000], and O_2-diffusion [Brillas and Casado 2002] cathodes. This reaction in acid medium can be written as follows:

$$O_{2(g)} + 2H^+ + 2e^- \rightarrow H_2O_2 \tag{1.5}$$
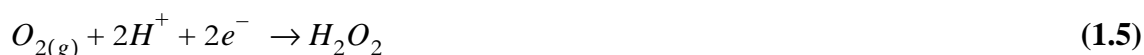
1.4.3 Advanced Photochemical Oxidation Processes

An interesting class of AOP consists of the so called Advanced Photochemical Oxidation (APO) processes[US.EPA 1998]. APO processes are characterised by a free radical mechanism initiated by the interactions of photons of a proper energy level with the molecules of chemical species present in the solution or with a catalyst.

The most used APO technologies can be broadly divided into the following groups: (1) heterogeneous photocatalysis, (2) homogeneous photocatalysis, and (3) the photo-Fenton process. These APO technologies are briefly described below.

1.4.3.1 Heterogeneous photocatalysis

Since 1972, when Fujishima and Honda [Fujishima and Honda 1972] reported the photocatalytic decomposition of water on TiO_2 electrodes, photocatalysis has been used with great success in the degradation of a wide variety of contaminants, including alkanes, alcohols, carboxylic acids, alkenes, phenols, dyes, PCBs, aromatic hydrocarbons, halogenated alkanes and alkenes, surfactants, and pesticides [Ollis and Ekabi 1993; Blake 2001].

Heterogeneous photocatalysis is a technology based on the irradiation of a catalyst, usually a semiconductor, which may be photoexcited to form electron-donor sites (reducing sites) and electron-acceptor sites (oxidising sites), providing great scope as redox reagents. The process is heterogeneous because there are two active phases, solid and liquid.

Among several semiconductors, TiO_2 has proven to be the most suitable for widespread environmental applications. Titanium dioxide is stable to photo- and chemical corrosion, and inexpensive. TiO_2 has an appropriate energetic separation between its valence (VB) and conduction band (CV), which can be surpassed by the energy of a solar photon. The VB and CB energies of the TiO_2 are estimated to be +3.1 and -0.1 volts, respectively, which means that its band gap energy is 3.2 eV and absorbs in the near UV light (λ<387 nm).

To date, there is evidence supporting the idea that hydroxyl radical ($^\bullet$OH) is the main oxidizing species responsible for photo-oxidation of the majority of the studied organic compounds [Legrini et al. 1993]. The first event, after absorption of near ultraviolet radiation at λ<387 nm, is the generation of electron/hole pairs (Eq. 1.6) separated between the CB and VB.

$$TiO_2 + h\upsilon \rightarrow TiO_2(e^- + h^+)$$ **(1.6)**

Some of the many events which take place after the UV light absorption by TiO_2 particles and the subsequent generation and separation of electrons (e^-_{CB}) and holes (h^+_{VB}) are presented in Fig. 1.8. Three oxidation reactions have been experimentally observed: electron transfer from RX, H_2O, and $^-$OH adsorbed on the catalyst surface.
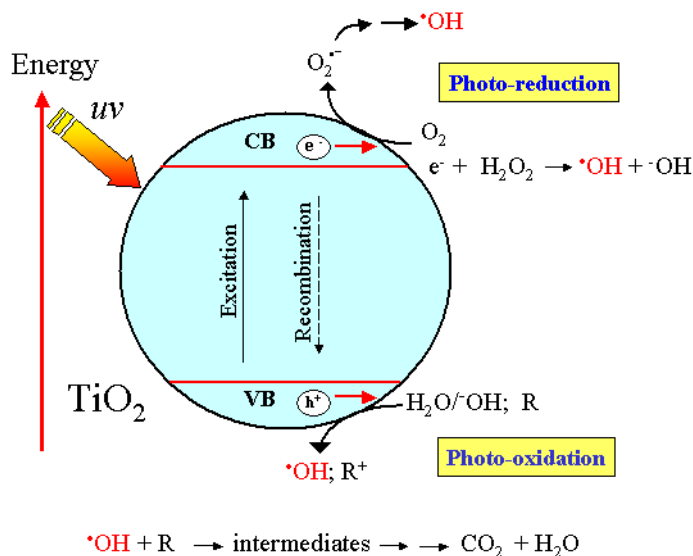
FIGURE 1.8   *TiO$_2$-semiconductor photocatalytic process. Scheme showing some photochemical and photophysical events that might take place on an irradiated semiconductor particle.*

It has been shown that the photocatalytic degradation of a water contaminant can be enhanced by addition of H$_2$O$_2$, a better electron acceptor than O$_2$ [Ollis et al. 1991; Pichat et al. 1995; Diller et al. 1996]. This effect has been explained by the formation of hydroxyl radicals during the reaction with CB electrons by:

$$H_2O_2 + e_{CB}^{-} \rightarrow {}^\bullet OH + OH^- \tag{1.7}$$

It limits the electron-hole recombination rate and increases the hydroxyl radical concentration at the TiO$_2$ surface.

1.4.3.2   Homogeneous photodegradation

The former applications of homogeneous photodegradation (single-phase system) to treat contaminated waters, concerned the use of UV/H$_2$O$_2$ and UV/O$_3$. The use of UV light for photodegradation of pollutants can be classified into two principal areas: (1) direct photodegradation, which proceeds following direct excitation of the pollutant by UV light and (2)

photo-oxidation, where light drives oxidative processes principally initiated by hydroxyl radicals. The latter process involves the use of an oxidant to generate radicals, which attack the organic pollutants to initiate oxidation. Three major oxidants used are: hydrogen peroxide, ozone, and Photo-Fenton system (Fe^{3+}/H_2O_2).

UV/H_2O_2: UV oxidation with H_2O_2 was first applied to wastewater treatment by Koubeck [Koubeck 1975]. The most commonly accepted mechanism for the photolysis of H_2O_2 is the cleavage of the molecule into hydroxyl radicals with a quantum yield of two $^\bullet OH$ radicals formed per quantum of radiation absorbed (Eq. 1.8). This reaction is observed only at $\lambda < 300$ nm for concentrations of H_2O_2 of 10^{-1} mol l^{-1}. On the other hand, H_2O_2 is known to dismute (Eq. 1.9).

$$H_2O_2 + h\upsilon \rightarrow 2^\bullet OH \qquad\qquad\qquad\qquad \textbf{(1.8)}$$

$$H_2O_2 + HO_2^- \rightarrow O_2 + H_2O + OH^- \qquad\qquad\qquad \textbf{(1.9)}$$

The use of UV/H_2O_2 is very common for the treatment of contaminated water [Pichat et al. 1995; Rodriguez et al. 2000] due to several practical advantages: (i) H_2O_2 is available as an easily handled solution that can be diluted in water to give a wide range of concentrations, (ii) there are no air emissions, and (iii) a high-quantum yield of hydroxyl radicals is generated. The major drawback of using H_2O_2 is its low molar extinction coefficient at the near UV-region [Legrini et al. 1993]. The H_2O_2/UV photoprocess needs low pressure mercury lamps emitting short UV-radiation (254 nm), which is not available in the solar radiation. The high operation costs of the UV lamps reduce the feasibility of application of this system on a large scale [Bauer et al. 1999].

O_3/UV: Ozone is widely used as an oxidant in pollution abatement in aqueous media. It has the advantage that it is an environmentally friendly oxidant as its use is residue-free. However, with many pollutants it reacts so slowly [Reisz et al. 2003] that for all practical purposes they must be considered ozone-refractory. For this reason, procedures are being applied where the oxidative power of the ozone is "activated", i.e., by a combination of ozone with H_2O_2 [Safarzadeh-Amiri 2001], with H_2O_2/UV radiation [Beltran et al. 1997; Ku et al. 2000; Esplugas et al. 2002], with Fe(III)/UV [Contreras et al. 2001] or Cu(I)/UV [Canton et al. 2003].

The reaction between ozone and organic matter can proceed in two different ways depending on the ozonising conditions (pollutants, pH and ozone dose fed): Through direct reactions of molecular ozone and the pollutants, or indirectly through radical reactions (mainly through reactions with $^\bullet$OH).

Photolysis of ozone dissolved in water leads to the production of hydrogen peroxide (Eq. 1.10) and the subsequent formation of $^\bullet$OH (Eq. 1.8), which oxidizes the organic compounds.

$$O_3 + H_2O + h\upsilon \rightarrow O_2 + H_2O_2 \qquad\qquad (1.10)$$

The O_3/UV process is considered as an advanced water treatment for the effective oxidation and destruction of toxic and refractory organics [Canton et al. 2003], bacteria, and viruses in water but it has the same problem as hydrogen peroxide process for the use of solar energy since O_3 does not absorb light at $\lambda > 300$ nm.

Application of solar irradiation to the homogeneous photochemical process, is only possible for the photo-Fenton reaction, which can be active at wavelengths up to 600 nm (35% of the solar irradiation).

1.4.3.3 Fenton photo-assisted reactions

The Fenton reaction was discovered by H.J.H Fenton in 1894 [1894]. Forty years later the Haber-Weis mechanism was postulated [Haber and Waiser 1934], which revealed that the effective oxidative agent in the Fenton reaction is the hydroxyl radical ($^\bullet$OH). Since then, some groups have tried to explain the whole mechanism [Walling 1975; Prousek 1995; Sychev and Isak 1995]. The Fenton reaction can be outlined as follows:

$$M^{n+} + H_2O_2 \rightarrow M^{(n+1)+} + OH^- + {}^\bullet OH \qquad\qquad (1.11)$$

where M is a transition metal as Fe or Cu.

In absence of light and complexing ligands other than water, the most accepted mechanism of H_2O_2 decomposition in acid homogeneous aqueous solution, involves the formation of

hydroxyperoxyl ($HO_2^\bullet/O_2^-$) and hydroxyl radicals ($^\bullet OH$) [De Laat and Gallard 1999; Gallard and De Laat 2000].

The $^\bullet OH$ radical, once in solution attacks almost every organic compound. The metal regeneration can follows different paths. For Fe^{2+}, the most accepted scheme is described in Equations 1.12 to 1.18 [Sychev and Isak 1995].

$$Fe^{2+} + H_2O_2 \rightarrow Fe^{3+} + OH^- + {}^\bullet OH \qquad K=63 \ l \ mol^{-1}s^{-1} \tag{1.12}$$

$$Fe^{3+} + H_2O_2 \rightarrow Fe^{2+} + HO_2^\bullet + H^+ \qquad K=3.1 \times 10^{-3} \ l \ mol^{-1}s^{-1} \tag{1.13}$$

$$Fe^{2+} + {}^\bullet OH \rightarrow Fe^{3+} + OH^- \qquad K=3 \times 10^8 \ l \ mol^{-1}s^{-1} \tag{1.14}$$

$$^\bullet OH + H_2O_2 \rightarrow HO_2^\bullet + H_2O \qquad K=3.3 \times 10^7 \ l \ mol^{-1}s^{-1} \tag{1.15}$$

$$Fe^{3+} + HO_2^\bullet \rightarrow Fe^{2+} + H^+ + O_2 \qquad K=2 \times 10^3 \ l \ mol^{-1}s^{-1} \tag{1.16}$$

$$Fe^{3+} + O_2^{\bullet -} \rightarrow Fe^{2+} + O_2 \qquad K=5 \times 10^7 \ l \ mol^{-1}s^{-1} \tag{1.17}$$

$$Fe^{2+} + HO_2^\bullet \rightarrow Fe^{3+} + HO_2^- \qquad K=1.2 \times 10^6 \ l \ mol^{-1}s^{-1} \tag{1.18}$$

Fenton reaction rates are strongly increased by irradiation with UV/visible light [Rupert et al. 1993; Sun and Pignatello 1993; Bandara et al. 1996], this type of photoassisted reaction is referred to as the «photo-Fenton reaction» [Zepp et al. 1992].

$$Fe^{3+} + H_2O + h\upsilon \rightarrow Fe^{2+} + {}^\bullet OH + H^+ \tag{1.19}$$

The positive effect of irradiation on the degradation rate is due to the photochemical regeneration of ferrous ions (Fe^{2+}) by photoreduction of ferric ions (Fe^{3+}) [Faust and Hoigne 1990]. The new generated ferrous ion reacts with H_2O_2 generating a second $^\bullet OH$ radical and ferric ion (Eq. 1.12), and the cycle continues. In these conditions, iron can be considered as a real catalyst.

The main advantage of the photo-Fenton process is the light sensitivity up to a wavelength of 600 nm (35% of the solar radiation) [Safarzadehamiri et al. 1997]. The depth of light penetration is high and the contact between pollutant and oxidising agent is close, since homogeneous solution is used [Bauer et al. 1999; Fallmann et al. 1999].

Fenton and photo-Fenton processes have been used with great success to treat a wide variety of contaminants, including phenols [Kiwi et al. 1994; Gernjak et al. 2003], dyes [Bandara et al. 1996], halogenated alkanes and alkenes [Buyuksonmez et al. 1999], and pesticides [Fallmann et al. 1999; Parra et al. 2000].

Several parameters governing or influencing the kinetics of the photo-Fenton system have been studied: pH [Scott et al. 1995], iron concentration [Krutzler and Bauer 1999], iron species [Cuzzola et al. 2002], H_2O_2 concentration [Safarzadehamiri et al. 1997], initial pollutant concentration [Rupert et al. 1993], temperature [Sagawe et al. 2001; Rodriguez et al. 2002], the irradiation source [Rodriguez et al. 2002], the presence of radical scavengers [Chen and Pignatello 1997; Kiwi et al. 2000]. The effect of pH, initial iron and H_2O_2 concentrations are briefly discussed below.

• Effect of the pH

The Fenton and photo-Fenton systems have a maximum catalytic activity at pH of about 2.8. The pH value influences the generation of $^{\bullet}OH$ radicals and thus the oxidation efficiency. For pH values above 4 the degradation strongly decreases since iron precipitates as hydroxide derivative, reducing the Fe^{2+} availability and the radiation transmission [Faust and Hoigne 1990; Ghaly et al. 2001].

The need for acidification of a waste water stream is one of the major obstacles towards an industrial application of the Photo-Fenton reaction. Thus a possible extension of the useful pH range towards more neutral solutions would be of utmost interest.

• Effect of the initial hydrogen peroxide concentration

Degradation rates increase with H_2O_2 concentration which is explained by the effect of the additionally produced $^{\bullet}OH$ radicals [Parra et al. 2000]. However, above a certain H_2O_2

concentration, the reaction rate levels off and sometimes is negatively affected, by the progressive increase of the hydrogen peroxide concentration. This may be due to auto-decomposition of H_2O_2 to oxygen and water and recombination of $^\bullet OH$ radicals (Eq. 1.15). Therefore, H_2O_2 should be added to treated wastewater an optimal concentration to achieve the best degradation. This optimal H_2O_2 concentration depends on the iron concentration and on the nature and concentration of the pollutant.

• Effect of the initial iron concentration

As in the case of H_2O_2, degradation rate increase with the concentration of iron, but after an optimum the efficiency decreases. This may be due to the increase of a brown turbidity that hinders the absorption of the light required for the photo-Fenton process or by the recombination of $^\bullet OH$ radicals. In this case, Fe^{2+} reacts with $^\bullet OH$ radicals as a scavenger (Eq. 1.14).

It is desirable for the ratio of H_2O_2 to Fe^{2+} or Fe^{3+} to be as low as possible, so recombination can be avoided and iron complex production reduced. An optimal H_2O_2/iron molar ratio between 10 and 25 has been proposed by several authors [Tang and Huang 1996; Kim et al. 1997; Beltran-Heredia et al. 2001]. The effect that H_2O_2 and iron concentrations have on the degradation of a model compound is discussed in section "3.3.2".

The limitation inherent to the Fenton and photo-Fenton systems in homogeneous solution is that all the reactants including the catalyst are in solution, and the recovery of iron is complicated and expensive. It is important to keep in mind the level of iron in water allowed by environmental legislation. For example, in Switzerland [Conseil Fédéral Suisse 1998] the upper limit of iron in an effluent that goes to be discharged in natural waters (2 mg l^{-1}) or to a biological wastewater treatment plant (20 mg l^{-1}).

The development of Fenton catalyst supported on inert materials has recently become interesting in order to avoid the need for iron separation from the treated water. Photo-Fenton studies on supported Fe-ions have involved perfluorinated membranes [Fernandez et al. 1999], Nafion-silica composites [Dahananjeyan et al. 2001], polyethylene copolymers [Dhananjeyan et al. 2001], and silica loaded fabrics [Bozzi et al. 2002]. At the same time, different possibilities for heterogeneous iron photo-assisted processes for the treatment of wastewater have been explored,

such as using zero valent iron [Pulgarin et al. 1995; Ghauch 2001], iron oxide [Pulgarin and Kiwi 1995; Bandara et al. 2001; Herrera et al. 2001], and iron load zeolith [Pulgarin et al. 1995].

1.5 Integration of photochemical and biological processes for water treatment

A major drawback of APO processes is their relatively high operational costs compared to those of biological treatments. However, the use of APO processes as a pretreatment step for the enhancement of the biodegradability of wastewater containing recalcitrant or inhibitory compounds can be justified when the intermediates resulting from the reaction can be readily degraded by microorganisms. Therefore, combinations of APO processes as preliminary treatments with inexpensive biological processes, seem very promising from an economical point of view.

Previous studies have attempted the strategy of combining chemical and biological processes to treat contaminants in wastewater. These studies, extensively reviewed by Scott and Ollis [1995; 1997] suggested potential advantages for water treatment. Recently, some interesting coupled systems (APO-Biological) have been proposed to treat various types of industrial wastewaters. Table 1.2 presents a survey of publications, realized within the last five years, involving the use of coupling APO-biological processes for water treatment, based on the structure proposed by Scoot and Ollis [1995]. Wastewaters under study are coming from: textile, pulp and paper, surfactants, and explosive military industries, as well as from olives washing, and pesticides contaminated effluents.

For the 16 cases presented in Table 1.2, two waters were previously pretreated by biological means to remove the easily biodegradable fraction of pollution before leading to APO-biological treatment in which the aim of the APO is to produce biodegradable intermediates.

The proposed systems include: $h\nu/H_2O_2$ - aerobic batch activated sludge (BAS) [Adams and Kuzhikannil 2000]. TiO_2-assisted photocatalytic reduction in series with fungal mineralization by phanerochaete chrysosporium [Hess et al. 1998]. $h\nu/TiO_2$-supported in glass rings followed by bacterial degradation using Pseudomonas paucimobilis (S37) and Burkholdeira cepacia (PZK) [Yeber et al. 2000]. Ledakowicz et al. [2001] explored $h\nu/O_3$ and $h\nu/H_2O_2$ systems as a

TABLE 1.2   Studies utilizing photochemical and biological coupled systems for the degradation of organic compounds

Authors	Chemical degraded	Concentration	APO	Biological Oxidation	Biodegradability test	Order of schema	Overall efficiency
[Hess et al. 1998]	TNT	0.44 mmol l^{-1}	hv/TiO$_2$	Fungal (Phanerochaee chrysosporidium)			++
[Reyes et al. 1998]	Kraft effluents		hv/ZnO immobilized	Fungal (Lentinula edodes)		B-B-AOP AOP-B	+ ++
[Pulgarin et al. 1999]	p-nitro-o-toluenesulfonic acid	330 mg C l^{-1}	hv/Fe^{3+}/H$_2$O$_2$	FBR	BOD$_5$/COD Micotox	AOP-B	++
[Adams and Kuzhikannil 2000]	Alkildimethzlbenzyl-Ammonium-ChloridesDioctyl-dimethyl-Ammonium-Chlorid	COD=1000 mg l^{-1}	hv/H$_2$O$_2$	BAS essay	BAS essay	AOP-B	++
[Yeber et al. 2000]	&-chlorovanillin	186 ppm	hv/TiO$_2$ immobilized	Pseudomonas Parcimobilis (S37) and Burkholdera Cepai (PKZ)	Bacterial growth rate	AOP-B	0
[Parra et al. 2000]	Isoproturon Metobromuron	0.2 mmol l^{-1}	hv/Fe^{3+}/H$_2$O$_2$	Fixed Bed Reactor (FBR)	BOD$_5$/COD Micotox	AOP-B	++ 0
[Benitez et al. 2001]	Olives washing wastewaters	COD=2.7g l^{-1} BOD=1.56g l^{-1}	hv/O$_3$	Acclimated activted sludge culture	Kinetic measure. (Contois model)	B-AOP AOP-B	+ ++
[Ledakowicz et al. 2001]	Synthetic textile wastewater	COD=2154 mg O$_2$ l^{-1} BOD=1050 mg	hv/O$_3$ hv/H$_2$O$_2$	Acclimated activated sludge culture	Kinetic. measure. (Monod model)	AOP-B	++
[Sarria et al. 2001]	AMBI	3 mmol l^{-1}	hv/Fe^{3+}/H$_2$O$_2$	FBR	BOD$_5$/COD Micotox	AOP-B	++
[Rodriguez et al. 2002]	Textile wastewater	900 mg C l^{-1}	hv/Fe^{3+}/H$_2$O$_2$	FBR	Zahn-Wellens test	AOP-B	0
[Parra et al. 2002]	Isoproturon	0.2 mmol l^{-1}	hv/TiO$_2$ immobilized	FBR	BOD$_5$/COD Micotox	AOP-B	++
[Sarria et al. 2003]	AMBI	1 mmol l^{-1}	hv/Fe^{3+}/O$_2$ (air)	FBR	AOS	AOP-B	++

pretreatment followed by activated sludge. Benitez et al. [2001] compared a variety of oxidation schemes: aerobic biological pretreatment followed by either $h\nu/O_3$ or $h\nu/H_2O_2$, and $h\nu/O_3$ or $h\nu/H_2O_2$ pretreatments followed by aerobic biodegradation. Reyes et al. [1998] tested a photo-pretreatment using ZnO immobilized on sand followed by a fungal mineralization by Lentinula edodes. Three different combined systems were developed at EPFL, using photo-Fenton reaction [Parra et al. 2000; Sarria et al. 2001; Rodriguez et al. 2002], $h\nu/Fe^{3+}/O_2$ [Sarria et al. 2003] or $h\nu/$ TiO_2-supported in glass rings [Parra et al. 2002]. In all cases this was followed by a biological step with an immobilized biomass system. All these processes are carried in sequential batch reactors at laboratory scale treating 1 to 3 litres of polluted water.

- **Used APO process**

The three commonly used photoassisted APO are: (i) the photodecomposition of hydrogen peroxide ($h\nu/H_2O_2$) [Adams and Kuzhikannil 2000], (ii) photolysis of ozone ($h\nu/O_3$) [Benitez et al. 2001], (iii) heterogeneous photocatalysis ($h\nu/TiO_2$) [Hess et al. 1998] and $h\nu/ZnO$ [Reyes et al. 1998]. More improving works are now concentrated on fixing the catalyst on a support, in order to work at neutral pH and reuse the catalyst several times [Parra et al. 2002].

Among AOP, the photo-Fenton system ($h\nu/Fe^{3+}/H_2O_2$) has shown to be one of most promising for remediation of contaminated waters [Pulgarin et al. 1999]. The $h\nu/Fe^{3+}/O_2$ system has been explored [Sarria et al. 2003] as an alternative to the photo-Fenton system ($h\nu/Fe^{3+}/$ H_2O_2). The advantage of this method is that the addition of H_2O_2 is avoided.

- **Used biological oxidation system**

The choice of the biological oxidation system is a very important point for the development of a coupled system. Same as the choice of AOP, the appropriated biological system depends on the characteristics of the wastewater to be treated, and specifically on the goal of the treatment.

Immobilized-cell aerobic technology, which involves the colonization of microorganisms onto inorganic supports forming a biofilm, has been used in the APO-Biological coupled systems for the biodegradation of different types of wastewaters [Sarria et al. 2002]. The immobilized-cell bioreactor or Fixed Bed Reactor (FBR) offers several advantages over conventional suspended growth systems, such as the capacity to handle shock loads [Martienssen 2000]. Moreover, it is more

resistant to antimicrobial agents, allows the recycling of the biological catalysers, and functions at very high cell concentration without rheological or mass transfer limitations. FBR operating in continuous mode do not suffer of decrease in the metabolic activity due to product accumulation; the use of substrates is optimal even at low concentration. Due to the localized concentration of nutrients and hydrolytic coenzymes at the support-substrate/interface, cells are used in their stationary phase where the metabolic chains are more active.

Other biological process i.e. the fungal biotreatment has been successfully used to mineralize photo pre-treated solutions of 2,6,6,-trinitroleluene (TNT) [Hess et al. 1998] and 6-chlorovanillin [Reyes et al. 1998].

- **Biodegradability test**

The biodegradability of the AOP pretreated solutions of initial biorecalcitrant wastewaters is followed or assessed by means of: (i) analyzing global parameters, such as Biological Oxygen Demand (BOD_5), Chemical Oxygen Demand (COD), Dissolved Organic Carbon (DOC), and Oxygen uptake (respirometric methods); (ii) estimating the ratio BOD_5/COD or the Average Oxidation State (AOS); (iii) measuring the bacterial growth rate, (iv) assessing toxicity by measuring the EC_{50} value by Microtox test, or (v) using kinetic models, which according to Esplugas and Ollis [Esplugas and Ollis 1993; Scott and Ollis 1996; Ollis 2001], is a crucial way to impulse the practical application and design of these coupled systems.

Ledakowicz et al. [2001] used the Monod model, which describes the effect of nutrient concentration S on the microbial growth (dX/dt) rate.

$$\frac{dX}{dt} = \frac{\mu_{max}S}{K_mS + S}X \tag{1.20}$$

Here, μ_{max} is the maximum specific growth rate and K_1 is the saturation constant for substrate (Monod constant).

Benitez et al. [2001] employed the Contois model, which relates de specific substrate decomposition rate q to the substrate concentration S.

$$q = q_{max}\frac{S}{K_iX + S} \tag{1.21}$$

In Eq. 1.21 q_{max} is the maximum rate of substrate utilisation and K_i is the Contois saturation constant.

- **Overall efficiency**

The indicators of overall effectiveness for combined oxidation studies are presented in Table 1.2 (last column). The following convention where used: (++) for a dramatic increase, (+) for a modest increase and (0) for a negligible increase. Coupled systems generally lead to increase the degradation of target compounds. Among the 16 cases of Table 1.2, dramatic increase (++) noted in 11 cases, modest increase (+) in 2 cases, and a negligible increase (0) in 3 cases. The negative results were attributed to the formation of uncharacterized biorecalcitrant intermediates and complexes [Adams and Kuzhikannil 2000; Parra et al. 2000; Rodriguez et al. 2002].

In general, works summarized in Table 1.2, confirm the convenience of application of sequential photochemical and biological oxidation of biorecalcitrant containing wastewater. Nevertheless, to date do not exist study that explore the possible combination of solar and biological processes at pilot scale.

1.6   Study case: AMBI a biorecalcitrant water pollutant

This thesis work focuses on the treatment of one industrial wastewater containing a biorecalcitrant pollutant, 5-amino-6-methyl-2-benzimidazolone (AMBI), a representative of chemicals having a structure impossible to be degraded by bacteria. Fig. 1.9 shows the 2d and 3d representation of the chemical structure of AMBI.
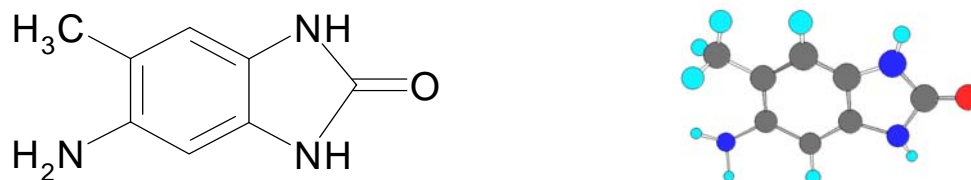
FIGURE 1.9   *2D and 3D chemical structure of the 5-amino-6-methyl-2-benzimidazolone*

Physicochemical characteristics of the wastewater under study are summarized in Table 1.3 The AMBI contaminated wastewater is characterized by a very low biodegradability (expressed by BOD_5/COD ratio). According to the Zahn-Wellens biodegradability test [OECD 1996], only 32% and 51% of DOC were eliminated in 3 and in 9 days, respectively. A supplementary test to assess the biodegradation of AMBI wastewater was carried out in batch mode with a Fixed Bed Reactor. Even under theoretically favourable conditions, as the presence of co-substrates and adapted bacteria, as well as a strict control of pH, temperature and aeration, this test confirms the low biodegradability of AMBI containing wastewater.

TABLE 1.3 *Physicochemical characteristics of the wastewater under study*

DOC (mg C l^{-1})	BOD$_5$ (mg O$_2$ l^{-1})	COD (mg O$_2$ l^{-1})	Cl$^-$ (mg l^{-1})	NH$_4^+$ (mg l^{-1})	PO$_4^{3-}$ (mg l^{-1})	NO^{3-} (mg l^{-1})	pH
4368	136	18105	6265	6.8	0.9	0.0	9.3

1.7 References

Adams C D, Kuzhikannil J J (2000). Effects of UV/H2O2 preoxidation on the aerobic biodegradability of quaternary amine surfactants. *Water Research* **34** (2) 668-672.

Adewuyi Y G (2001). Sonochemistry: Environmental Science and Engineering Applications. *Ind. Eng. Chem. Res.* **40** (22) 4681-4715.

Andreozzi R, Caprio V, Insola A, Marotta R (1999). Advanced oxidation processes (AOP) for water purification and recovery. *Catal.Today* **53** (1) 51-59.

Bahnemann D, Cunningham J, Fox M A, Pelizzetti E, Pichat P, Serpone N (1994). Photocatalytic Treatment of Waters. Aquatic and Surface Photochemistry. Helz G R, Zepp R G, Crosby D G, Ed. Lewis Publishiers, Boca Raton. p 261-316.

Bandara J, Mielczarski J A, Lopez A, Kiwi J (2001). Sensitized degradation of chlorophenols on iron oxides induced by visible light comparison with titanium oxide. *Appl. Appl. Catal. B*. **34** 321-333.

Bandara J, Morrison C, Kiwi J, Pulgarin C, Peringer P (1996). Degradation/Decoloration of Concentrated-Solutions of Orange-II - Kinetics and Quantum Yield for Sunlight- Induced Reactions via Fenton Type Reagents. *J. Photochem. Photobiol. A* **99** (1) 57-66.

Bauer R, Waldner G, Fallmann H, Hager S, Klare M, Krutzler T, Malato S, Maletzky P (1999). The photo-fenton reaction and the TiO2/UV process for waste water treatment - novel developments. *Catal.Today* **53** (1) 131-144.

Beltran F J, Encinar J M, Gonzalez J, F. (1997). Industrial wastewater advanced oxidation. Ozone combined with hydrogen peroxide or UV radiation. *Water Research* **31** (10) 2415-2448.

Beltran-Heredia J, Torregrosa J, Dominguez J R, Peres J A (2001). Comparison of the degradation of p-hydroxybenzoic acid in aqueous solution by several oxidation process. *Chemosphere* **42** 351-359.

Benitez F J, Acero J L, Gonzalez T, Garcia J (2001). Ozonation and Biodegradation Processes in Batch Reactors Treating Black Table Olives Washing Wastewaters. *Ind. Eng. Chem. Res* **40** (14) 3144 - 3151.

Blake D (2001). Bibliography of work on the heterogeneous photocatalytic removal of hazardous compounds from water and air. Update number 4 to October 2001, NREL/TP-510-31319. National Technical Information Service (NTIS), U.S. Department of commerce, Springfield, VA 22161.

Bolton J R, Cater S R (1994). Homogeneous photodegradation of pollutants in contaminated water: an introduction. Aquatic and Surface Photochemistry. Helz G R, Zepp R G, Crosby D G, Ed. Lewis Publishiers, Boca Raton. p 467-490.

Bossmann S H, Oliveros E, Gob S, Siegwart S, Dahlen E, Payawan L, Straub M, Worner M, Braun A (1998). New evidence against hydroxyl radicals as reactive intermediates in the thermal and photochemically enhanced Fenton reactions. *J. Phys. Chem* **102** 5542-5550.

Bozzi A, Yuranova T, Mielczarski E, Mielczarski J, Buffat P A, Lais P, Kiwi J (2002). Superior biodegradability mediated by immobilized Fe-fabrics of waste waters compared to Fenton homogeneous reactions. *Appl. Catal. B.* **42** (3) 289-303.

Brillas E, Casado J (2002). Aniline degradation by Electro-Fenton(R) and peroxi-coagulation processes using a flow reactor for wastewater treatment. *Chemosphere* **47** (3) 241-248.

Buyuksonmez F, Hess T F, Crawford R L, Paszczynski A, Watts R J (1999). Optimization of Simultaneous Chemical and Biological Mineralization of Perchloroethylene. *Appl. Environ. Microbiol.* **65** (6) 2784-2788.

Canton C, Esplugas S, Casado J (2003). Mineralization of phenol in aqueous solution by ozonation using iron or copper salts and light. *Appl. Catal. B.* **43** (2) 139-149.

Chen R Z, Pignatello J J (1997). Role of Quinone Intermediates as Electron Shuttles in Fenton and Photoassisted Fenton Oxidations of Aromatic-Compounds. *Environ. Sci. Technol.* **31** (8) 2399-2406.

Comninellis C, Pulgarin C (1991). Anodic oxidation of phenol for wastewater treatment. *J. Appl. Electrochem.* **21** 703-708.

Comninellis C, Pulgarin C (1993). Electrochemical Oxidation of Phenol for Waste-Water Treatment Using SnO2 Anodes. *J. Appl. Electrochem.* **23** (2) 108-112.

Conseil Fédéral Suisse (1998). Ordonnance sur la protection des eaux usées (OEaux) 814.201 du 28 octobre.

Contreras S, Rodriguez M, Chamarro E, Esplugas S (2001). UV- and UV/Fe(III)-enhanced ozonation of nitrobenzene in aqueous solution. *J. Photochem. and Photobiol. A.* **142** (1) 79-83.

CRC Hanbook of Chemistry and Physics (CRC Handbook). 1985. Edited by Weast R C, Astle M J and Beyer W H. CRC Press, inc. Boca Raton, Florida.

Cuzzola A, Bernini M, Salvadori P (2002). A preliminary study on iron species as heterogeneous catalysts for the degradation of linear alkylbenzene sulphonic acids by H2O2. *Appl. Catal. B.* **36** (3) 231-237.

Dahananjeyan M, Kiwi J, Albers P, Enea O (2001). Photo-Assisted Immobilized Fenton Degradation up to pH 8 of Azo Dye Orange II Mediated by Fe3+/Nafion/Glass Fibers. *Helv. Chim. Acta* **84** 3433-3441.

De Laat J, Gallard H (1999). Catalytic decomposition of hydrogen peroxide by Fe(III) in homogeneous aqueous solution: mechanism and kinetic modeling. *Environ. Sci. Technol.Environ. Sci. Technol.* **33** 2726-2732.

Dhananjeyan M R, Mielczarski E, Thampi K R, Buffat P, Bensimon M, Kulik A, Mielczarski J, Kiwi J (2001). Photodynamics and Surface Characterization of TiO2 and Fe2O3 Photocatalysts Immobilized on Modified Polyethylene Films. *J. Phys. Chem. B.* **105** (48) 12046-12055.

Diller R, Fornefett I, Siebers U, Bahnemann D W (1996). Photocatalytic degradation of trinitrotoluene and trinitrobenzene: influence of hydrogen peroxide. *J. Photochem. and Photobio. A.* **96** 231-236.

Do J-S, Chen C-P (1994). Kinetics of in situ degradation of formaldehyde with electrogenerated hydrogen peroxide. *Industrial & Engineering Chemistry Research* **33** (2) 387-394.

EEC (1992). *List of Council Directives 76/4647, European Economic Community, Brussels, Belgium.*

Enea O, Pulgarin C (2000). Strategie de caracterisation et de traitement des eaux residuaires industrielles: quel role pour la catalyse, l'electrocatalyse ou la photocatalyse solaire? *Entropie* (228) 16-21.

Esplugas S, Gimenez J, Contreras S, Pascual E, Rodriguez M (2002). Comparison of different advanced oxidation processes for phenol degradation. *Water Research* **36** (4) 1034-1042.

Esplugas S, Ollis D F, Eds. (1993). Process integration development: Reactor kinetic models for sequential and biological oxidation for water treatment. Chemical Oxidation Technologies for the Nineties IV. Lancaster, Technomic Publishing Company.

Fallmann H, Krutzler T, Bauer R, Malato S, Blanco J (1999). Applicability of the Photo-Fenton method for treating water containing pesticides. *Catal.Today* **54** (2-3) 309-319.

Faust B C, Hoigne J (1990). Photolysis of Fe(III) - hydroxy complexes as sources of OH radicals in clouds, fog and rain. *Atmos. Environ.* **24A** (1) 79-89.

Fenton H J H (1894). Oxidation of tartaric acid in presence of iron. *J. Chem. Soc. Trans.* **65** 899-910.

Fernandez J, Bandara J, Lopez A, Buffat P, Kiwi J (1999). Photoassisted Fenton degradation of non biodegradable azo dye (orange II) in Fe-free solutions mediated by cation transfer membranes. *Langmuir* **15** 185-192.

Francony A, Petrier C (1996). Sonochemical degradation of carbon tetrachloride in aqueous solution at two frequencies: 20 kHz and 500 kHz. *Ultrasonics Sonochemistry* **3** (2) S77-S82.

Fujishima A, Honda K (1972). Electrochemical photolysis of water at a semiconductor electrode. *Nature* **238** (7) 37-38.

Gallard H, De Laat J (2000). Kinetic modelling of Fe(III)/H2O2 oxidation reactions in dilute aqueous solution using atrazine as a model organic compound. *Water Research* **34** (12) 3107-3116.

Gernjak W, Krutzler T, Glaser A, Malato S, Caceres J, Bauer R, Fernandez-Alba A R (2003). Photo-Fenton treatment of water containing natural phenolic pollutants. *Chemosphere* **50** (1) 71-78.

Ghaly M Y, Hartel G, Mayer R, Haseneder R (2001). Photochemical oxidation of p-chlrophenol by UV/H2O2 and photo-Fenton process. A comparative study. *Waste Management* **21** 41-47.

Ghauch A (2001). Degradation of benomyl, picloram, and dicamba in a conical apparatus by zero-valent iron powder. *Chemosphere* **43** (8) 1109-1117.

Haber W G, Waiser J (1934). The catalytic decomposition of hydrogen peroxide by iron salts. *J. Proc. Roy. Soc. London* **A147** 332.

Herrera F, Lopez A, Mascolo G, Albers P, Kiwi J (2001). Catalytic decomposition of the reactive dye UNIBLUE a on hematite. modeling of the reactive surface. *Water Research* **35** (3) 750-760.

Hess T F, Lewis T A, Crawford R L, Katamneni S, Wells J H, Watts R J (1998). Combined photocatalytic and fungal treatment for the destruction of 2,4,6-trinitrotoluene (TNT). *Water Research* **32** (5) 1481-1491.

Hoffmann M, Martin S, Choi W, Bahnemann D (1995). Environmental Applications of semiconductor catalysis. *Chem. Rev.* **95** 69-96.

Hoigne J (1997). Inter-calibration of OH radical sources and water quality parameters. *Water Sci. and Technol.* **35** (4) 1-8.

Horan N J (1990). *Biological Wastewater Treatment Systems. Theory and Operation*. Chichester, England, Jhon Wiley & Sons Ltd.

Kim S-M, Geissen S-U, Vogelpohl A (1997). Landfill leachate treatment by a photoassisted fenton reaction. *Water Sci. and Technol.* **35** (4) 239-248.

Kiwi J, Lopez A, Nadtochenko V (2000). Mechanism and kinetics of the OH-radical intervention during fenton oxidation in the presence of significant amount of radical scavenger (Cl-). *Environ. Sci. Technol.* **34** (11) 2162-2168.

Kiwi J, Pulgarin C, Peringer P (1994). Effect of Fenton and Photo-Fenton Reactions on the Degradation and Biodegradability of 2-Nitrophenols and 4- Nitrophenols in Water-Treatment. *Appl. Catal. B.* **3** (4) 335-350.

Koubeck E (1975). Photochemical induced oxidation of refractory organics with hydrogen peroxide. *Ind. Eng. Chem. Process Des. Dev.* **14** 348.

Krutzler T, Bauer R (1999). Optimization of a Photo-Fenton Prototype Reactor. *Chemosphere* **38** (11) 2517-2532.

Ku Y, Wang W, Shen Y-S (2000). Reaction behaviours of decomposition of monocrotophos in aqueous solution by UV and UV/O3 processes. *J. of Hazardous Materials* **B72** 25-37.

Ledakowicz S, Solecka M, Zylla R (2001). Biodegradation, decolourisation and detoxification of textile wastewater enhanced by advanced oxidation processes. *J. of Biotechnology* **89** (2-3) 175-184.

Legrini O, Oliveros E, Braun A M (1993). Photochemical Processes for Water-Treatment. *Chem. Rev.* **93** (2) 671-698.

Luck F (1999). Wet air oxidation: past, present and future. *Catal.Today* **53** (1) 81-91.

Mantzavinos D, Lauer E, Hellenbrand R, Livingston A G, Metcalfe I S (1997). Wet Oxidation as a Pretreatment Method for Wastewaters Contaminated by Bioresistant Organics. *Water Sci. Sci. Technol.* **36** (2-3) 109-116.

Martienssen M (2000). Simultaneous catalytic detoxification and biodegradation of organic peroxides during the biofilm process. *Water Research* **34** (16) 3917-3926.

OECD (1996). *Guidelines for testing of Chemicals, test 302B.*

Ollis D F (2001). On the need for engineering models of integrated chemical and biological oxidation of wastewaters. *Water Sci. Technol.* **44** (5) 117-123.

Ollis D F, Ekabi H A (1993). *Photocatalytic purification and treatment of water and air.* Amsterdam.

Ollis D F, Pelizzetti E, Serpone N (1991). Destruction of water contaminants. *Environ. Sci. Technol.* **25** (9) 1523-1529.

Oturan M A (2000). Ecologically effective water treatment technique using electrochemically generated hydroxyl radicals for in situ destruction of organic pollutants: Application to herbicide 2,4-D. *J. of Applied Electrochemistry* **30** (4) 475-482.

Parra S, Malato S, Pulgarin C (2002). New integrated photocatalytic-biological flow system using supported TiO2 and fixed bacteria for the mineralization of isoproturon. *Appl. Catal. B.* **36** (2) 131-144.

Parra S, Sarria V, Malato S, Peringer P, Pulgarin C (2000). Photochemical versus coupled photochemical-biological flow system for the treatment of two biorecalcitrant herbicides: metobromuron and isoproturon. *Appl. Catal. B.* **27** (3) 153-168.

Pichat P, Guillard C, Amalric L, Renard A C, Plaidy O (1995). Assessment of the Importance of the Role of H2O2 and O-2(O-) in the Photocatalytic Degradation of 1,2- Dimethoxybenzene. *Solar Energ Mater Solar Cells* **38** (1-4) 391-399.

Ponce de Leon C, Pletcher D (1995). Removal of formaldehyde from aqueous solutions via oxygen reduction using a reticulated vitreous carbon cathode cell. *J. of Applied Electrochemistry* **25** (4) 307-314.

Prousek J (1995). Fenton reaction after a century. *Chem. Lisy.* **89** 11-21.

Pulgarin C, Invernizzi M, Parra S, Sarria V, Polania R, Peringer P (1999). Strategy for the coupling of photochemical and biological flow reactors useful in mineralization of biorecalcitrant industrial pollutants. *Catal.Today* **54** (2-3) 341-352.

Pulgarin C, Kiwi J (1995). Iron Oxide-Mediated Degradation, Photodegradation, and Biodegradation of Aminophenols. *Langmuir* **11** (2) 519-526.

Pulgarin C, Kiwi J (1996). Overview on Photocatalytic and Electrocatalytic Pretreatment of Industrial Non-Biodegradable Pollutants and Pesticides. *Chimia* **50** (3) 50-55.

Pulgarin C, Peringer P, Albers P, Kiwi J (1995). Effect of Fe-ZSM-5 Zeolite on the Photochemical and Biochemical Degradation of 4-Nitrophenol. *J. Mol. Catal. A.* **95** (1) 61-74.

Pulgarin C, Schwitzguebel J P, Peringer P, Pajonk G M, Bandara J, Kiwi J (1995). Abiotic Degradation of Atrazine on Zero-Valent Iron Activated by Visible-Light. *Abstr Pap Amer Chem Soc* **209** (APR) 232-ENVR.

Reisz E, Schmidt W, Schuchmann H P, Sonntag C (2003). Photolysis of Ozone in Aqueous Solutions in the Presence of Tertiary Butanol. *Environ. Sci. Technol.* **In press**.

Reyes J, Dezotti M, Esposito E, Villasenor J, Mansilla H, Durnan N (1998). Biomass photochemistry-XXII: Combined photochemical and biological process for treatment of Kraft El effluent. *Appl. Catal. B.* **15** (3-4) 211-219.

Robertson P (1996). Semiconductor photocatalysis: an environmentally acceptable alternative production technique and effluent treatment process. *J. Cleaner Prod.* **4** (3-4) 203-212.

Rodriguez M, Abderrazik N, Contreras S, Chamarro E, Gimenez J, Esplugas S (2002). Iron(III) photoxidation of organic compounds in aqueous solutions. *Appl. Catal. B.* **37** (2) 131-137.

Rodriguez M, Kirchner A, Contreras S, Chamarro E, Esplugas S (2000). Influence of H2O2 and Fe(III) in the photodegradation of nitrobenzene. *J. Photochem. Photobiol. A* **133** (1-2) 123-127.

Rodriguez M, Sarria V, Esplugas S, Pulgarin C (2002). Photo-Fenton treatment of a biorecalcitrant wastewater generated in textile activities: biodegradability of the photo-treated solution. *J. Photochem. and Photobio. A.* **151** 129-135.

Rodriguez M, Timokhin V, Michl F, Contreras S, Gimenez J, Esplugas S (2002). The influence of different irradiation sources on the treatment of nitrobenzene. *Catal. Today* **76** (2-4) 291-300.

Rupert G, Bauer R, Heisler G (1993). The photo-Fenton reaction-an effective photochemical wastewater treatment process. *J. Photochem. and Photobio. A.* **73** 75-78.

Safarzadeh-Amiri A (2001). O3/H2O2 treatment of methyl-tert-butyl ether (MTBE) in contaminated waters. *Water Research* **35** (15) 3706-3714.

Safarzadehamiri A, Bolton J R, Cater S R (1997). Ferrioxalate-Mediated Photodegradation of Organic Pollutants in Contaminated Water. *Water Res.* **31** (4) 787-798.

Sagawe G, Alexander L, Lübber M, Bahnemann D (2001). The insulated solar Fenton hybrid Process: fundamental investigations. *Helv. Chim. Acta* **84** 3742-3759.

Sarria V, Deront M, Peringer P, Pulgarin C (2003). Degradation of a biorecalcitrant dye precursor present in industrial wastewaters by a new integrated iron(III) photoassisted-biological treatment. *Appl. Catal. B.* **40** (3) 231-246.

Sarria V, Parra S, Adler N, Péringer P, Pulgarin C (2002). Recent developments in the coupling of photoassisted and aerobic biological processes for the treatment of biorecalcitrant compounds. *Catal. Today* **76** (2-4) 301-315.

Sarria V, Parra S, Invernizzi M, Péringer P, Pulgarin C (2001). Photochemical-biological treatment of a real industrial biorecalcitrant wastewater containing 5-amino-6-methyl-2-benzimidazolone. *Water Sci. Technol.* **44** (5) 93-101.

Scott J P, Ollis D F (1995). Integration of chemical and biological oxidation processes for water treatment: review and recommendations. *Environ. Progr.* **14** (2) 88-103.

Scott J P, Ollis D F (1996). Engineering Models of Combined Chemical and Biological Processes. *J. Environ. Eng.* **122** (12) 1110-1114.

Scott J P, Ollis D F (1997). Integration of Chemical and Biological Oxidation Processes for Water Treatment: II. Recent illustrations and experiences. *J. Adv. Oxid. Technol.* **2** (3) 374-381.

Scott M A, Hickey W J, Harris R F (1995). Degradation of atrazine by fenton's reagent: condition optimization and product quantification. *Environ. Sci. Technol.* **29** 2083-2089.

Sulzberger B, Canonica S, Egli T, Giger W, Klausen J, Gunter U (1997). Chimia **51** (12) 900-907.

Sun Y F, Pignatello J J (1993). Photochemical-Reactions Involved in the Total Mineralization of 2,4-D by Fe-3+/H2O2/UV. *Environ. Sci. Technol.* **27** (2) 304-310.

Sychev A Y, Isak V G (1995). Iron compounds and the mechanisms of the homogeneous catalysis of the activation of O2 and H2O2 and of the activation of organic substrates. *Russian Chemical Reviews* **64** (12) 1105-1129.

Tang W Z, Huang C P (1996). 2,4-dichlorophenol oxidation kinetics by Fenton's reagent. *Environ. Technol.* **17** 1371-1378.

Theron P, Pichat P, Petrier C, Guillard C (2001). Water treatment by TiO2 photocatalysis and/or ultrasound: Degradations of phenyltrifluoromethylketone, a trifluoroacetic-acid-forming pollutant, and octan-1-ol, a very hydrophobic pollutant. *Water Sci. and Technol.* **44** (5) 263-270.

UNESCO (2003). Water for people, water for live - UN World Water Development Report. Paris, UNESCO.

US.EPA (1998). Handbook on Advanced Photochemical Oxidation Processes. Cincinnati, Ohio 45268, U.S. Environmental Protection Agency.

Walling C (1975). Fenton's reagent revisted. *Acc. Chem. Res.* **8** 125-131.

Yeber M C, Freer J, Martinez M, Mansilla H D (2000). Bacterial response to photocatalytic degradation of 6-chlorovanillin. *Chemosphere* **41** (8) 1257-1261.

Zepp R G, Faust B, Hoigne J (1992). Hydroxyl radical formation in aqueous reactions (pH 3-8) of iron(II) with hydrogen peroxide. The photo-Fenton reaction. *Environ. Sci. Technol.* **26** 313-319.

E**XPLORATORY STUDY OF** SONOCHEMICAL, ELECTROCHEMICAL AND PHOTOCHEMICAL OXIDATION PROCESSES

Chapter 1 presented an overview of AOP and coupled AOP-biological systems for water treatment; Among different AOP, chapter 2 focuses on sonochemical, electrochemical and photochemical oxidation of AMBI. This chapter is organised around four major topics: (i) the biodegradability enhancement of AMBI wastewater by use of ultrasounds, (ii) the electrochemical oxidation, on Pt anodes, of industrial wastewaters containing AMBI, (iii) the study of some heterogeneous and homogeneous photocatalytic AOP and (iv) the economical comparison regarding the energy cost of the tested AOP. Among different process evaluated, we decide to go further into the study of the iron photo-assisted processes, since the homogenous character of these systems provides, with reasonable limitations, good engineering conditions for coupling them with a complementary biological treatment.

2.1   Introduction

Dye pollutants from the textile industry are an important source of environmental contamination. Indeed, these effluents are often toxic, mostly non-biodegradable and some times also resistant to destruction by physico-chemical treatment methods. [Aleboyeh et al. 2003].

5-amino-6-methyl-2-benzimidazolone (AMBI), is an important precursor in the industrial production of dyes. According to different biodegradability tests, it was characterized as a biorecalcitrant substance (see section "1.6").

As mentioned in chapter 1, AOP have been proposed in recent years as an attractive alternative for the treatment of this kind of non-biodegradable wastewaters. AOP are usually classified of different ways according to the reaction phase (homogeneous or heterogeneous) or to

the •OH generation methods (chemical, electrochemical, sonochemical, or photochemical). The present chapter presents an exploratory study on sonochemical, electrochemical and photochemical oxidation processes to degrade AMBI. This chapter is organised around four major topics: (i) the biodegradability enhancement of AMBI wastewater by use of ultrasounds, (ii) the electrochemical oxidation, on Pt anodes, of industrial wastewaters containing AMBI, (iii) the study of some heterogeneous and homogeneous photocatalytic AOP and (iv) the economical comparison regarding the energy cost of the tested AOP.

2.2   Sonochemical degradation of AMBI

As shown in section "1.2.1", sonochemical oxidation methods involve the use of ultrasonic waves (20 kHz to 10 MHz) to produce an oxidative environment via cavitation that yields localized microbubbles [Petrier and Francony 1997]. The collapse of these bubbles results in the generation of highly reactive species including hydroxyl, hydrogen and hydroperoxyl radicals, and hydrogen peroxide.

$$H_2O \left[\longrightarrow \ggg \right] H^{\bullet} + {}^{\bullet}OH$$

The exploratory study described herein was aimed to investigate the effectiveness of ultrasound for the degradation of AMBI.

2.2.1   Experimental

2.2.1.1   Reagents and materials

5-amino-6-methyl-2-benzimidazolone –AMBI- ($C_8H_9N_3O$) as well as samples of real industrial wastewater were received from Rohner, Basel-Switzerland. The chemicals for HPLC analysis were obtained from Fluka. Milli-Q water was used throughout for the preparation of aqueous solutions and as a component of the mobile phase, water-acetonitrile (HPLC grade) in HPLC analysis.

2.2.1.2 Ultrasonic reactor

Ultrasonic irradiations were performed in a cylindrical water-jacketed glass cell equipped with a Teflon holder (Fig. 2.1). The ultrasonic transducer (600 kHz) was made from a piezo-electric disc (diameter 4 cm) fixed on a titanium plate with the piezo-electric element connected to a high-frecuency power. The experiments were carried out with 300 ml of AMBI real wastewater described in section "2.1".
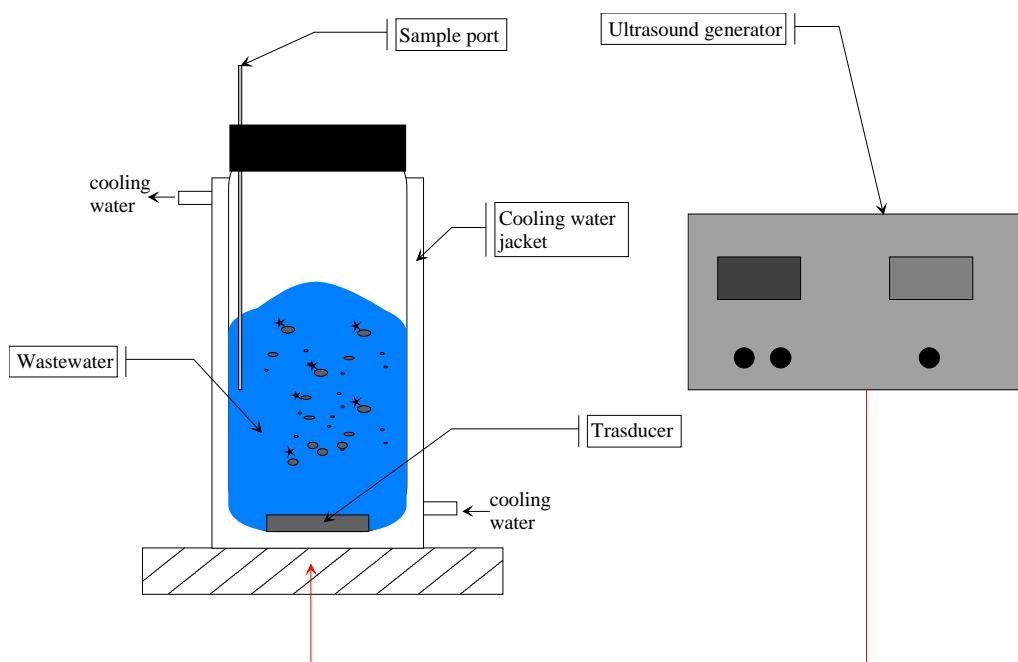
FIGURE 2.1   *Ultrasonic reactor*

2.2.1.3 Chemical and biological analysis

Dissolved Organic Carbon (DOC): A Shimadzu, model 5050A, TOC analyzer is used for DOC measurements. The instrument is equipped with an ASI automatic sample injector and it uses potassium phthalate solution as calibration standard. Acidification and stripping before analysis were sometimes necessary to keep the solutions free of atmospheric CO_2.

High Performance Liquid Chromatography (HPLC): The equipment used is a Varian 9065 unit provided with a Varian 9012 solvent delivery system, an automatic injector 9100, and a Varian

Pro Star variable (200-400 nm) diode array detector 9065 Polychrom. All the modules are piloted with a PC computer with the Varian Star 5.3 software for liquid chromatography. A reverse phase Spherisorb silica column ODS-2 and acetonitrile/water as mobile phase are used to run the chromatography in gradient mode. The signal for AMBI is detected at 302 nm.

Biological Oxygen Demand (BOD) was measured by means of a Hg free WTW 2000 Oxytop unit thermostated at 20 0C.

2.2.2 Results

It has been shown that energy intensity is an important factor in the sonochemical degradation process. In this work, experiments at two different energy intensities 30 and 90 W were performed and results are presented in Fig. 2.2.

As shown in Fig. 2.2, increasing energy input increases the degradation rate of AMBI. When 30W was used only 50% of initial AMBI concentration could be degraded in 3000 minutes.
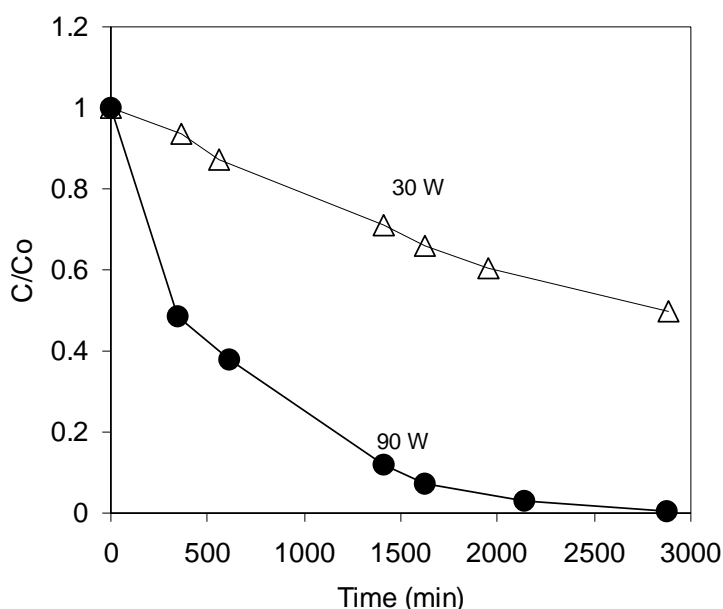
FIGURE 2.2   *Effect of ultrasonic input energy on the sonochemical degradation of AMBI wastewater. [AMBI]o = 5.0 mmol l^{-1}.*

The ultrasonic degradation of AMBI at 90 W was followed by means of HPLC and the chromatograms obtained as well as the UV/Vis spectra of the different picks are presented in Fig. 2.3. In this figure it is possible to observe the pick of AMBI, with a retention time of 3.92 min and the presence of four main intermediates of degradation. The last chromatogram taken at 3000 min, confirms the total degradation of AMBI but also the formation of remaining intermediates. The UV/Vis shows that some of these intermediates do not display important absorption in UV region, indicating that they probably are aliphatic compounds.

Ratios of BOD_5/COD obtained at the beginning and the end of the treatment were of 0.008 and 0.2, respectively. These values indicate that an improvement of the biodegradability of AMBI wastewater was reached at the end of the treatment.
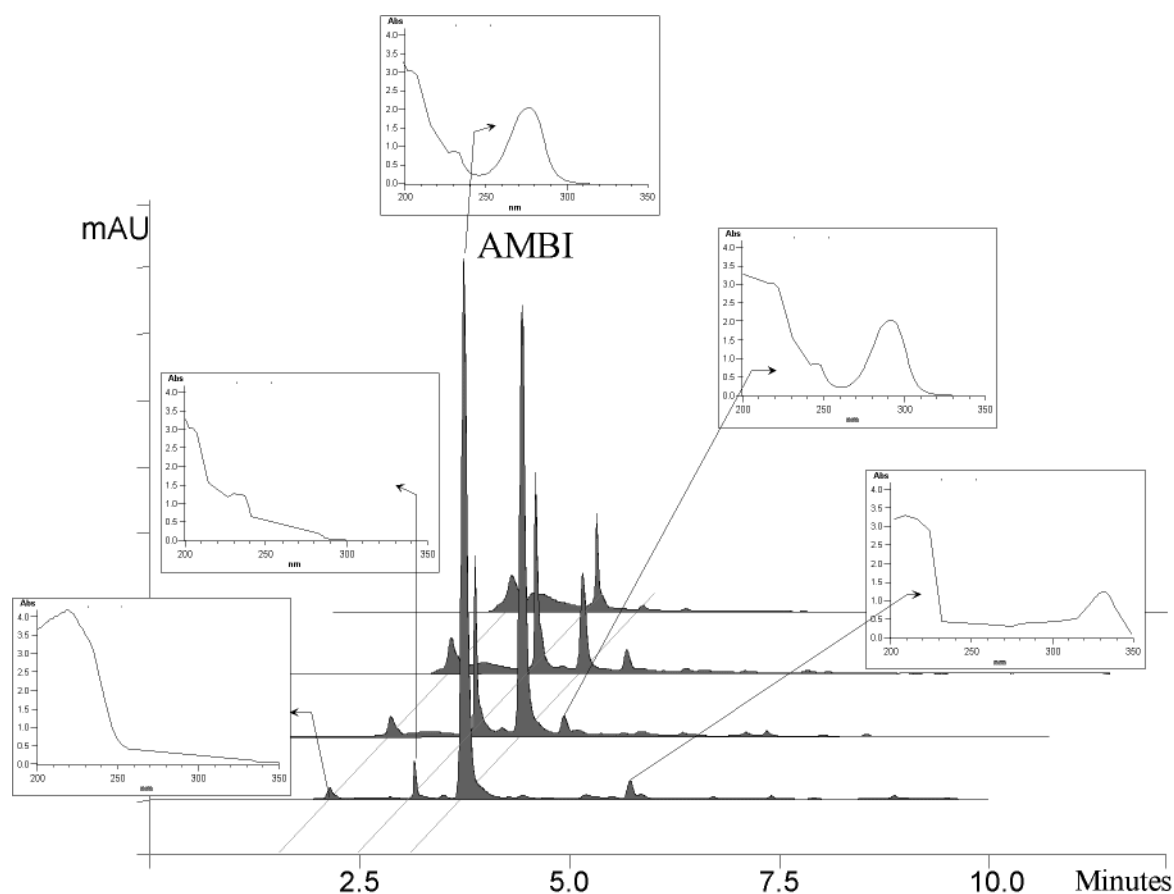
FIGURE 2.3   *Sonolytical degradation of AMBI wastewater at 90 W followed by HPLC analysis and UV/Vis spectra of the different picks.*

2.3 Electrochemical degradation of AMBI: toward an electrochemical-biological coupling

Electrochemical oxidation is a promising, versatile alternative method for pollutant degradation that has the potential to replace or complete already existing processes [Brillas et al. 1998]. Electrochemistry makes the treatment of liquids, gases and solids possible; it is amenable to automation and compatible with the environment because the main reagent, the electron, is a clean one [Jüttner et al. 2000]. Many studies on the anodic oxidation of organic pollutants have been carried out [Comninellis and Pulgarin 1991; Brillas et al. 1998]. Complete mineralization has only been obtained at anodes such as SnO_2 and PbO_2 materials that exhibit a high oxygen overvoltage [Comninellis and Pulgarin 1991, 1993]. However, commercial application of these electrodes is limited by their low stability and availability. In addition, they undergo corrosion processes that, in several cases, result in the release of toxic metal ions. Other anode materials, such as Ti/IrO_2, Ti/RuO_2, and Pt can achieve the partial degradation of organic pollutants to highly oxidized products after a series of electrochemical and chemical steps. Because these products are often biodegradable, in principle, this "electrochemical conversion" can be followed by a suitable biological treatment. Thus, the coupling of electrochemical and biological process might prove a judicious choice for the remediation of industrial wastewaters that contain recalcitrant compounds.

In this section, the electrochemical treatment of a real industrial wastewater containing AMBI was explored. The influence of several experimental variables such as temperature, pH, current density and wastewater concentration on the performance of the electrochemical reactor was analysed. The biocompatibility (toxicity and biodegradability) of the electrochemically treated solutions was evaluated. A test in which effluents of the electrochemical reactor were collected and further treated in a biological Fixed Bed Reactor (FBR) resulted in complete mineralization.

2.3.1 Experimental

2.3.1.1 Electrolytic cell

All electrochemical experiments were carried out in a single compartment electrolytic cell with a total volume of 150 ml Fig. 2.4. The anode was a 40 cm^2 Pt electrode and the cathode a zirconium spiral electrode. The cell current and was kept constant at 2 A. The initial pH of the electrolysis medium was adjusted by addition of aqueous NaOH or H$_2$SO$_4$. Periodic samples were taken from the electrolytic cell for chemical analysis.
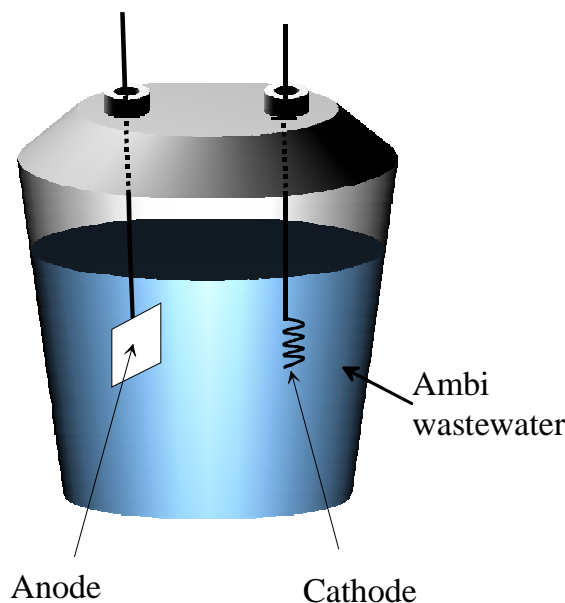
FIGURE 2.4   *Electrolytic cell*

2.3.1.2 Chemical analysis

DOC and HPLC analyses were performed using the same methodology described in section "2.2.1.3".

Chemical Oxygen Demand (COD): This analysis is carried out via a Hach-2000 spectrophotometer using dichromate solution as the oxidant in strong acid medium. Test solution (2 ml) is pipetted into the dichromate reagent and digested at 150°C for two hours. Colour is

developed during the oxidation and measured against a water blank using a Hach DR/890 colorimeter. The optical density for the change of colour of the dichromate solution was determined at λ = 430 nm.

Chloride analysis was performed with a Chlor-o-counter Mark II provided by Fhlor Instruments.

2.3.1.3 Biological analysis

The BOD measures the oxygen required for the biochemical degradation of organic material. This analysis is made by means of a Hg free WTW 2000 Oxytop unit thermostated at 20°C. The pH of the samples are adjusted between 6.8 and 7.5 followed by addition (20% v/v) of decanted sludge (inoculum) from the biological plant of Vidy, Lausanne, Switzerland and of nutrients substances (solutions A, B, and C) and trace elements necessary for the bacterial activity.

- Solution A: $FeCl_3.6H_2O$ (0.5 g), HCl 1N (1 ml) in 100 ml of distilled water.

- Solution B: $MgSO_4.7H_2O$ (2.0 g), $CaCl_2$ (2.5 g), NH_4Cl (quantity depending of carbon concentration to degrade to have always a ratio C/N of 20) in 500 ml of distilled water.

- Solution C: Na_2HPO_4 (6.8 g), KH_2PO_4 (2.8 g) in 1000 ml of distilled water.

- Solution A+B: 50 ml of solution A, 500 ml solution B in 1000 ml of distilled water.

- Solution trace elements: $FeSO_4.7H_2O$ (200 mg), $ZnSO_4.7H_2O$ (10 mg), $MnCl_2.4H_2O$ (3 mg), H_3BO_3 (30 mg), $CoCl_2.6H_2O$ (20 mg), $CuCl_2.2H_2O$ (1 mg), $NiCl_2.6H_2O$ (2 mg), $Na_2MoO_4.2H_2O$ (3 mg), in 1000 ml of distilled water.

For each BOD determination, 20 ml l^{-1} of solution A+B, 50 ml l^{-1} of C and 2 ml l^{-1} of trace elements are added for 400 mg C of the test solution. The BOD values are calculated according to Eq. 2.1.

$$BOD = \frac{BOD_{sample} - 0.01(\% \, inoculum \times BOD_{inoculum})}{0.01 \times (100 - \% \, inoculum)} \qquad \textbf{(2.1)}$$

Zahn-Wellens biodegradability test: The Zahn-Wellens test was adapted in 1981 as OECD Guideline 302 B for determining inherent biodegradability [OECD 1996]. A mixture containing the test substance, mineral nutrients (the same as for BOD determination), and a relatively large

amount of activated sludge (0.2 - 1 g l^{-1})in aqueous medium is agitated and aerated at 20-25$^{\text{o}}$C in the dark or in diffuse light for up to 28 days. Blank controls, containing activated sludge and mineral nutrients but no test substance, are run in parallel. The biodegradation process is monitored by determination of DOC and by HPLC analysis of the test substance. The Zahn-Wellens Biodegradability test is applied with bacterial concentration of 1 g l^{-1}. The biomass from the biological activated sludge plant of Vidy, Lausanne, Switzerland, is previously aerated for 24 hours and subsequently centrifuged.

Microtox® rapid toxicity testing system: During the photochemical pretreatment, the toxicity is assessed using the Microtox® test system. The basic technology of this system is based upon the use of luminescent bacteria, specifically the strain *Vibrio fischeri* NRRL B-11177, to measure toxicity from environmental samples. When properly grown, luminescent bacteria produce light as a by-product of their cellular respiration. Cell respiration is fundamental to cellular metabolism and all associated life processes. Bacterial bioluminescence is tied directly to cell respiration, and any inhibition of cellular activity (toxicity) results in a decreased rate of respiration and a corresponding decrease in the rate of luminescence.

The tests are carried out using a Microtox Model 500 Analyzer, which is a laboratory-based temperature controlled photometer (15-27$^{\text{o}}$C) that maintains the luminescent bacteria reagent and test samples at the appropriate test temperature. This self-calibrating instrument measures the light production from the luminescent bacteria reagent. The sample toxicity is determined by measuring the effective concentration at which 50% of the light is lost due to compound toxicity (EC$_{50}$).

2.3.2   Results

2.3.2.1   Effect of the initial AMBI concentration in anodic degradation

Original wastewater samples contained ca. 25 mmol l^{-1} AMBI. For the electrochemical degradation experiments, however, the original samples were diluted in order to evaluate the effect of the initial concentration of AMBI on the yield of the electrochemical process. Fig. 2.5 shows the amount of AMBI removed in the first 15 min (3.3 Ah l^{-1} or 1.8×10^3 Coulombs) of electrochemical oxidation as a function of initial AMBI concentration. The cell ran at a constant current density (50

mA cm^{-2}), at 70 $^{\circ}$C and pH 6.3. As the initial AMBI concentration increases, AMBI removal first increases and then decreases with best removal attained at ~ 5.0 mmol l^{-1} AMBI. In the first minutes of electrolysis, at high initial concentrations, a yellowish deposit appears on the Pt anode surface and then disappears.

These results indicate that, at low initial AMBI concentrations, the electrochemical process is controlled by diffusion. However, as the initial AMBI concentration increases, transitory, partial electrode passivation may occur. However, this phenomenon does not result in overall passivation of the electrode because the same anode can be used in several runs with no significant loss of current efficiency. The nature of the anode deposit has to be further investigated. Hence, 5.0 mmol l^{-1} AMBI solutions were used in further experiments.
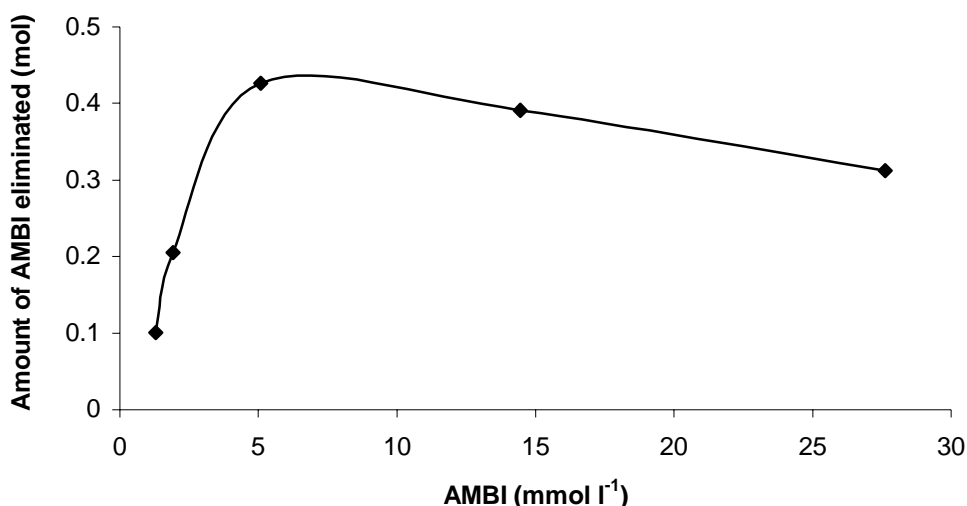
FIGURE 2.5 *Effect of initial AMBI concentration on the amount eliminated within the first 15 min of electrolysis on Pt electrodes, at 25 mA cm^{-2} and 70 $^{\circ}$C.*

2.3.2.2   Current density and temperature

Several AMBI degradation curves, bulk AMBI concentration vs. electrical charge (not shown), were obtained at constant current densities in the range between 25 and 75 mA cm^{-2}. Upon electrolysis, pH naturally decreases from ca. 6.3 to 4 in the first 15 min of electrolysis. All

degradation curves were practically superimposable on one another. Thus, in the selected density range, degradation rates are limited by the mass transfer of AMBI to the anode. After passing 45 min (10 Ah l^{-1} or 5.4×10^3 Coulombs), practically 100% AMBI degradation was attained.

A new set of degradation experiments was carried out at constant temperatures in the range between 30 and 70 $^\circ$C at 50 mA cm^{-2}. In all cases, foam is formed as the reaction proceeds. However, this side effect considerably decreases as the reaction temperature rises. Other than that, for electrolysis of AMBI on Pt anodes, degradation curves (AMBI concentration vs. electrical charge) are practically independent of temperature, indicating that AMBI itself is not thermolabile. For analytical purposes, we decided to avoid foam formation and subsequent experiments were done at 70 $^\circ$C. However, in order to keep the costs of the process low and favourable conditions for the subsequent biological treatment, working at room temperature would be desirable.

2.3.2.3 Effect of pH

The electrolytic degradation of five-fold diluted wastewater at three different pH media is presented in Fig. 2.6. Error bars represent standard deviations of the data. The initial pH values were 3, 6.3 (natural initial pH), and 11. In the effluent, AMBI degrades much faster in solutions at pH 6.3 than at pH 3 or 11. After 15 min of electrolysis (3.3 Ah l^{-1}), at pH 6.3, the concentration of AMBI decayed by ca. 75%. At the same reaction time, at pH 3 or 11, only 35% was removed.

As shown in Table 1.3 (Ch. 1) real wastewater containing AMBI has an important concentration of Cl^{-1}, which can play an important role in the electrochemical degradation of AMBI. Consequently, the evolution of concentration of ions chloride was followed during the degradation at pH 6.3 (see inset in Fig. 2.6).

The degradation of AMBI in this five-fold diluted wastewater is accompanied by a decrease of Cl^- (as shown in the inset) and pH (from 11 to 8 and from 6.3 to 4).

AMBI is a basic species, which can be protonated to AMBIH$^+$ [Sarria et al. 2003]. At room temperature, the pKa value for the deprotonation reaction is 4.7 (see more details in section "3.3.1.1"). Therefore, in the experiments at pH 6.3 and 11, the most probable initial oxidation sites,

the amino or the imidazolone groups, are unprotonated and one would expect AMBI oxidation rates to be pH independent.
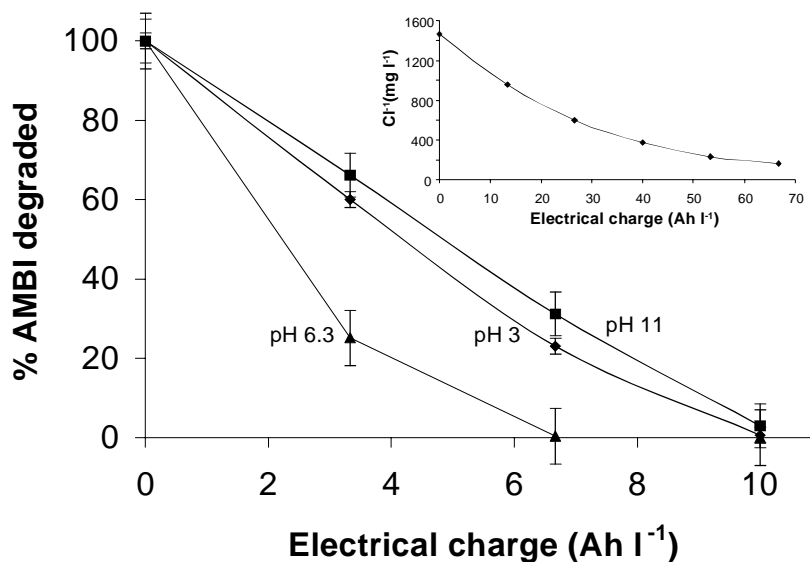
FIGURE 2.6   *Electrolysis of five-fold diluted industrial wastewater at different pH values. 25 mA cm^{-2} and 70 ^{o}C. The inset shows the variation of Cl^{-} concentration upon electrolysis at the natural initial pH (6.3). [AMBI] = 5.0 mmol l^{-1}.*

Fig. 2.7 shows results from a control experiment in which synthetic solutions containing 5.0 mmol l^{-1} AMBI + 50 g l^{-1} sodium sulphate underwent electrolysis at pH 3, 7 and 11 (continuous lines with black diamonds, triangles, and squares, respectively). This experiment shows that pH itself does not play an important role in the degradation of AMBI. Observe, however, that adding NaCl to the synthetic solution (1.46 g l^{-1} Cl^{-}), at pH 7 results in a better degradation of AMBI (dashed lines with white triangles).

The lesson from Fig. 2.7 is that the results displayed in Fig. 2.6 can be explained by considering the role of chloride ions (which are already present in the wastewater).
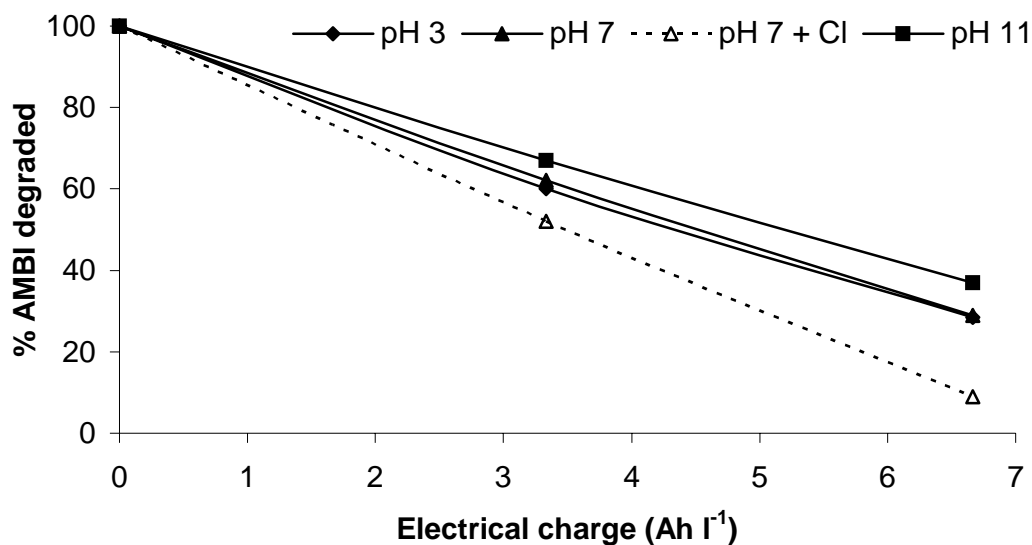
FIGURE 2.7   *Electrochemical degradation of synthetic wastewater at different pH values. 25 mA cm^{-2} and 70 ^{o}C.*

Electrochemical oxidation of Cl$^-$ occurs readily on Pt surfaces to produce chlorine, according to Eq. 2.2.

$$2Cl^- \rightarrow Cl_2 + 2e^- \tag{2.2}$$

Further oxidation and hydrolysis of chlorine yields hypochlorous acid (HOCl) or the hypochloride ion (OCl$^-$) depending on the solution pH. Thus, at sufficiently high applied potentials, Cl$_2$ is the main chlorine species at pH < 3, HOCl in the region 3 < pH < 7, and OCl$^-$ at pH >7. As among these species, HOCl is the strongest oxidant, the high AMBI oxidation rates attained at pH = 6.3 can be attributed to the predominant formation of HOCl [Rajeshwar and Ibañez 1997]. The observed pH decay is probably a result of parallel anodic oxidation of water through Eq. 2.3:

$$2H_2O \rightarrow 4H^+ + O_2 + 4e^- \tag{2.3}$$

2.3.2.4 Variation of oxidation state indicators upon electrolysis

We ran a new set of electrolytic experiments of wastewater, this time by using the "optimized" experimental parameters (dilution factor: 1/5, pH 6.3, 70 ^{0}C, 50 mA cm^{-2}). The experiments were monitored by HPLC and TOC (Fig. 2.8). AMBI concentration decays was fast and it disappears in 45 min of reaction (10 Ah l^{-1} or 5.4×10^3 Coulombs). This is in contrast with the evolution of TOC, which changes little in the first 10 min (2.2 Ah l^{-1} or 1.2×10^3 Coulombs), and then, in the following 35 min, slowly decreases to 20%. This is consistent with accumulation of intermediates rather than direct mineralization. TOC decrease is more important only after total elimination of AMBI. By 135 min (30 Ah l^{-1} or 1.6×10^4 Coulombs), TOC has decreased by nearly 70%, suggesting that most intermediates are readily mineralised. After that, the change of TOC is very slow, indicating the presence of organic compounds, which, at work conditions, are not further degraded by the electrochemical process.
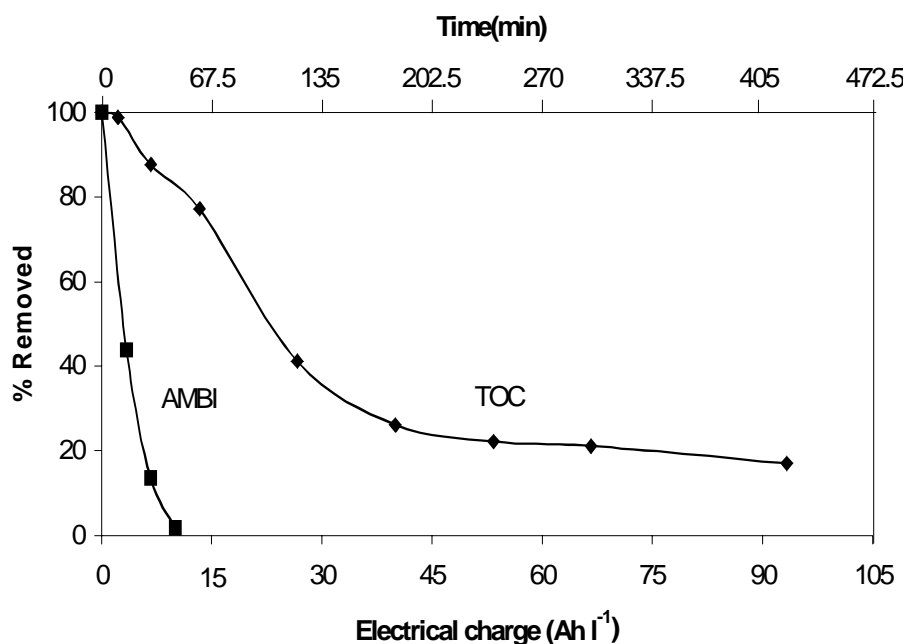
FIGURE 2.8   *Electrochemical treatment of five-fold diluted industrial AMBI wastewater. 25 mA cm-2 and 70 $^{\circ}$C. Evolution of AMBI and TOC concentration.*

TOC evolution does not say anything about the toxicity and the biocompatibility of the electro-treated solutions. In several occasions, the electrochemical treatment may lead to the formation of substances which are less biodegradable or more toxic than those in the untreated waters [Ribordy et al. 1997]. A biological step can be attempted for complete treatment of the

solution resulting from electrolysis only if the electrolysis effluent proves to be biocompatible. Therefore, its chemical and biological characteristics must be studied.

2.3.2.5 Average oxidation state of electrotreated solutions

A comparison of experimental TOC and COD values yields the Average Oxidation State (AOS), Eq. 2.4, which is an indicator of the oxidation degree of complex solutions and gives indirect information on their probability of biodegradation.

$$AOS = \frac{4(TOC - COD)}{TOC}$$

(2.4)

TOC and COD are expressed in moles of C l^{-1} and moles of O_2 l^{-1}, respectively. AOS takes values between +4, for CO_2, and –4, for CH_4. As Fig. 2.9 shows, AOS increases with the electrochemical treatment and attains a value of 1.8 after 180 min (40 Ah l^{-1} or 2.2×10^4 Coulombs). This positive value probably indicates that the solution now contains highly oxidized aliphatic compounds mainly. Although high AOS values are frequently associated to biocompatible solutions, this is not always the case as traces of highly toxic compounds (such as organic chlorides) may remain.
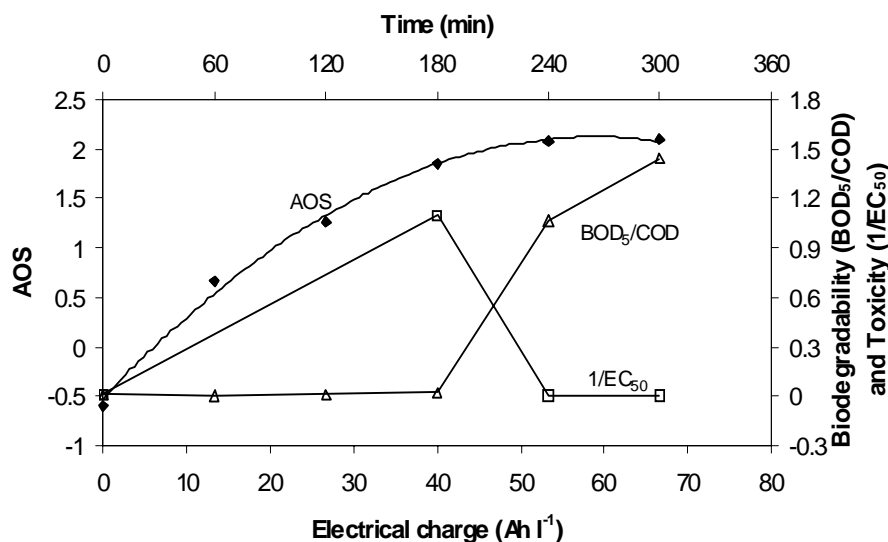
FIGURE 2.9   *Chemical and biological characteristic of wastewater upon electrolysis. Initial concentration: 5.0 mmol l^{-1} AMBI, 25 mA cm^{-2} and 70 °C.*

2.3.2.6 Biological characteristics of electrotreated solutions

Additional tests (toxicity and biodegradability) were carried out to study the biocompatibility of solutions and to choose the best conditions under which the electrochemical process can be coupled to a biological one for complete treatment of wastewater containing AMBI. Two curves in Fig. 2.9 show the biodegradability (as indicated by the BOD_5/COD ratio) and the toxicity expressed by ($1/EC_{50}$) upon electrolysis. The toxicity increases and the biodegradability remains quite low during the first 3 h. This behaviour can be explained in terms of the possible formation of organic chlorides and, perhaps quinones, which are highly bio-recalcitrant and toxic, even in very small concentrations. At later times, the toxicity (expressed by $1/EC_{50}$) decays abruptly and the BOD_5/COD ratio increases. At ca. 4 h (53.3 Ah l^{-1} or 2.9×10^4 Coulombs), the toxicity is very low and the ratio BOD_5/COD is high. A wastewater is considered biodegradable and acceptable for discharge when the BOD_5/COD is higher than 0.4 [Marco et al. 1997]. The extremely high BOD_5/COD ratio (higher than 0.9) attained at the end of electrolysis is not only linked with the presence of biodegradable intermediates but might be also due to the development of nitrification conditions (consuming oxygen), which are known to give a positive bias to the BOD_5 test.

The most relevant conclusion from Fig. 2.9 is that, after 4 h (53.3 Ah l^{-1} or 2.9×10^4 Coulombs), the solution becomes biocompatible. At this time, a biological treatment can be set up for the complete mineralization of the effluent from electrolysis.

2.3.2.7 Evaluation of the biodegradability of electrotreated solutions in a FBR

The effluent from electrolysis was neutralized and then tested for biodegradability in a FBR. The test was carried out under theoretically favourable conditions, that is, and a strict control of pH, temperature and aeration. Fig. 2.10 shows the evolution of DOC during the biodegradability test. DOC decays to zero in ca. 4.5 h. No need for acclimatisation or a period for bacterial growth.

Therefore, the FBR test indicates that coupling between electrochemistry and microbiology for the treatment of wastewaters that contain AMBI is extremely successful.
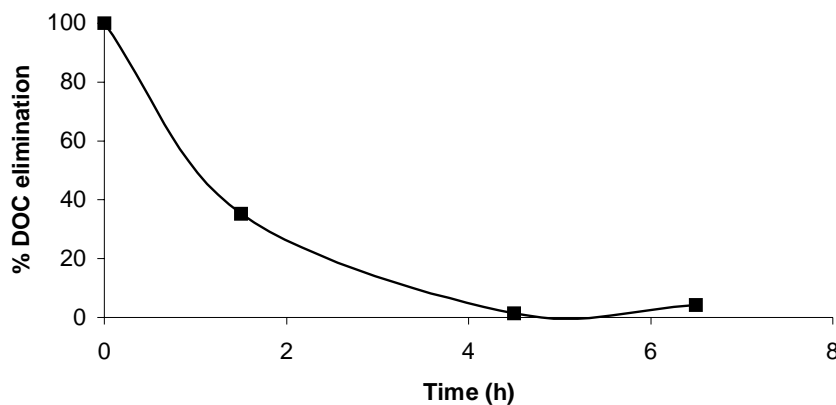
FIGURE 2.10   *Biological degradation test of the electrolysis effluent in a FBR.*

This study shows that constant current electrolysis of diluted wastewaters containing AMBI is mainly influenced by the concentration of chloride ions. Highly oxidizing chlorine species boost the degradation rates of AMBI and its intermediates. The pH medium has a little effect on kinetics of AMBI degradation. Temperature and current densities do not affect the degradation process.

Toxic and non-biodegradable intermediates are produced. However, once these intermediates are further degraded, the toxicity decreases sharply and the biodegradability increases significantly. Thus, the solution reaches the status of biocompatibility after prolonging the electrolysis to 4 h (53.3 Ah l^{-1} or 2.9×10^4 Coulombs). Effluents from the electrolytic cell can rapidly undergo biodegradation in a FBR reactor.

2.4   Photochemical degradation of AMBI

An interesting class of advanced oxidation processes consists of the so called Advanced Photochemical Oxidation (APO) processes[US.EPA 1998]. APO processes are characterised by a free radical mechanism initiated by the interactions of photons of a proper energy level with the molecules of chemical species present in the solution or with a catalyst.

APO has been considered as a promising technology for the treatment of contaminated water. Matrices to which APO has been applied include the following: contaminated groundwater, industrial wastewater, municipal wastewater, drinking water, landfill leachate, contaminated surface water. APO has been tested on the following types of waterborne contaminants: volatil organic compounds (VOC), semivolatil organic compounds (SVOC), polychlorinated byphenyls (PCB), pesticides and herbicides, dioxins and furans, explosives and their degradation products, humic substances, inorganics and dyes (see detailed reviews: [Legrini et al. 1993; Hoffmann et al. 1995; Goswami 1997; Mills and Le Hunte 1997; Alfano et al. 2000; Blake 2001; Malato et al. 2002]. That is why we considered that in degradation of AMBI the APO processes would be effective.

In this section, the photochemical treatment of a real industrial wastewater containing AMBI was explored. Some experiments were made to find the most convenient APO. The systems with light energy (hν), oxygen peroxide or oxygen from air and homogeneous (Fe^{3+}) and heterogeneous (TiO$_2$) catalyst were compared: hν/H$_2$O$_2$, hν/Fe^{3+}/O$_2$, hν/TiO$_2$, hν/TiO$_2$/H$_2$O$_2$ and hν/Fe^{3+}/H$_2$O$_2$.

2.4.1 Experimental

The photocatalytic experiments were performed using 40 ml Pyrex flask with a cut-off at λ = 290 nm placed into a Hanau Suntest Simulator (Fig. 2.11).

The radiation source employed is a xenon lamp where the total radiant flux (80 mW cm^{-2}) was measured with a YSI Corporation powermeter. The lamp has a l distribution with about 0.5% of the emitted photons at wavelengths shorter than 300 nm and about 7% between 300 and 400 nm. The profile of the photons emitted between 400 and 800 nm followed the solar spectrum. The aqueous suspensions were magnetically stirred throughout irradiation, opened to air. Extreme care was taken to ensure uniform experimental conditions during the degradation rate determination. Samples were taken periodically and the disappearance of each substance was monitored by DOC analysis (section "2.2.1.3") after filtration with millipore filters (0.45 μm) to remove the catalyst.

The oxidant: H$_2$O$_2$ (30% w/w) analysis grade (p.a.) was from Fluka.

The catalyst: $FeCl_3.6H_2O$ was from Fluka and TiO_2 was Degussa P-25, mainly Anatase, surface area 50 $m^2\,g^{-1}$.

DOC analysis was performed using the methodology describe in section "2.2.1.3".
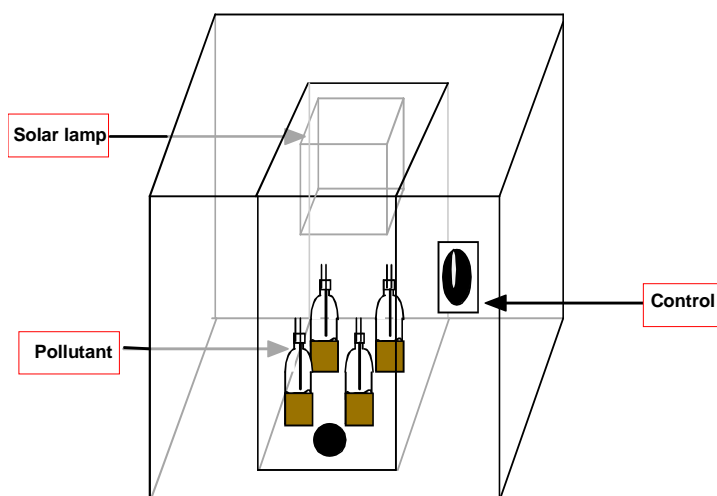
FIGURE 2.11 *Picture and schematic representation of the suntest simulator*

2.4.2 Results

Fig. 2.12 shows the degradation of DOC of a 3.0 mmol l^{-1} AMBI containing wastewater by various APO. The experiments were performed in the Suntest Fig. 2.11 using a real wastewater. The

concentrations of H_2O_2 (50 mmol l^{-1}), TiO_2 (0.2 g l^{-1}), and Fe^{3+} (2.0 mmol l^{-1}) used, were fixed considering previous researches [Parra et al. 2000].
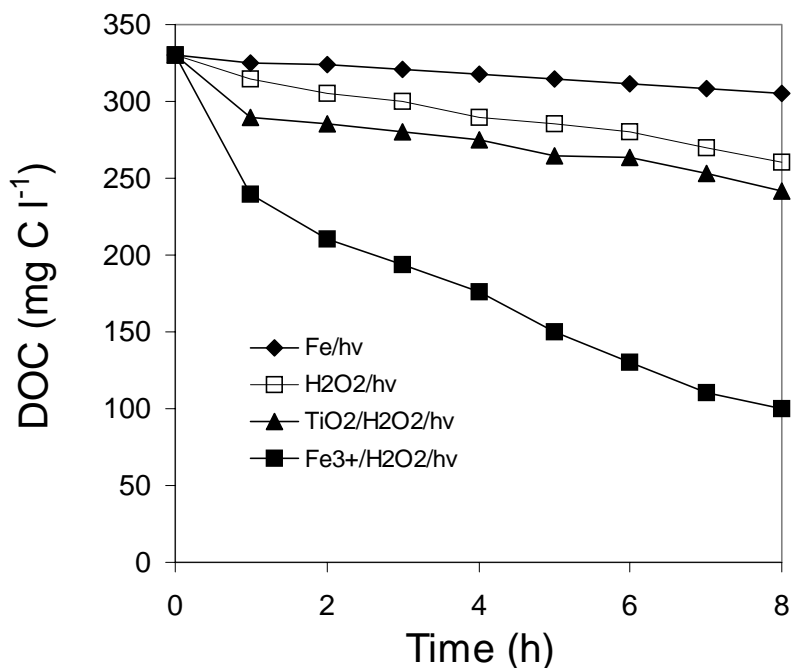
FIGURE 2.12 *DOC evolution of AMBI containing wastewater as function of irradiance time in the Suntest. Study of some APO. [AMBI]o = 3.0 mmol l^{-1}.*

As shown in Fig. 2.12, the photo-Fenton system ($h\nu/Fe^{3+}/H_2O_2$), far superior to the other methods, is able to mineralise 70% of the initial DOC in 8 hours. The $h\nu/TiO_2/H_2O_2$ and $h\nu/H_2O_2$ systems, only arrive to a maximum of about 26 and 21%, respectively. The system $h\nu/Fe^{3+}/O_{2(air)}$ was found to be the least effective, which only reaches to a maximum of 7%. To explain this observation, the different absorption cross-sections of the light absorbing species have to be taken into account, as well as the emission spectrum of the UV-lamp used (Fig. 2.13).
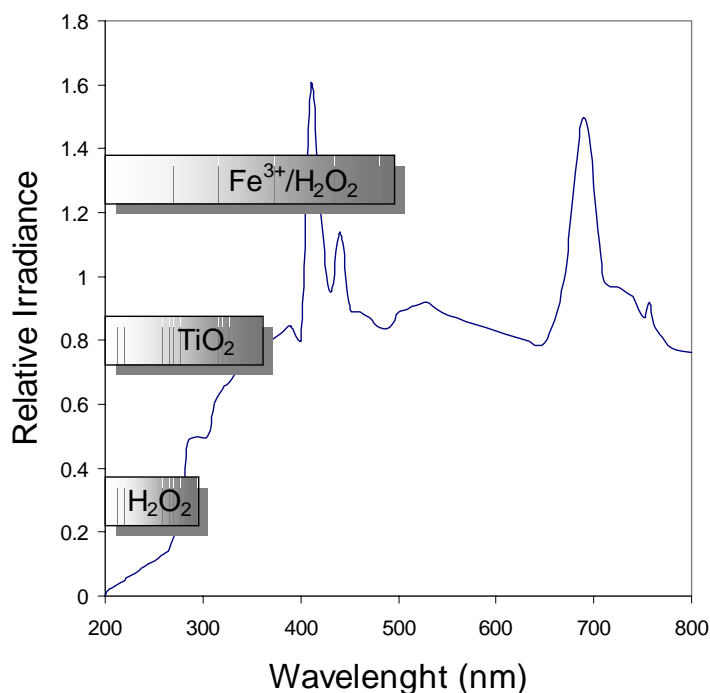
FIGURE 2.13   *Emission spectra of the UV-lamp used in the Suntest and the different absorption cross-sections of the H_2O_2, TiO_2 and Fenton systems.*

The H_2O_2 does not absorb significantly beyond 300 nm and absorbs only weakly in the range 200-300 nm. The Anatase form of TiO_2 absorbs in the range 300-400 nm. Therefore these systems are able to utilise only 1 and 7% of the lamp radiation respectively. On the contrary, the absorption spectrum of the photo-Fenton system presents an increased light sensitivity up to a wavelength of 500 nm and can absorb and utilize about 35% of the lamp radiation, thus making use of the lamp output more efficient. On the other hand, in the photo-Fenton system, the depth of light penetration is high and the contact between pollutant and oxidising agent is close, since homogeneous solution is used.

However the system $h\nu/Fe^{3+}/O_{2(air)}$ appears also as advantageous because addition of commercial H_2O_2 can be avoided, representing an economic gain, that could compensate in certain cases the longer illumination times when compared with those observed with the system $h\nu/Fe^{3+}/H_2O_2$.

2.5   Comparison of sonochemical electrochemical and photo-chemical processes

In order to compare different degradation processes a valuable criterion is the economical evaluation of applied methods. However, except economics, there are a number of important factors in selecting a waste-treatment technology including: regulations, effluent quality goals, operation (maintenance, control, safety) and robustness (flexibility to change/upsets). Although all these factors are important, economics is often the most important [Bolton et al. 1996].

To asses a economical comparison of AOP, Bolton [Bolton et al. 1996] proposed a figure-of-merit, the so called Electrical Energy per order of pollutant removal (EE/O). EE/O is the electrical energy in kilowatt hours (kWh) required to bring about the degradation of a contaminant C by one order of magnitude in 1 m^3 (1000 l) of contaminated water, which can be calculated, in the case of batch operation, by:

$$\mathrm{EE}/O \;=\; \frac{P \times t \times 1000}{V \times 60 \times \log(C_i/C_f)} \tag{2.5}$$

where P is the rated power (kW) of the AOP system. V is the volume (in litres, l) of water in the time t (min). C_i and C_f are the initial and final concentrations of C and the factor of 1000 converts g to kg.

The EE/O of the sonochemical, electrochemical and photo-Fenton processes used in this chapter were estimated and are presented in "Table 2.1". The following assumptions were made: (i) Only energy cost was estimated, not the investment cost for chemicals, apparatus and buildings. (ii) Additional operations like neutralization and filtration will be necessary in some cases. The cost are not include either. (iii) Energy consumption of the laboratory equipment per unit wastewater used for the calculation is higher than in an optimized large scale plant. (iv) The price of electrical energy in Switzerland is almost 0.13 US\$ per kWh (vi) The degradation time, represents the time necessary to mineralization of 50% of initial DOC.

TABLE 2.1 *Electric energy cost estimates for various AOP for the degradation of AMBI containing wastewater. [DOC] initial = 800 mg C l⁻¹.*

System	Degradation time (h)	Energy demand (kWh m³)	Volumic costs (US$ m⁻³)
Sonochemical	2	1266	165
Electrochemical	5	540	70
Photochemical (photo-Fenton)	4	500	65

The electric energy cost of the Photo-Fenton system, 65 US$ m^{-3}, is about 90% of the electrochemical treatment and 40% of the sonochemical treatment. In conclusion on the basis of this calculation, we can confirm that from the energetic point of view, the photo-Fenton system is the most advantageous when the power source is electricity. More detailed study was performed in this direction (see section "5.3.6.2").

The exploratory study effectuated in this chapter, comparing electric energy consumption of three AOP systems, does not allow reaching a definitive conclusion that indicates which system is the best. But, as even for the most interesting system, the photochemical, the energy cost is quite high. Nevertheless the utilisation in this case of direct solar radiation to act on photocatalytic reactors could represent an economic approach with potential of application in sunny regions particularly these located in developing countries. The development of a solar energy-autonomous photoreactor could be extremely interesting, since it is known that electrical energy can represent a major fraction of the operating cost of photocatalytic decontamination systems [Matthews 1993].

According to these criteria, the APO process adjust better than the electrochemical and ultrasounds systems, since in AOP:

- Solar energy could be used, which represent an important economic gain (see section 1.2.3.2 and chapter 5).

- The reactor is simple and can be easily constructed.

- The catalyst is iron, a cheap substance, and in many cases, can be present naturally in water [Olivié-Lauquet et al. 1999].

2.6   References

Aleboyeh A, Aleboyeh H, Moussa Y (2003). "Critical" effect of hydrogen peroxide in photochemical oxidative decolorization of dyes: Acid Orange 8, Acid Blue 74 and Methyl Orange. *Dyes and Pigments* **57** (1) 67-75.

Alfano O M, Bahnemann D, Cassano A E, Dillert R, Goslich R (2000). Photocatalysis in water environments using artificial and solar light. *Catal. Today* **58** (2-3) 199-230.

Blake D (2001). Bibliography of work on the heterogeneous photocatalytic removal of hazardous compounds from water and air. Update number 4 to October 2001, NREL/TP-510-31319. National Technical Information Service (NTIS), U.S. Department of commerce, Springfield, VA 22161.

Bolton J R, Bircher K G, Tumas W, Toman C A (1996). Figures-of-merit for the technical development and application of advanced oxidation processes. *J. Adv. Oxid. Technol.* **1** (1) 13-17.

Brillas E, Mur E, Sauleda R, Sánchez L, Peral J, Domènech X, Casado J (1998). Aniline mineralization by AOP's: anodic oxidation, photocatalysis, electro-Fenton and photoelectro-Fenton processes. *Appl. Catal. B.* **16** 31-42.

Comninellis C, Pulgarin C (1991). Anodic oxidation of phenol for wastewater treatment. *J. Appl. Electrochem.* **21** 703-708.

Comninellis C, Pulgarin C (1993). Electrochemical Oxidation of Phenol for Waste-Water Treatment Using SnO2 Anodes. *J. Appl. Electrochem.* **23** (2) 108-112.

Goswami D Y (1997). A riview of engineering developments of aqueous phase solar photocatalytic detoxification and desinfection processes. *J. Solar Energy Eng.* **119** 101-107.

Hoffmann M, Martin S, Choi W, Bahnemann D (1995). Environmental Applications of semiconductor catalysis. *Chem. Rev.* **95** 69-96.

Jüttner K, Galla U, Schmieder H (2000). Electrochemical approaches to environmental problems in the process industry. *Electrochem. Acta.* **45** 2575-2594.

Legrini O, Oliveros E, Braun A M (1993). Photochemical Processes for Water-Treatment. *Chem. Rev.* **93** (2) 671-698.

Malato S, Blanco J, Vidal A, Richter C (2002). Photocatalysis with solar energy at a pilot-plant scale: an overview. *Appl. Catal. B.* **37** (1) 1-15.

Marco A, Esplugas S, Saum G (1997). How and why combine chemical and biological processes for wastewater treatment. *Water Sci. and Technol.* **35** (4) 321-327.

Matthews R W (1993). Photocatalysis in water purification: possibilities, problems and prospects. Photocatalytic Purification and Treatment of Water and Air. Ollis D F, Al-Ekabi H, Ed. Elsevier Science Amsterdam.

Mills A, Le Hunte S (1997). An overview of semiconductor photocatalysis. *J. Photochem. and Photobio. A.* **108** 1-35.

OECD (1996). *Guidelines for testing of Chemicals, test 302B.*

Olivié-Lauquet G, Allard T, Benedetti M, Muller J P (1999). Chemical distribution of trivalent iron in riverine meterail from a tropical ecosystem: a quantitative EPR study. *Wat. Res.* **33** (11) 2726-2734.

Parra S, Sarria V, Malato S, Peringer P, Pulgarin C (2000). Photochemical versus coupled photochemical-biological flow system for the treatment of two biorecalcitrant herbicides: metobromuron and isoproturon. *Appl. Catal. B.* **27** (3) 153-168.

Petrier C, Francony A (1997). Incidence of wave-frequency on the reaction rates during ultrasonic wastewater treatment. *Water Sci. and Technol.* **35** (4) 175-180.

Rajeshwar K, Ibañez J (1997). *Environmental Electrochemistry Fundamentals and applications in pollution abatement*. San Diego, California, USA, Academic Press.

Ribordy P, Pulgarin C, Kiwi J, Peringer P (1997). Electrochemical Versus Photochemical Pretreatment of Industrial Wastewaters. *Water Sci. Technol. Technol.* **35** (4) 293-302.

Sarria V, Deront M, Peringer P, Pulgarin C (2003). Degradation of a biorecalcitrant dye precursor present in industrial wastewaters by a new integrated iron(III) photoassisted-biological treatment. *Appl. Catal. B.* **40** (3) 231-246.

US.EPA (1998). Handbook on Advanced Photochemical Oxidation Processes. Cincinnati, Ohio 45268, U.S. Environmental Protection Agency.

IRON PHOTOASSISTED DEGRADATION OF AMBI

Chapter 2 explored sonochemical, electrochemical and photochemical degradation systems; Chapter 3 focuses on the degradation of AMBI by means of the hν/Fe(III)/O$_{2\text{(air)}}$ *and* hν/Fe(III)/H$_2$O$_2$ *systems using an artificial irradiation source. The transformation of AMBI photoinduced by Fe(III) is mainly attributed to three simultaneous process: direct photolysis of the [Fe^{3+}---AMBI] complex, the attack by •OH radicals generated by the photolysis of the Fe(OH)$^{2+}$ and by the Fenton-like reactions. The effect of AMBI, Fe^{3+} and H$_2$O$_2$ for the degradation of AMBI wastewater in the photo-Fenton process was discussed and optimal conditions were found.*

3.1 Introduction

Among different AOP evaluated in chapter 2, we decide to go further into the study of the iron photo-assisted processes, which offer several advantages for the development of a wastewater treatment technology in sunny regions:

- Solar radiation could be used, which represents an important economic gain.

- Iron is the fourth most abundant element in the earth's crust and it is present in natural systems [Pracht et al. 2001].

- O$_2$ or H$_2$O$_2$ the electron acceptors are ecologically ideal oxidants, which are reduced in presence of iron compounds, generating highly reactive superoxide and hydroxyl radicals [Sychev and Isak 1995].

- The homogeneous character of these systems provides, with reasonable limitations, good engineering conditions for coupling them with a complementary biological treatment [Sarria et al. 2002].

Previous investigations have shown that on irradiation by UV/visible light, iron(III) salts can promote the photooxidation organic compounds including: 2,6-dimethylphenol [Mazellier and Bolte 1997], Tetraacetylethylendiamine, [Brand et al. 1997], Alkylphenol ehoxylates [Brand et al. 1998], 4-chlorophenol [Mazellier et al. 1999], 4-dodecylbenzenesulphonate [Mailhot et al. 2000], Alcohol ehoxylates [Brand et al. 2000], 3-chlorophenol [Mazellier and Bolte 2001], Dibutyl phthalate [Bajt et al. 2001], Napthalene [Hykrdova et al. 2002], Dibutyl phthalate [Mailhot et al. 2002], Atrazine [Krysova et al. 2003].

The agent responsible for these reactions could be the hydroxyl radical formed by photochemical dissociation of Fe(III)-hydroxy complex, $Fe(OH)^{2+}$. The reaction can be simply expressed as below [Faust and Hoigne 1990]:

$$Fe(OH)^{2+} + h\nu \rightarrow Fe^{2+} + {}^{\bullet}OH \qquad (3.1)$$
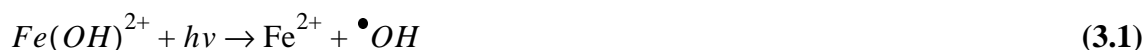
This reaction presents interesting quantum yields (e.g., $\phi_{Fe(II)} = 0.14 \pm 0.04$ at 333 nm; $\phi_{lOH} = 0.195 \pm 0.033$ at 310 nm) [Benkelberg and Warneck 1995]. However, it greatly increases when Fe(III) is complexed with an organic ligand. The reduction of Fe(III) to Fe(II), through a photoinduced ligand to metal charge transfer (LMCT), can occur over the ultraviolet and into the visible (out to ~ 550 nm) [Balzani and Carassiti 1970], and subsequently, the electron-deficient organic ligands further reduce O_2 to $O_2^{\bullet-}$ undergoing a oxidation processes. This pathway can be represented as:

$$[Fe^{3+}L_n] + h\nu \; = \; [Fe^{2+}L_{n-1}] + L^{\bullet} \qquad (3.2)$$

$$L^{\bullet} + O_2 \rightarrow O_2^{\bullet} + \text{oxidized org} \qquad (3.3)$$

O_2 (Eq. 3.4) and H_2O_2 (Eq. 3.5) can participate on the reoxidation of the photoproduced Fe(II) to Fe(III) conferring an interesting catalytic aspect to the process.

$$Fe^{2+} + H^+ + O_2 \rightarrow Fe^{3+} + HO_2^{\bullet} \tag{3.4}$$

$$Fe^{2+} + H_2O_2 \rightarrow Fe^{3+} + OH^- + {}^{\bullet}OH \tag{3.5}$$

The case of using H_2O_2 as oxidant constitutes the typical Fenton process [Fenton 1894], which was presented in detail in the section "1.2.3.3".

The aim of this chapter is to study the viability of the $h\nu/Fe(III)/O_{2(air)}$ and $h\nu/Fe(III)/H_2O_2$ systems for the degradation of AMBI using an artificial irradiation source (suntest simulator). The following topics were also studied: (a) the characterisation of AMBI and Fe(III) in aqueous solution, (b) the involvement of ${}^{\bullet}OH$ radicals and oxygen, and the effect of AMBI, Fe(III) and H_2O_2 concentrations on the performances of the photo-Fenton degradation.

3.2 Experimental

Chemicals and reagents were the same as described in section "2.3.1". The analytical methods DOC and HPLC were described in section "2.2.1.3", COD analysis was described in section "2.3.1.2". The photocatalytic experiments were performed using 40 ml Pyrex flask placed into a Hanau Suntest Simulator (Fig. 2.10) as described in section "2.4.1".

Hydrogen peroxide analysis: Concentrations of H_2O_2 are determined by the Merck Merckoquant$^{®}$ peroxide analytical test strips and by permanganate titration. The latter method utilizes the reduction of potassium permanganate ($KMnO_4$) by hydrogen peroxide in sulfuric acid (see also: http://www.h2o2.com/intro/highrange.html).

Fe(II) concentration was determined by complexometry with o-phenantroline, according with the methodology proposed by Calver and Pitts [Calvert and Pitts 1966].

3.3 Results

3.3.1 Iron photoassisted - oxygen system (hν/Fe(III)/O$_2$) system

3.3.1.1 Characterisation of AMBI and Fe(III) in aqueous solution

Fe(III): The hydrolysis of Fe(III) is very complex phenomenon and has been largely studied [Faust and Hoigne 1990]. It has been observed that the Fe(OH)$^{2+}$ is the predominant species in an iron solution freshly prepared at the pH range of 2.9 to 3.5 [Bajt et al. 2001]. In the pH range ≤ 4 at least four different Fe(III) ions, which are well characterized, coexist in aqueous solution: Fe^{3+}, Fe(OH)$^{2+}$, Fe(OH)$_2$$^+$ and the dimer Fe$_2$(OH)$_2$$^{4+}$. The species distribution is governed by the following hydrolysis equilibria (Eqs 3.6 -3.8) [Faust and Hoigne 1990].

$$Fe^{3+} + H_2O \rightarrow Fe(OH)^{2+} + H^+ \qquad K_1 = 2.7 \times 10^{-3} \qquad \textbf{(3.6)}$$

$$Fe^{3+} + 2H_2O \rightarrow Fe(OH)_2^+ + 2H^+ \qquad K_2 = 1.3 \times 10^{-8} \qquad \textbf{(3.7)}$$

$$2Fe^{3+} + 2H_2O \rightarrow Fe_2(OH)_2^{4+} + 2H^+ \quad K_3 = 6.0 \times 10^{-4} \qquad \textbf{(3.8)}$$
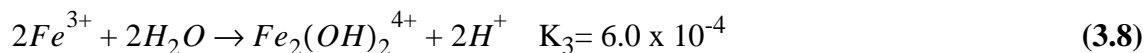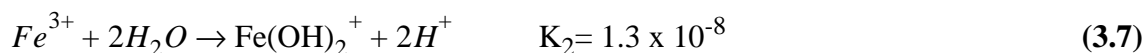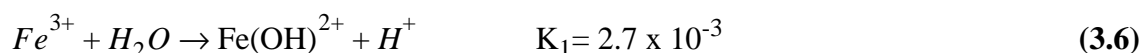
AMBI: In order to interpret accurately the photochemical degradation of AMBI, it is crucial to know the behaviour of AMBI aqueous solution as a function of pH. Fig. 3.1 presents the variation of the UV absorption spectra of AMBI at different pH in the range of 1.92 – 9.2. In Fig. 3.1 it is possible to observe the presence of two isosbestic points (IP), indicating that two different species of AMBI are in equilibrium. By analogy to [Wong-Wah-Chung et al. 2001] we can consider that the AMBI exists in two different forms according to the pH: AMBI and its monoprotonated (AMBIH$^+$) form.
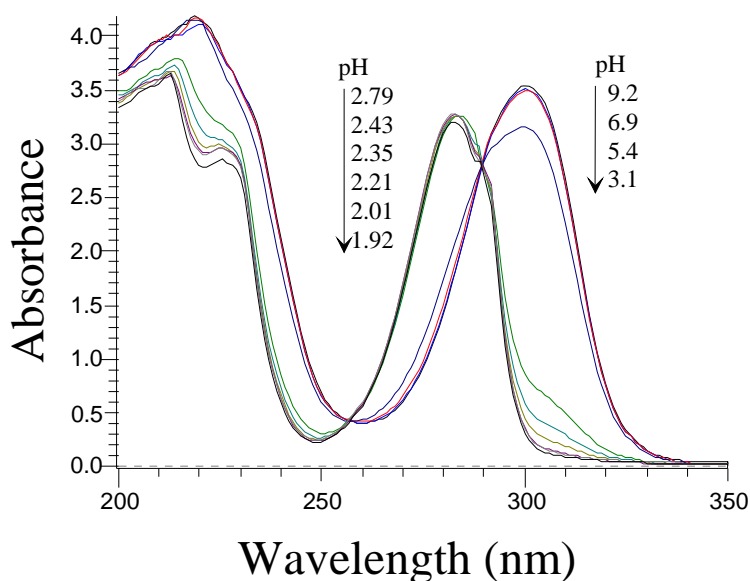
FIGURE 3.1   *Absorption spectra of AMBI (1 mmol l^{-1}) in water at room temperature as a function of pH.*

The process of mono-protonation of AMBI is represented in the Fig. 3.2, where we can observe the two different forms of AMBI.
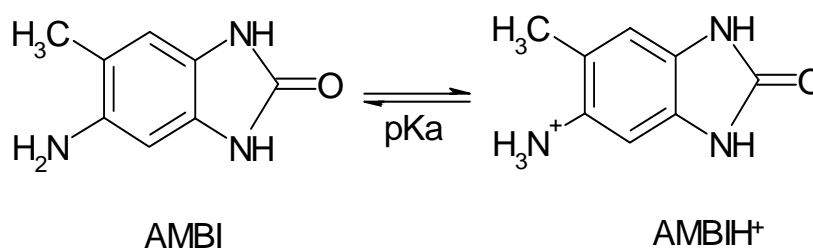
FIGURE 3.2   *AMBI protonation*

A pKa value of 4.7 has been measured [Sarria et al. 2003]. The monoprotonated form AMBIH$^+$ is predominant at pH < 4.7 whereas the molecular form AMBI is mainly present at pH > 4.7. In all cases, The UV visible spectrum of the AMBI presents absorption up to 350 nm, which means that photodegradation using solar light irradiation is not possible and the utilisation of a catalyst is necessary. Considering this, we investigate the efficiency of Fe(III), to promote the photo-degradation of AMBI in aerated water.

Fe(III)/AMBI mixture in aqueous solution: The absorption spectra of Fe(III), AMBI, as well as the Fe(III)/AMBI mixtures are presented in the Fig. 3.3.

The spectres of AMBI and Fe(III) have a maximums at 300 and 297 nm respectively. The spectra of the mixture [Fe(III)]/[AMBI] have a maximums at 284, 440 and 475 nm. The mixture of AMBI and Fe(III) lead presumably to the formation of a complex, which have significant absorption in the visible region, where neither AMBI nor Fe(III) absorbs. In the visible region, a rapid growth of the absorption is observed when the ratio R = [Fe(III)]/[AMBI] increase between 1 and 4, at the same time, a reduction of the absorption is observed in the maximum a involvement nm. To explain this observation, a formation of an outer-sphere complex [Stumm and Morgan 1981] is suggested, which maybe conformed by 4 atoms of Fe(III) and 1 atom of AMBI. Nevertheless, a detailed study would be necessary to confirm this observation.
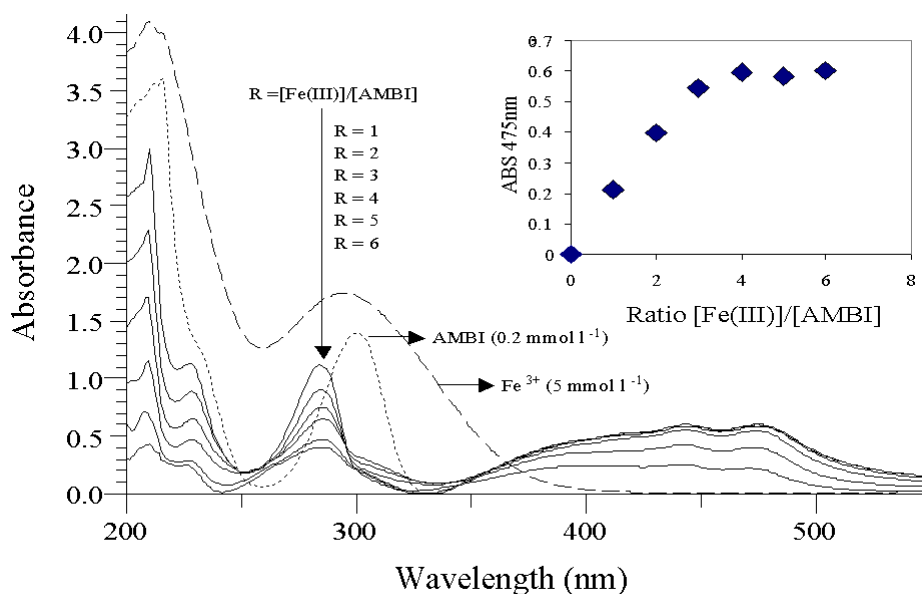
FIGURE 3.3   *UV-Vis spectra of aqueous solution of AMBI (0.2 mmol l^{-1}), and several mixtures of AMBI and Fe(III), where the ratio R=[Fe(III)]/[AMBI] varies between 1 and 6.*

The complex formed by AMBI and iron was thermally stable, provided the ratio R=[Fe(III)])/[AMBI] < 1. All attempts to reverse the complexation between AMBI and Fe(III), such addition of strong chelating agents (EDTA, o-phenantroline, ascorbic acid), as well as pH

modification (acid and basic) failed, which indicates that AMBI is a strong chelating ligand. At higher ratio values (R ≥1), a fast thermal redox process, presumably inside the complex, leading to the diminution of the maxima a 284 nm and the reduction of Fe(III) into Fe(II) was observed.Fig. 3.4 presents a typical spectral evolution of the mixture R=[Fe(III)])/[AMBI] = 4 as a function of time.
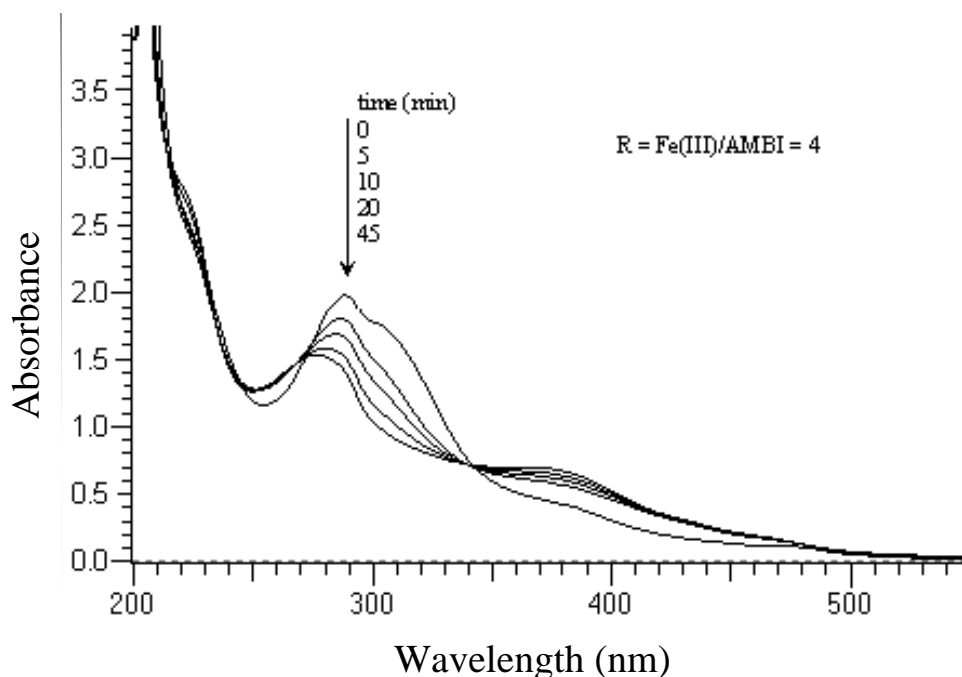
FIGURE 3.4   *Spectral evolution for a mixture [Fe(III)]$_o$ = 0.8 mmol l^{-1} and [AMBI] = 0.2 mmol l^{-1}.*

3.3.1.2   Fe(III) photoinduced degradation of AMBI in aqueous solution under air atmosphere

To evaluate the photochemical reactivity of a mixture containing AMBI (1 mmol l^{-1}) and Fe(III) (1 mmol l^{-1}), some experiments were performed using a Suntest simulator. Fig. 3.5 shows the kinetic evolution of AMBI and DOC as a function of phototreatment time. A rapid complexation and conversion of AMBI occurs during the first minutes, accompanied by relatively small diminution in DOC. It can be seen that after 300 min, about 90% of the AMBI has been oxidised, while only about 30% of the DOC has been removed. This can be presumably due to the formation of more oxidised intermediates, which generally have a lower reactivity toward hydroxyl

radicals or other oxidants [Scott and Ollis 1995] and consequently are more difficult to photo-oxidise than AMBI.
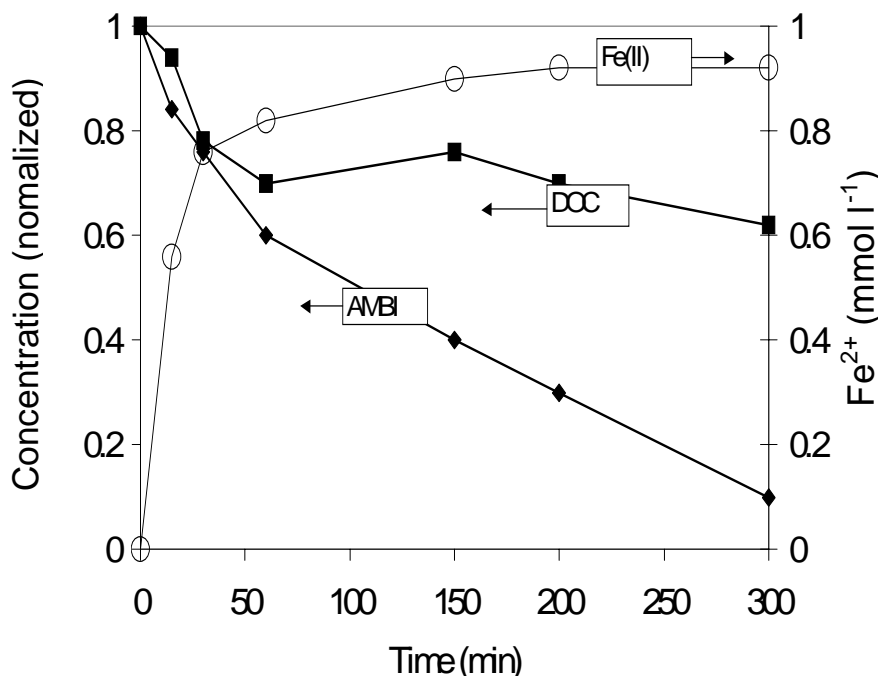
FIGURE 3.5 *Concentration profile of AMBI, DOC and Fe(II) during photodegradation experiment in a suntest. Both [AMBI] and [Fe(III)] = 1.0 mmol l^{-1}.*

In the first 15 min (Fig. 3.5), we observe that almost 80% of initial Fe(III) is reduced to Fe(II). After that the Fe(II) concentration increases until reached a plateau. However we have to note that the oxidation of AMBI was going on even after Fe(II) had reached its plateau value. According to some authors [Mazellier and Bolte 2001] a reoxidation of Fe(II) to Fe(III) regenerating the photoreactive Fe(III) specie Fe(OH)$^{2+}$ seems probable. The general mechanisms proposed involve a reaction of Fe(II) with:

(i) the hydroperoxyde radical (HO$_2^\bullet$/O$_2^{\bullet-}$) Eq. 3.9. HO$_2^\bullet$/O$_2^{\bullet-}$ is formed by the single-electron reduction of molecular oxygen (see Eq. 3.4).

$$Fe(II) + HO_2^\bullet/O_2^\bullet + 3H^+ + h\nu \rightarrow Fe(III) + 2H_2O_2 \tag{3.9}$$
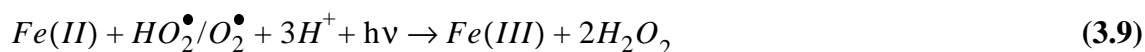
(ii) the $^\bullet$OH produced in the reaction bulk Eq. 3.10:

$$Fe(II) + {}^{\bullet}OH + h\nu \rightarrow Fe(III) + OH^{-} \qquad \textbf{(3.10)}$$

This last reaction appears to be detrimental in the whole oxidative process.

3.3.1.3   Involvement of $^{\bullet}$OH radicals and oxygen

With the objective to better understand the mechanism of the iron photoassisted degradation processes, we carried out different experiments in presence of one $^{\bullet}$OH radical scavenger (isopropanol), and under O_2 and He_2 atmospheres, the results obtained are presented in Fig. 3.6.
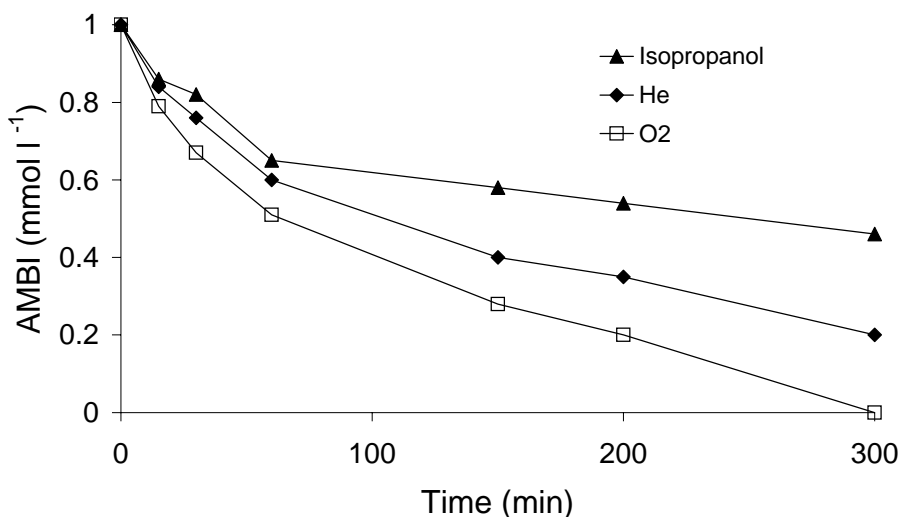
FIGURE 3.6   *Kinetics of AMBI disappearance as a function of irradiation time in a suntest at different conditions: «O_2» means under O_2 atmosphere: «He» means under Helium atmosphere; «isopropanol» means under 10 mmol l^{-1} isopropanol was added. Both [AMBI] and [Fe(III)] = 1.0 mmol l^{-1}.*

Photodegradation of AMBI carried out in the presence of isopropanol (10 mmol l^{-1}), as radical scavenger, was considerably inhibited. This observation is indirect evidence that $^{\bullet}$OH radicals are involved in the iron photoassisted process. The isopropanol scavenged the $^{\bullet}$OH radicals, which are produced in the bulk by means of different mechanisms such as the photolysis of Fe(III), as in Eq 3.1.

The photolysis rate of the mixture Fe(III)/AMBI is higher in the presence of oxygen in comparison to the absence of this compound, under He_2 atmosphere. As mentioned by Sun and

Pignatello [Sun and Pignatello 1993], oxygen plays an important role in the iron photoassisted reactions. Oxygen enhancement can be attributed to the following mechanisms:

- Oxygen reacts with intermediate organoradicals, as show in the Eq. 3.3, to give products containing hydroxyl and carboxyl functional groups, which then form photolabile Fe(III) complexes, thereby promoting overall photodegradation.

- The oxygen participates in the reoxidation of Fe(II) to Fe(III) as show in Eq. 3.10.

- In agreement with Zuo and Hoigné [Zuo and Hoigné 1992], oxygen participates in the generation of H_2O_2 in the solution. The mechanism involved the single-electron reduction of molecular oxygen to form intermediate superoxide ion and its conjugate acid (Eq. 3.4), the hydroperoxyl radical. The subsequent disproportionation of this specie leads to H_2O_2 and O_2 formation, Eq. 3.11.

$$HO_2^\bullet / O_2^{\bullet -} + H^+ \rightarrow H_2O_2 + O_2 \qquad (3.11)$$

The H_2O_2 formed can participate in the Fenton (Eq. 3.12) and Fenton-like reactions.

$$Fe^{2+} + H_2O_2 \rightarrow Fe^{3+} + OH^- + {}^\bullet OH \qquad (3.12)$$

3.3.1.4 Degradation pathway of AMBI by $h\nu/Fe^{3+}/O_{2(air)}$

According to these observations, we attribute the AMBI photodegradation to three main processes that can be represented by the Fig. 3.7, which is inspired from the literature *[Catastini et al. 2002]*:

(i) An intermolecular photoredox process: photolysis of the Fe^{3+}---L complex (Eq. 3.2). It occurs by dissociation of Ligand To Metal Charge Transfer (LMCT) [Sun and Pignatello 1993]. The organic radical formed (AMBI$^\bullet$) is object of the subsequent degradation reactions chain. A possible reduction of the Fe^{3+} inside the complex, which also happens in the dark, was also observed. The reduced complex can capture

one electron of a water molecule and produce an $^\bullet$OH radical. A more detailed study is needed to confirm this observation.

(ii) The attack of $^\bullet$OH radicals generated by the photochemical dissociation of Fe(III)-hydroxy complex, $Fe(OH)^{2+}$.

(iii) The attack of $^\bullet$OH radicals generated by the Fenton and photo-Fenton like reactions, due to the presence of Fe(II) and H_2O_2 formed in the solution.
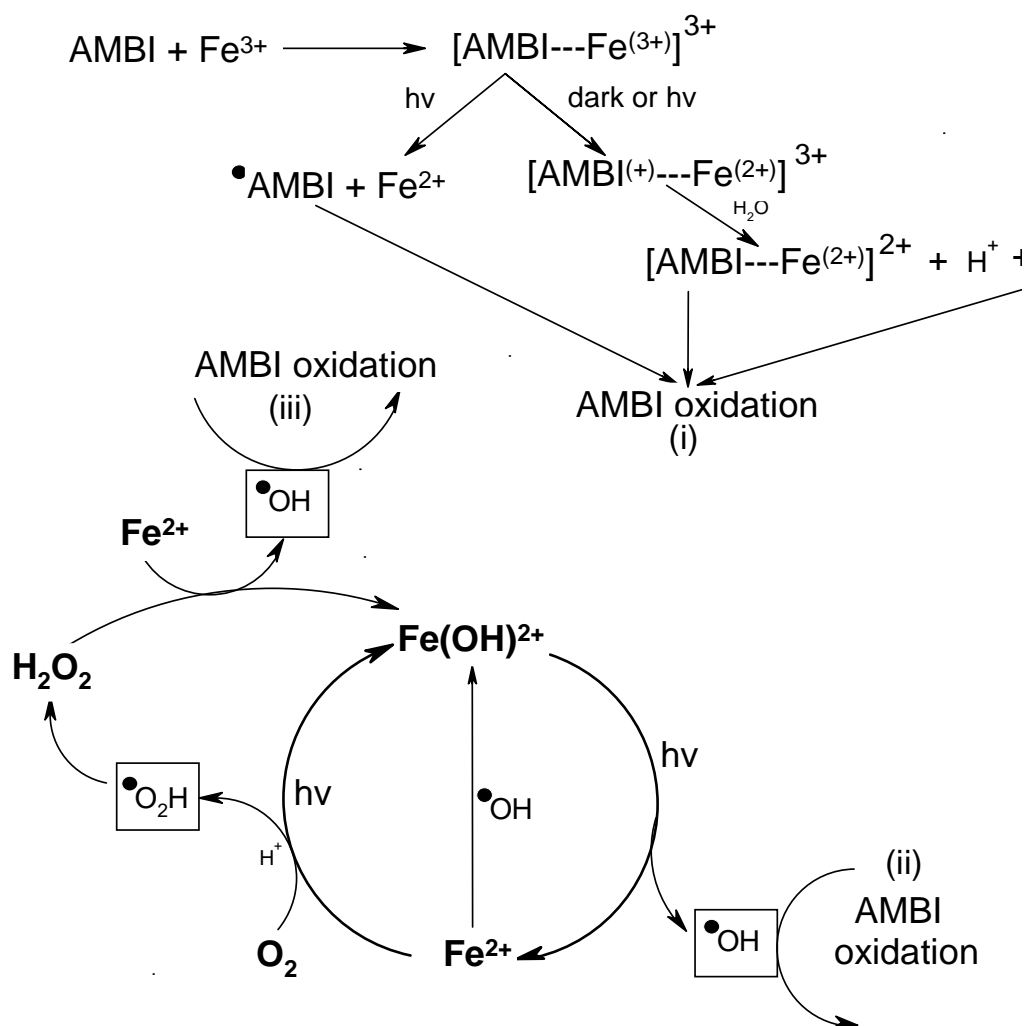
FIGURE 3.7   *Proposed pathways of AMBI degradation by the iron photoassisted reactions, inspired from [Catastini et al. 2002].*

3.3.2 Photo-Fenton system (hν/Fe(III)/H$_2$O$_2$)

The case of using H_2O_2 as oxidant constitutes the typical Fenton process [Fenton 1894], which was presented in detail in the section "1.2.3.3".

As shown in sections "1.2.3.3" the optimal concentration of initial compound, Fe^{3+} and H_2O_2 are key factors for the photo-Fenton system and need to be determined. Degradation of AMBI can be described assuming a pseudo-first order reaction (Eq. 3.13):

$$-\frac{d(DOC)}{dt} = k(DOC) \tag{3.13}$$

where k is the pseudo-first order reaction rate constant. Integration of Eq. 3.13 leads to:

$$\ln(DOC/DOCo) = -kt \tag{3.14}$$

A plot of $\ln(DOC_o)/(DOC)$ against time of irradiation (t) gives a straight line with a slope of k, which has been calculated and used to study the effect of different concentrations of AMBI, Fe^{3+}, and H_2O_2.

3.3.2.1 Effect of the initial AMBI concentration on degradation of real wastewater using Suntest

It was observed that the initial concentration of the target compound could have an important influence in the photo-Fenton processes [Chen and Pignatello 1997]. In order to obtain the optimal AMBI concentration, some experiments were carried out in the Suntest using real wastewater (Fig. 3.8). H_2O_2 and Fe^{3+} initial concentrations were 25 and 1.0 mmol l^{-1}, respectively.

A significant enhancement of degradation efficiency was observed when AMBI concentration was increased from 0.5 to 1 mmol l^{-1}. Above this concentration, the rate of AMBI oxidation was negatively affected by progressive increase of AMBI concentration. This may be attributed to the increase of darkness in the solution generated by high concentrations of AMBI, which hinders the absorption of the UV light required for the photo-Fenton process. This result

suggests also, that the pollutant and/or another species present in solution (e.g. any products of pollutant oxidation, anions, etc.) compete with each other for the oxidant, decreasing its activity.
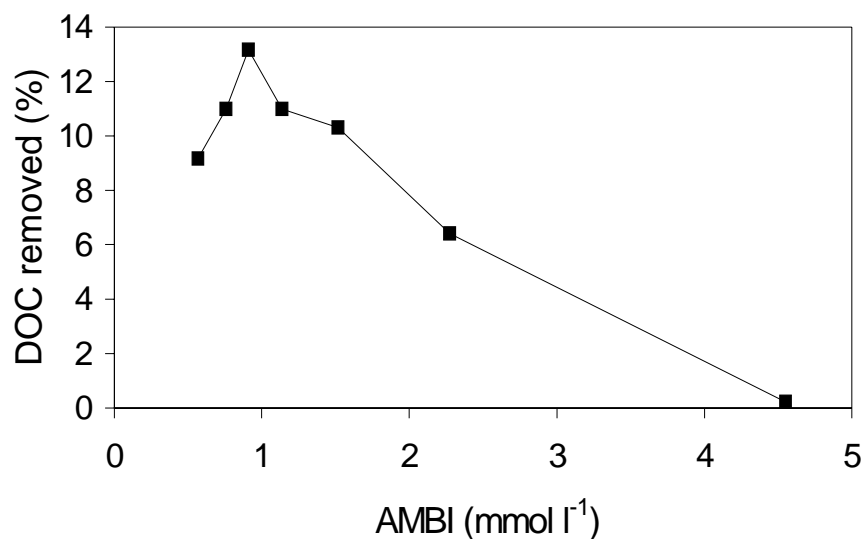
FIGURE 3.8   *Effect of initial AMBI concentration on the amount of AMBI eliminated in the first 15 min of photo-Fenton treatment.*

The optimal concentration of AMBI was about 1 mmol l^{-1}. At this moment a molar AMBI:Fe^{3+} ratio of 1:1 was reached.

3.3.2.2   Effect of the initial Fe^{3+} concentration on degradation of synthetic and real wastewater using two different illumination systems

To further elucidate the role of Fe^{3+} concentration on the photo-degradation of AMBI in the $Fe^{3+}/H_2O_2/h\nu$ system, a series of experiments varying the concentration of iron were carried out. The experiments were performed in the Suntest using real and synthetic wastewater. The results are presented in Fig 3.9:

(i)   In all cases, for low initial concentrations of Fe^{3+}, decomposition rates increase with the amount of Fe^{3+} and reach a broad maximum. After this maximum, higher initial

concentrations result in decreased degradation rates. This may be due to 3 different factors:

 ⬥ Increase of darkness in the solutions during the photo-treatment, which hinders the absorption of the UV light required for the photo-Fenton process.

 ⬥ Excessive formation of Fe^{2+}, which will be competing with the pollutant in solution for $^{\bullet}OH$ radicals.

$$Fe^{2+} + {^{\bullet}OH} \rightarrow Fe^{3+} + OH^{-} \tag{3.15}$$

 ⬥ The fixed H_2O_2 concentration can become the limiting factor of the oxidation-reduction reaction when high concentrations of Fe^{3+} are used.

(ii) The degradation constant of synthetic wastewater is higher than that of real wastewater. A reason for this may be the higher concentration of inorganic ions present in real wastewater (see Table 2.1 in section "2.3"). It must to be take into account, that photo-Fenton reaction is extremely sensitive to anions, and phosphate ions in particular will seriously suppress the Fenton ability to oxidize organic pollutants [Lu et al. 1997].
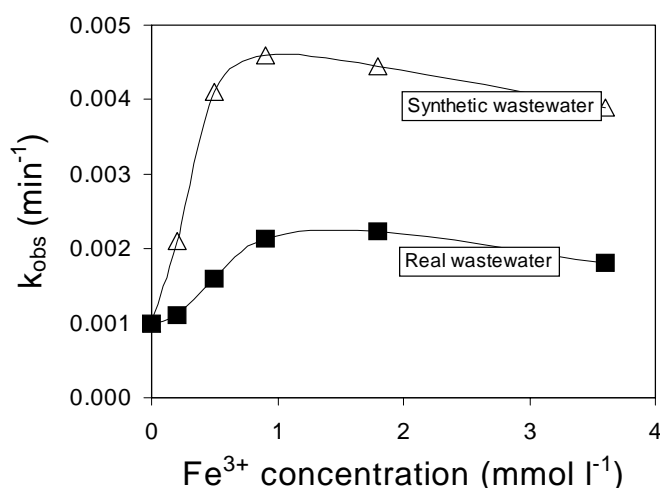
FIGURE 3.9   *The rate constant of photo-Fenton oxidation of synthetic and real AMBI wastewater at different Fe^{3+} concentrations using two different illumination systems.*

3.3.2.3 Effect of H_2O_2 concentration on degradation of synthetic and real waste-water using the Suntest

Another important point to consider in the photo-Fenton oxidation is the amount of H_2O_2 required for efficient AMBI treatment. Several experiments were carried in the Suntest using real wastewater, and results are presented in Fig. 3.10.
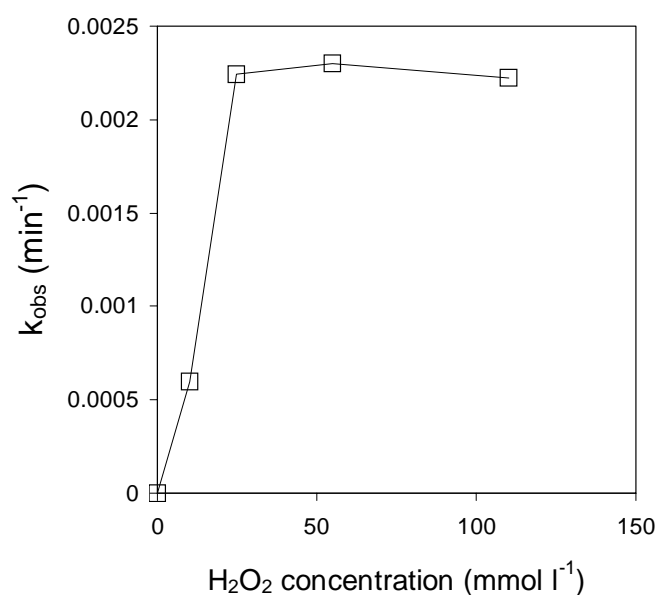
FIGURE 3.10   *The rate constant of photo-Fenton oxidation of AMBI containing wastewater at different H_2O_2 concentrations.*

As shown in Fig. 3.10, a significant enhancement of degradation efficiency was verified when the H_2O_2 concentration was increased from 0 to 25 mmol l^{-1}. Above this concentration, the rate of AMBI oxidation is not affected by the progressive increase of H_2O_2 up to 120 mmol l^{-1}. This is probably due to both, the auto-decomposition of H_2O_2 into oxygen and water (Eq. 3.16), and the scavenging of hydroxyl radicals by H_2O_2. Excess of H_2O_2 will react with $^\bullet OH$ (Eq. 3.17) competing with organic pollutants and consequently reducing the efficiency of the treatment.

$$2H_2O_2 \rightarrow 2H_2O + O_2 \tag{3.16}$$

$$H_2O_2 + {}^\bullet OH \rightarrow {}^\bullet O_2H + H_2O \tag{3.17}$$

Through this work we have found that the optimal concentration of H_2O_2 is 25 mmol l^{-1} for the degradation of AMBI containing wastewater. There was no significant difference observed between the results obtained with synthetic and real wastewater.

3.3.2.4   Degradation pathway of AMBI by $h\nu/Fe^{3+}/H_2O_2$

According to the previous observations, is possible to represent the AMBI degradation by the following simplified schema (Fig. 3.11). A reduction-oxidation cycle of Fe(III)-Fe(II) and the photolysis of Fe(III) aqueous complexes generating $^{\bullet}$OH radicals and the formation of a photoactive complexes [AMBI---Fe(III)] seems to be possible ways for the photo-Fenton degradation of AMBI.
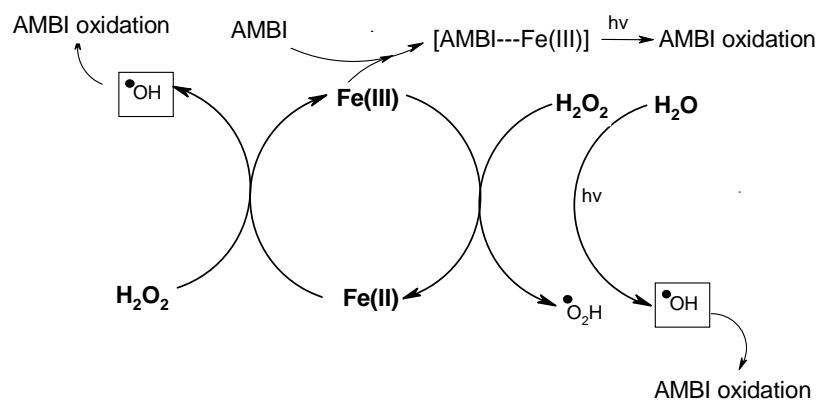
FIGURE 3.11   *Simplified schematic representation of photo-Fenton degradation of AMBI*

3.4   Conclusions

This chapter focuses on the degradation of AMBI by means of the $h\nu/Fe(III)/O_{2(air)}$ and $h\nu/Fe(III)/H_2O_2$ systems using an artificial irradiation source. Concerning the application of the system $h\nu/Fe(III)/O_{2(air)}$ for the degradation of AMBI, the following conclusions can be pointed out:

AMBI exits in two different forms according to the pH: AMBI and its monoprotonated (AMBIH^{+}) form.

The mixture of AMBI and Fe(III) lead presumably to the formation of a complex, which have significant absorption in the visible region, with maximums at 284, 440 and 475 nm. This complex is thermally stable, in the case of the ratio R = [Fe(III)/]/[AMBI] < 1. At higher ratio values (R ≥ 1), a fast thermal redox process, inside the complex, leading to the diminution of the maximum at 284 nm and reduction of Fe(III) to Fe(II) was observed.

The illuminated Fe(III) induced the photo-degradation of AMBI. This process is mainly attributed to three simultaneous process: direct photolysis of the $[Fe^{3+}$---AMBI] complex, the attack of the complex by $^{\bullet}$OH radicals generated by the photolysis of $Fe(OH)^{2+}$, and by the attack of supplementary $^{\bullet}$OH radicals generated by the Fenton and photo-Fenton like reactions, which are induced by the H_2O_2 that have been formed "in situ". When higher concentrations of H_2O_2 are added to AMBI---Fe(III) solution, Fenton and photo-Fenton reactions are considerably improved.

Concerning the application of the system $h\nu/Fe(III)/H_2O_2$ for the degradation of AMBI, the following conclusions can be pointed out:

The optimal concentrations of AMBI, Fe^{3+} and H_2O_2 are 1, 1 and 25 mmol l^{-1}, respectively, for the degradation of AMBI containing wastewater in the photo-Fenton process. Neither Fe^{3+} nor H_2O_2 should be overdosed due to their scavenging effect of hydroxyl radicals. Inhibition of degradation rate was observed at higher concentrations of AMBI probably due to the increase of the darkness of the solution, which hinders the absorption of the UV light required for the photo-Fenton process.

3.5   References

Bajt O, Mailhot G, Bolte M (2001). Degradation of dibutyl phthalate by homogeneous photocatalysis with Fe(III) in aqueous solution. *Appl. Catal. B.* **33** (3) 239-248.

Balzani V, Carassiti V (1970). Photochemistry of Coordination Compounds, Ed. London. p 161-183.

Benkelberg H-J, Warneck P (1995). Photodecomposition of iron(III) hydroxo and sulfato complexes in aqueous solution. Wavelength dependance of OH and SO4- Quantum yields. *J. Phys. Chem.* **99** 5214-5221.

Brand N, Mailhot G, Bolte M (1997). Degradation and photodegradation of tetraacetylethylendiamine (TAED) in the presence of iron(III) in aqueous solution. *Chemosphere* **34** (12) 2637-2648.

Brand N, Mailhot G, Bolte M (1998). Degradation photoinduced by Fe(III). method of alkylphenol ethoxylates removal in water. *Environ. Sci. Technol.* **1998** (32) 2715-2720.

Brand N, Mailhot G, Bolte M (2000). The interaction "light, Fe(III)" as a tool for pollutant removal in aqueous solution: degradation of alcohol ethoxylates. *Chemosphere* **40** (4) 395-401.

Calvert J G, Pitts J N (1966). Photochemistry, Ed. John Wiley & Sons, Inc. New York. p 783-786.

Catastini C, Sarakha M, Mailhot G, Bolte M (2002). Iron (III) aquacomplexes as effective photocatalysts for the degradation of pesticides in homogeneous aqueous solutions. *The Science of The Total Environment* **298** (1-3) 219-228.

Chen R Z, Pignatello J J (1997). Role of Quinone Intermediates as Electron Shuttles in Fenton and Photoassisted Fenton Oxidations of Aromatic-Compounds. *Environ. Sci. Technol.* **31** (8) 2399-2406.

Faust B C, Hoigne J (1990). Photolysis of Fe(III) - hydroxy complexes as sources of OH radicals in clouds, fog and rain. *Atmos. Environ.* **24A** (1) 79-89.

Fenton H J H (1894). Oxidation of tartaric acid in presence of iron. *J. Chem. Soc. Trans.* **65** 899-910.

Hykrdova L, Jirkovsky J, Mailhot G, Bolte M (2002). Fe(III) photoinduced and Q-TiO2 photocatalysed degradation of naphthalene: comparison of kinetics and proposal of mechanism. *J. Photochem. and Photobio. A.* **151** (1-3) 181-193.

Krysova H, Jirkovsky J, Krysa J, Mailhot G, Bolte M (2003). Comparative kinetic study of atrazine photodegradation in aqueous Fe(ClO4)3 solutions and TiO2 suspensions. *Appl. Catal. B.* **40** (1) 1-12.

Lu M C, Chen J N, Chang C P (1997). Effect of Inorganic-Ions on the Oxidation of Dichlorvos Insecticide with Fentons Reagent. *Chemosphere* **35** (10) 2285-2293.

Mailhot G, Asif A, Bolte M (2000). Degradation of sodium 4-dodecylbenzenesulphonate photoinduced by Fe(III) in aqueous solution. *Chemosphere* **41** (3) 363-370.

Mailhot G, Sarakha M, Lavedrine B, Caceres J, Malato S (2002). Fe(III)-solar light induced degradation of diethyl phthalate (DEP) in aqueous solutions. *Chemosphere* **49** (6) 525-532.

Mazellier P, Bolte M (1997). Iron(III) promoted degradation of 2,6-dimethylphenol in aqueous solution. *Chemosphere* **35** (10) 2181-2192.

Mazellier P, Bolte M (2001). 3-chlorophenol elimination upon excitation of dilute iron(III) solution: evidence for the only involvement of Fe(OH)2+. *Chemosphere* **42** (4) 361-366.

Mazellier P, Sarakha M, Bolte M (1999). Primary mechanism for the iron(III) photoinduced degradation of 4-chlorophenol in aqueous solution. *New J. Chem.* **23** (2) 133-135.

Pracht J, Boenigk J, Isenbeck-Schroter M, Keppler F, Scholer H F (2001). Abiotic Fe(III) induced mineralization of phenolic substances. *Chemosphere* **44** (4) 613-619.

Sarria V, Deront M, Peringer P, Pulgarin C (2003). Degradation of a biorecalcitrant dye precursor present in industrial wastewaters by a new integrated iron(III) photoassisted-biological treatment. *Appl. Catal. B.* **40** (3) 231-246.

Sarria V, Parra S, Adler N, Péringer P, Pulgarin C (2002). Recent developments in the coupling of photoassisted and aerobic biological processes for the treatment of biorecalcitrant compounds. *Catal. Today* **76** (2-4) 301-315.

Scott J P, Ollis D F (1995). Integration of chemical and biological oxidation processes for water treatment: review and recommendations. *Environ. Progr.* **14** (2) 88-103.

Stumm X, Morgan X (1981). Aquatic Chemistry, Ed. Interscience USA. p 161-183.

Sun Y F, Pignatello J J (1993). Photochemical-Reactions Involved in the Total Mineralization of 2,4-D by Fe3+/H2O2/UV. *Environ. Sci. Technol*. **27**(2) 304-310.

Sun Y F, Pignatello J J (1993). Photochemical-Reactions Involved in the Total Mineralization of 2,4-D by Fe-3+/H2O2/UV. *Environ. Sci. Technol.* **27** (2) 304-310.

Sychev A Y, Isak V G (1995). Iron compounds and the mechanisms of the homogeneous catalysis of the activation of O2 and H2O2 and of the activation of organic substrates. *Russian Chemical Reviews* **64** (12) 1105-1129.

Wong-Wah-Chung P, Mailhot G, Bolte M (2001). 4,4'-Diaminostilbene-2,2'-disulfonate (DSD) behaviour: under irradiation in water. Decrease of its activity as a fluorescent whitening agent. *J. Photochem. and Photobiol. A.* **138** (3) 275-280.

Zuo Y, Hoigné J (1992). Formation of hydrogen peroxide and depletion of oxalic acid in atmospheric water photolysis of iron(III)-oxalato complexes. *Environ. Sci. Technol.* **26** 1014-1022.

COUPLED PHOTOCATALYTIC-BIOLOGICAL PROCESS AT LAB SCALE

Chapter 3 evaluated the iron photoassisted degradation of AMBI; Chapter 4 focuses on coupling iron photoassisted process with a biological system at lab scale. In this chapter a general strategy to develop combined photochemical and biological systems for biorecalcitrant wastewater treatment is proposed. For the development of this strategy, the following points were taken into account: the biodegradability of the initial pollutant, the chemical and biological characteristics of the phototreated solutions, the definition of the optimal pretreatment time, and the efficiency of the coupled reactor. Following this strategy, two kinds of combined systems were developed using for the photocatalytic pretreatment $h\nu/Fe^{3+}/O_2$ (air) or $h\nu/Fe^{3+}/H_2O_2$ and in both cases immobilized activated sludge culture for the biological step. Both coupled systems were successfully employed for the treatment of AMBI.

4.1 Introduction

As mentioned in chapter 1, Advanced Oxidation Processes (AOP) have been used to enhance the biotreatability of wastewater containing various organics that are non-biodegradable and/or toxic to common microorganisms. Although these processes are very effective in complete mineralization of pollutants, applied alone, they are expensive. A promising alternative to complete oxidation of biorecalcitrant wastewater is the use of an AOP as a pretreatment step to convert initially biorecalcitrant compounds to more readily biodegradable intermediates, followed by biological oxidation of these intermediates to biomass, CO_2 and water.

We developed a general strategy that can be used to develop a combined photoassisted AOP and biological process for biorecalcitrant wastewater treatment (Fig. 4.1). This general way has sometimes to be adapted in order to get water quality that will fulfil the local and other legislation requirements at the lowest financial cost.

WASTEWATER

- Biodegradable? — partly / yes / no
- Toxic at low conc.? — no / yes
- Biodeg. at low conc.? — yes / no
- Biorecalcitrant effluent
- Toxic and/or non-biodegradable effluent
- Biodegradable non-toxic effluent
- Bacterial adaptation and/or selection
- Pretreatment AOPS
- Biodegradable — no / yes
- Specific biological treatment
- biological treatment
- Legislation requirements achieved? — no / yes

EFFLUENT

FIGURE 4.1   *General strategy for coupling photochemical and biological water treatments*

Due to the high cost of photochemical treatments, as a first it must be confirmed that target pollutants are definitively non-biodegradable since for biodegradable compounds, classical biological treatments are, at the present, the cheapest and most environmentally compatible.

In coupled systems, the AOP pretreatment is meant to modify the structure of pollutants by transforming them into less toxic and easily biodegradable intermediates, which allows the subsequent biological degradation to be achieved in a shorter time and in a less expensive way.

The solution resulting from the phototreatment stage is considered to be biologically compatible after the elimination of:
- the initial biorecalcitrant compound,
- the inhibitory and/or non-biodegradable intermediates, and
- the residual H_2O_2, or other inhibitory electron acceptors, whenever they are utilized for the phototreatment.

These requirements, together with information concerning the evolution of toxicity and biodegradability of the phototreated solutions, allow the determination of an optimal phototreatment time, which corresponds to the best cost-efficiency compromise. The phototreatment time must be as short as possible to avoid a high energy consumption, which represents about 60% of the total operational cost when using electric light sources [Matthews 1993]. However, if the fixed pretreatment time is too short, the intermediates remaining in solution could still be structurally similar to initial biorecalcitrant compounds and therefore, non-biodegradable. Furthermore, at short phototreatment time, the residual H_2O_2 concentration or other oxidant may be high enough to inhibit the biological stage of the coupled reactor. Chemical, biological, and kinetic studies must always be carried out to ensure that the photochemical pretreatment induces beneficial effects on the biocompatibility of the treated wastewater.

The aim of this chapter is to combine photoassisted AOP and aerobic biological processes at lab scale to degrade biorecalcitrant, non-biodegradable, and/or toxic pollutants. Two kinds of combined systems were developed using for the photocatalytic pretreatment $h\nu/Fe^{3+}/O_{2(air)}$ or $h\nu/Fe^{3+}/H_2O_2$ systems and in both cases immobilized activated sludge culture for the biological step. Both coupled systems were employed for the treatment of AMBI.

4.2 Experimental

4.2.1 Materials and procedures

AMBI and real industrial wastewater containing AMBI were supplied by Rohner (Basel, Switzerland), $FeCl_3.6H_2O$ was purchased from Fluka and was used without further purification. In the biological reactor the nutrient salts used (P, N, K and metal traces) were added from standard solutions during biological degradation. All solutions were prepared with Millipore water ($\rho = 18.2$ $M\Omega$ cm). Taking into account that the monomeric species $Fe(OH)^{2+}$, the most photoactive specie, strongly depends on the age of the ferric solution (before and after dilution) and on the starting concentration [Mailhot et al. 2000], all solutions were prepared immediately prior to irradiation. For reactions under O_2 and He_2 atmosphere, solutions were bubbled with gas 0.5 h before irradiation. The reaction flask was fitted with a serum stopper.

4.2.2 Coupled photocatalytic-biological flow reactor

The coupled system used for the total mineralization of AMBI wastewater is presented in the Fig. 4.2 and is conformed by one coil photochemical reactor and one biological reactor, which are described a continuation:

Coil photochemical reactor: In the coil photochemical reactor, shown at the left hand side of Fig. 4.2, the contaminated water circulates through and 8 mm-diameter glass spiral of about 20 m long. A 400 W, 40 cm long, medium pressure Hg-lamp (Applied Photophysics) is positioned in such a way that its centre line passes through the axis of the coiled reactor. The predominant radiation is at 366 nm with output equivalent to ~15 Watt. The reactor was designed for different flow rates, organic loads, recirculation rates, and oxidant addition rates. The runs are carried out at room temperature (25^oC). The pollutant solution, H_2O_2 and Fe(III) solution are automatically added by means of peristaltic pumps into the mixing-vessel. The solution is recirculated in batch mode at 22 $l\,h^{-1}$ through the illuminated part of the photoreactor. In order to prepare the photo treated water for biological treatment, the solution is neutralized by means of NaOH at the photoreactor outlet, into the conditioning recipient.

.

PHOTOCHEMICAL REACTOR

BIOLOGICAL REACTOR
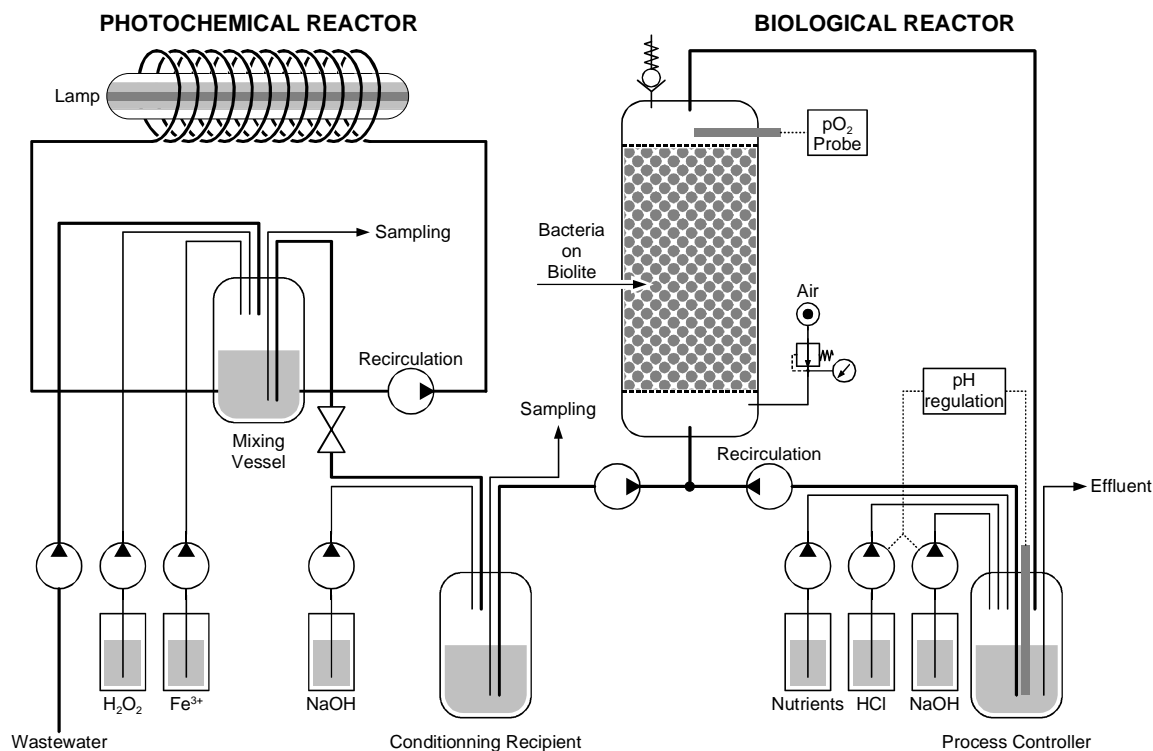
FIGURE 4.2   *Coupled photochemical and biological flow reactor*

Biological reactor: The fixed bed reactor (FBR), shown at the right hand side of Fig. 4.2, consists of a column of 1 l of capacity containing biolite colonised by activated sludge from the municipal wastewater treatment plant (Vidy, Lausanne – Switzerland). The effluent of the photochemical stage is circulated through the bottom of the column, which operated as an up-flow reactor. To assure a good contact of the phototreated solution with the biomass, the water is recirculated at 6 $l\,h^{-1}$ through the column. The pH is controlled by a probe and adjusted at 7.0 by means of HCl or NaOH; depending of the case. The required nutrients (N, P, K and mineral medium) for the bacterial activity are also added. The aeration is about $150\,l\,h^{-1}$ and the O_2 concentration is checked by means of a pO_2 probe on the top of the column.

The coupled reactor was operated in semi continuous (Fed-batch) mode: (i) the solution is recirculated in batch mode in the photoreactor during a pre-defined time; (ii) the pretreated solution is collected in the conditioning recipient, where it is neutralized. (iii) the solution is fed into the FBR in continuous mode.

4.2.3 Chemical and biological analysis

The analytical methods used in this section, DOC, COD, HPLC, BOD, Zahn-Wellens biodegradability test, Microtox and H_2O_2 analysis were described in experimental sections of chapters 2 and 3.

4.3 Results and Discussion

4.3.1 Integration of Fe(III)/hν/O$_{2(air)}$ processes with a biological treatment

In section "3.3.1.2" , it was observed that the iron photoassisted process is able to remove the initial biorecalcitrant compound, but not to mineralize the solution, since the DOC is weakly decreased. Nevertheless, different biodegradability test using Zahn-Wellens procedures [OECD 1996] as well as the bioreactor working with immobilized biomass, shown at right hand side of the Fig. 4.2, demonstrate that the residual DOC remaining in the phototreated solution becomes biodegradable after the total elimination of AMBI. Therefore, the complete mineralization can be achieved in a further biological treatment. To test this hypothesis, a photochemical-biological coupled reactor described in the experimental section was operated in a semi-continuous mode in order to try to carry out the complete mineralization of AMBI wastewater. The coupled system uses a hν/Fe(III)/O$_{2(air)}$ pretreatment under air atmosphere followed by an aerobic biological system with an immobilized activated sludge culture. The phototreatment goal was to remove or transform the biorecalcitrant compound (AMBI) in order to complete the total mineralization of intermediates by the subsequent biological treatment step.

4.3.1.1 Assessment of the optimal pretreatment time for synthetic wastewater

To define the optimal pretreatment time for the degradation of the AMBI in the coupled system, different experiments were carried out in the illumination range of 0-600 min. Each illumination time was applied maintaining the operation of the whole coupled system during at least 5 days after reaching steady state to check and assure the stability of the system during a meaningful period of time. The individual and overall performances of the coupled system, as a function of the

photochemical pretreatment time, are summarised in the Fig. 4.3, which were calculated using the Eq. 2.1 to Eq. 2.3 adapted from [Esplugas and Ollis 1993]:

$$\% \text{ of the initial DOC removed in the photoreactor } = \frac{DOC_{ip} - DOC_{fp}}{DOC_{ip}} \qquad \textbf{(4.1)}$$

$$\% \text{ of the initial DOC removed in the bioreactor } = \frac{DOC_{ib} - DOC_{fb}}{DOC_{ip}} \qquad \textbf{(4.2)}$$

$$\% \text{ of DOC removed in the coupled reactor } = \frac{DOC_{ib} - DOC_{fb}}{DOC_{ip}} \qquad \textbf{(4.3)}$$

where DOC = Dissolved Organic Carbon, the subscript ip = initial DOC entering photo-treatment, fp = ib final DOC leaving photo-treatment, ib= initial DOC entering biotreatment and fb = final DOC leaving biotreatment.
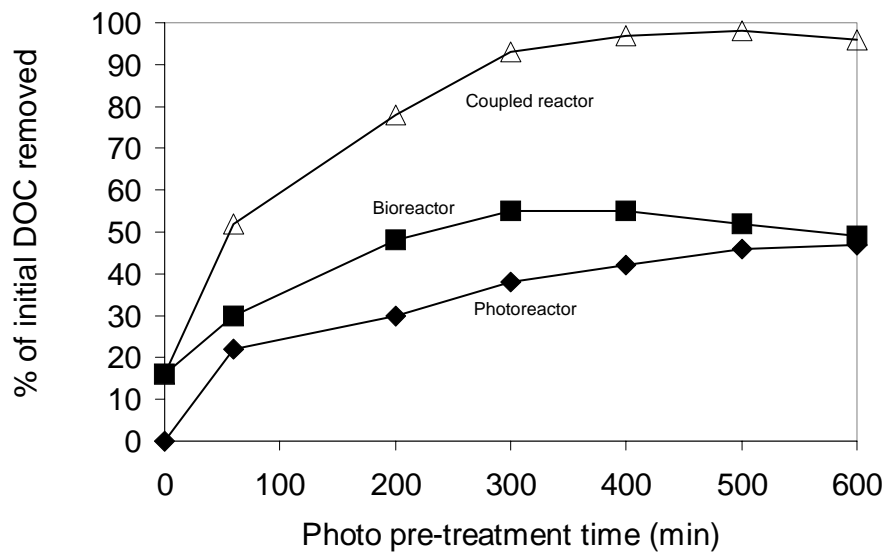
FIGURE 4.3   *DOC degradation by the photoreactor, the bioreactor and the overall coupled system as a function of the of photo-treatment time.*

In Fig. 4.3, it can be seen that the photochemical and biological processes accomplished different percentages of the total degradation. Similar shapes of the curves were obtained by Scoot and Ollis [Scott and Ollis 1996] using a mathematical simulation for the continuous process of a coupled chemical and biological reactor using first order oxidation and Monod rate.

The most interesting time to stop the phototreatment and switch over to the biological (low cost) treatment is around 300 min. At this time, the higher biological efficiency has been attained. Extension of the pretreatment beyond 300 min lead to a greater efficiency of the photochemical treatment but the biological efficiency is negatively affected. This can be attributed to an excessive photochemical treatment result in the degradation of oxidized products possessing a high metabolic value for the microorganisms. In the opposite way, a shorter photochemical treatment than 300 min is maybe not enough to eliminate the biorecalcitrant compound. As a consequence, in order to obtain a compromise between the highest overall efficiency and the shortest photochemical treatment, 300 min. of photochemical pretreatment was applied.

4.3.1.2   Treatment of a real wastewater with the coupled system

Further experiments were made in order to assess the possible application of the coupled iron photoassisted-biological system for the treatment of a real industrial wastewater in which the principal component is AMBI (94% of the initial DOC). The physicochemical characteristics of this wastewater have been described in section "1.4" . With the aim of respect the environmental restrictions in Switzerland [Conseil Fédéral Suisse 1998] concerning the upper limit of iron in an effluent that goes to be discharged in natural waters (2 mg l^{-1}) or to a biological wastewater treatment plant (20 mg l^{-1}). The concentrations of Fe(III) used in this experiments with real wastewater were 2.0 mg l^{-1} and 16,8 mg l^{-1}, and the results are shown in the Table 4.1.

TABLE 4.1   *Initial DOC removed (%) by the individual and overall coupled reactor in the treatment of a real AMBi wastewater.*
[AMBI] = 2.0 mmol l^{-1}

Conditions		Initial DOC removed (%) by		
Initial [Fe(III)] (mg l^{-1})	Phototreatment time (min)	Photoreactor	Bioreactor	Coupled system
2.00	480	28.4	30.8	59.3
16.8	240	17.6	63.2	80.8
16.8	480	36.4	55.5	91.6

From Table 4.1 it is possible to observe that the individual and overall performance of the coupled reactor are considerably affected by the Fe(III) concentration. If this is of 2.0 mg l^{-1}, in

order to respect the norm for natural waters, a slight global yield of 59,3% is only reached in 480 min of illumination. If the concentration of Fe(III) is increased to 16.8 mg l^{-1}, the individual and overall performances of the coupled reactor are almost two times higher. From these results is possible to conclude that in our case, for the treatment of a real sample of AMBI wastewater 12 fold diluted, is possible to use a Fe(III) at a concentration of 16.8 mg l^{-1} (0.3 mmol l^{-1}). In that case the limit of iron concentration in an effluent that can be discharged to a biological wastewater treatment plant is respected.

4.3.2   Integration of photo-Fenton (Fe^{3+}/hν/H_2O_2) and biological processes

A second coupled system using the classical photo-Fenton system in the photochemical pretreatment was tested. The chemical and biological characteristics of the pretreated solutions, fundamental point, in the development of the coupled system were analysed.

4.3.2.1   Chemical and biological characteristics of photo-treated solutions

Dissolved Organic Carbon (DOC), Chemical Oxygen Demand (COD), Biological Oxygen Demand (BOD_5) and the BOD_5/COD ratio were measured to assess the effect of photo-Fenton pretreatment on the biodegradability of synthetic and real wastewater. Table 4.2 shows the values of these parameters before and after photo-Fenton treatment.

TABLE 4.2   *Characteristics of initial and photo-Fenton treated AMBI containing wastewater*

Wastewater	Synthetic		Real	
	Initial	Final	Initial	Final
DOC	330	150	1660	1000
COD	966	162	6430	1380
BOD_5	96	66	51	496
BOD_5/COD	0.1	0.4	0.01	0.35

For synthetic and real wastewater respectively, a mineralization (DOC decreased) of 45.5% and 60.2% was observed. The COD decreased of 16.8% and 21.5% for synthetic and real wastes. BOD_5 may increase or decrease during chemical oxidation. The direction of BOD_5 change depends on the relative initial fractions of non-biodegradable and biodegradable compounds. For synthetic wastewater containing AMBI a reduction of BOD_5 was observed, by contrast to the real wastewater, which present an increment of BOD_5 value. The initial BOD_5/COD ratio of AMBI wastewater was nearly zero. This means that this wastewater is not easily biodegradable. When photo-Fenton treatment was applied, the new BOD_5/COD ratio registered was significantly increased to reach a value of 0.4. It indicates that the biodegradability of the wastewater has been enhanced. As a reference, a domestic wastewater typically has a BOD_5/COD ratio in the range of 0.3-0.5 [Marco et al. 1997]. Due to this fact, photo-Fenton treatment appears to be useful for increasing biodegradability of real and synthetic wastewater containing AMBI.

The toxicity of the photo-treated solutions has an important impact on the biological treatment and on wastewater quality, and that is why it was evaluated during the pretreatment and results are presented in Fig. 4.4. Results observed explain the good BOD_5/COD ratios obtained above since the photo-Fenton treatment significantly decreased the toxicity of synthetic wastewater (7). Specifically, $1/EC_{50}$ values decreased from 0.066 to 0.01, which represents a considerable diminution of its toxicity. This is a highly significant result and suggests that photo-Fenton pretreatment may be an effective means of reducing the toxicity of AMBI-containing wastewater.

The Average Oxidation State (AOS) of the photo-treated solution was also calculated and its evolution is shown in the Fig. 4.4 using the scale at the right hand side. The AOS was estimated according to the Eq. 2.4 (See section "2.3.2.5").

The data show conclusively that the original wastewater was drastically altered, as shown in Fig. 4.4, the AOS attains a broad maximum after approximately 200 minutes of treatment and has a value close to 2.5 (this value is representative of very oxidised substances). These results suggest that after 200 minutes the chemical nature of the intermediates does not vary anymore.
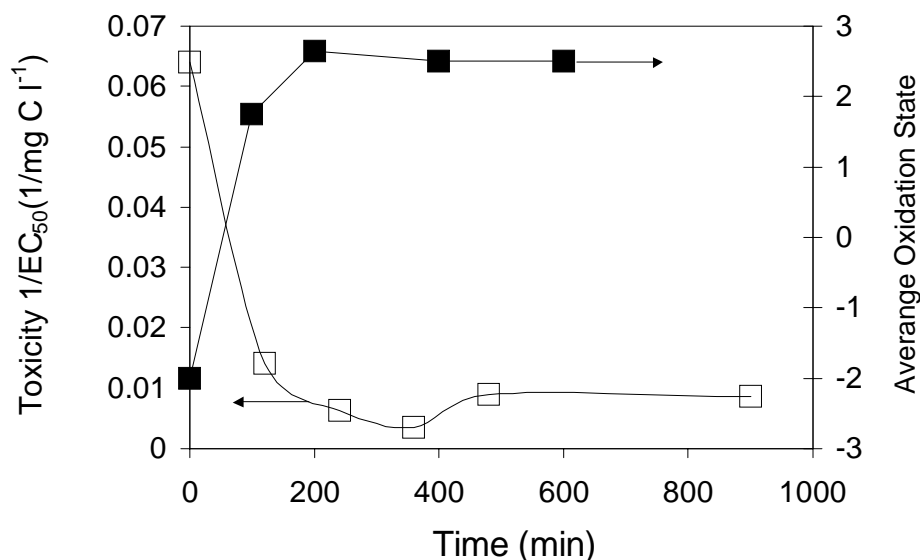
FIGURE 4.4   *Toxicity (□) and Average Oxidation State (■) evolution of real wastewater during the phototreatment as a function of time.*

The DOC evolution in this batch system seems to be directly correlated with both the toxicity level and AOS evolution, and also attains a plateau after 200 min, when between 50-60% of DOC is mineralised. Consequently, when the stabilization of these parameters is reached, the photo-treated solution may be considered as biocompatible. The stabilization of these parameters also indicates that the chemical oxidation is stopped and the photo-Fenton system seems to be no longer effective. In view of this, a biological treatment is required to complete mineralization of this wastewater.

4.3.2.2   Evaluation of biodegradability of photo-treated solution in a Fixed Bed Reactor (FBR)

The biodegradability of the wastewater before and after the photo-Fenton treatment was evaluated in a FBR, using the unacclimated municipal sludge as inoculum. The results of these evaluations are reported in Fig. 4.5, based on DOC evolution. Fig. 4.5 clearly indicates that the biological mineralization of AMBI wastewater is notably improved by photo-Fenton treatment. Additionally this figure demonstrates that biological DOC removal of pretreated AMBI waste requires some days of acclimatisation and growth of bacteria period (traces A and B) to reach an

optimal biological activity (trace C). The chemical and biological characteristics of the photo-treated solutions, suggest that the photo-Fenton process is an effective pretreatment method. Therefore, the integration of photochemical-biological systems appears to be advantageous and necessary to achieve the complete mineralization of AMBI wastewater.
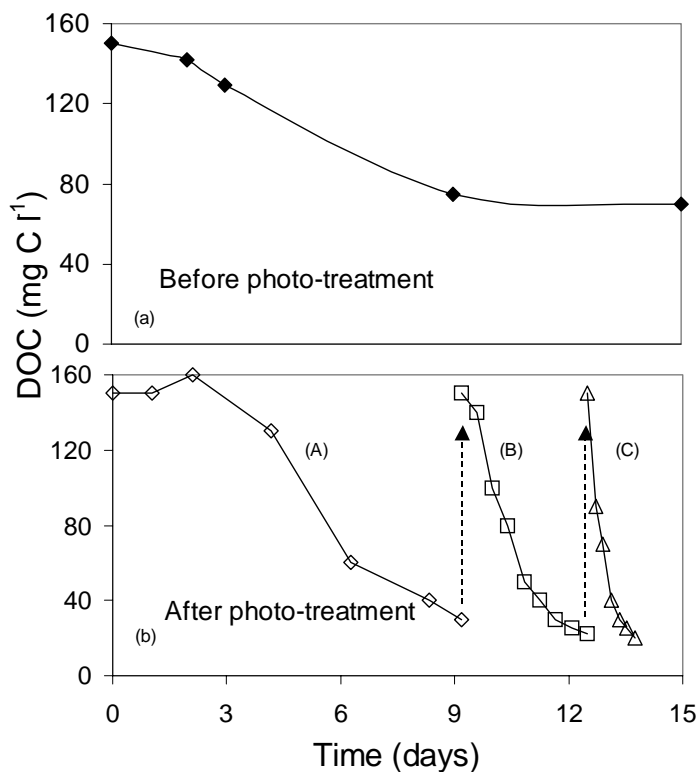
FIGURE 4.5   *Biodegradation of synthetic AMBI wastewater. (a) before and (b) after 1 hour of photo-treatment. (A, ◇) First, (B, □) second and (C, △) third biodegradation cycle after photodegradation.*

4.3.2.3   Photochemical and biological coupled flow treatment

The coupled photochemical-biological treatment in a flow reactor, described in experimental section, was operated for the degradation of real wastewater containing AMBI. The coupled system uses a photo-Fenton pretreatment followed by a biological degradation system with immobilised biomass (acclimatized biomass obtained in the biodegradability essays). This physicochemical pretreatment is necessary to modify the structure of the pollutant by transforming it into less toxic and easily biodegradable by-products. This allows the subsequent biological procedure of destruction to be achieved in a short time. The photo-treatment stage of the coupled system was

intended to obtain a solution biologically compatible in order to eliminate: a) the initial bio-recalcitrant compound, b) the inhibitory intermediates, and c) the residual H_2O_2. This oxidant, required for the photo-treatment oxidation, is known as a bactericide at concentrations higher than 10 mg l^{-1}, and consequently would inhibit the bacterial activity.

These requirements and the information obtained earlier (chemical and biological characteristics of photo-treated solutions) concerning the toxicity and the biodegradability evolution of the photo-treated solution of AMBI wastewater allow us to fix an optimal photo-treatment time in the illuminated part of the coupled reactor. This time corresponds to the moment when the best compromise between the efficiency of the photo-treatment and the cost is reached. To define the optimal operating conditions for the degradation of the AMBI wastewater by the coupled system, different experiments are carried out. The individual and overall performances of the coupled system are summarised in Table 3. As shown in this table 100% of AMBI was eliminated in the Photoreactor and a maximal DOC removal efficiency of 80.3% was attained with an overall (Photoreactor and bioreactor) residence time of 3.5 h.

TABLE 4.3   *Performances of the coupled photochemical-biological system reactor operated in semi-continuous mode for AMBI degradation.*

	Parameter	Photochemical Reactor (0.4 L)	Biological Reactor (1.0 L)	Coupled System
Conditions	Input flow rate (L/h)	0.4	0.4	0.4
	Dilution rate, D (h^{-1})	1.0	0.4	1.4
	Residence time (h)	1.0	2.5	3.5
	Input concentration (mg C l^{-1})	340	156	340
Results	Output conc. (mg C l^{-1})	156	34.5	34.5
	AMBI removed (%)	100.0	-----	100
	DOC removed (%)	44.6	35.7	80.3
	DOC degradation rate (mg C h^{-1})	73.6	48.6	122.2
	Specific DOC degrad. Rate (mg C h^{-1} per liter of reactor)	184	48.6	87.3

4.3.3 O_2 vs. H_2O_2 as electron acceptors in the photo pretreatment

The effectiveness of the aerated system $h\nu/Fe(III)/O_{2(air)}$ against the well-known photo-Fenton system ($h\nu/Fe(III)/H_2O_2$) as pretreatment when they are coupled with a biological final treatment was studied. The performances of both systems are presented in Fig. 4.6. Individual and overall performances of both coupled systems were calculated using the Eqs 4.1 to 4.3 (section "4.3.1.1").

Using the photo-Fenton reaction as a pretreatment step (with H_2O_2) after 2 hours, 65 percent of DOC was degraded in this first step. If the aerated system (without H_2O_2) is applied, only 36 percent was degraded in the photoreactor even after 5 hours of run. It is clear that the addition of H_2O_2 increases the photodegradation rate and efficiency of the photochemical reactor but in both cases almost the same global efficiency was reached (~90%).
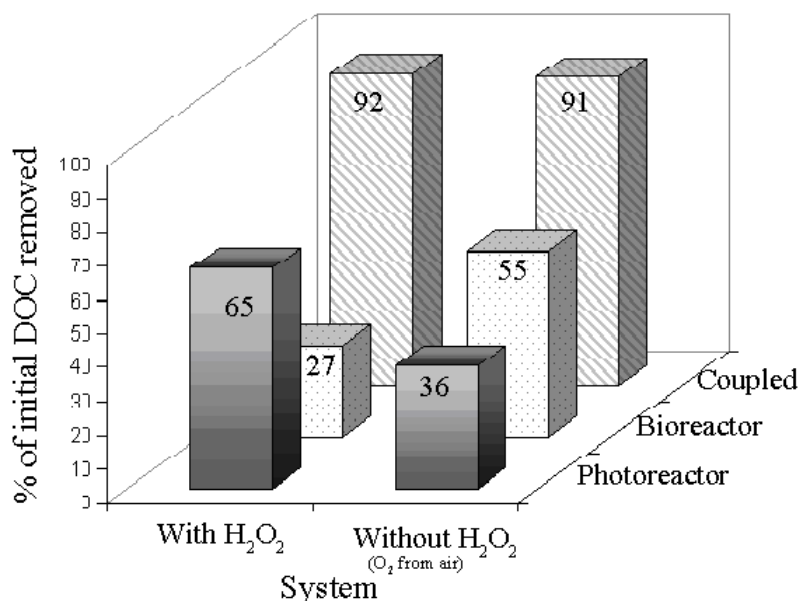
FIGURE 4.6   *Initial DOC removed (%) by the individual and the whole coupled system in the photochemical-biological flow reactor treating AMBI. Phototreatment times were 2 and 5 h, respectively with and without H_2O_2. In both cases AMBI was completely eliminated in the photochemical part of the treatment.*

The higher biological efficiency was observed in the system with O_2 from air (55%), against 27% for the photo-Fenton pretreatment. Nevertheless to make a balance between both options,

other parameters as the residence time must be more deeply considered. Table 2 summarized the performances for AMBI degradation of the both coupled system under study.

TABLE 4.4   *Performances for AMBI degradation by the coupled iron photo-assisted-biological systems*

	Parameter	Pretreatment	
		$h\nu/Fe(III)/H_2O_2$	$h\nu/Fe(III)/O_{2(air)}$
Photoreactor	Input flow rate (ml h^{-1})	438	219
	Residence time (h)	2	5
	Input concentration (mg C l^{-1})	234	217
	Output concentration (mg l^{-1})	81	138
	DOC removed (%)	65	36
	AMBI removed (%)	100	100
	Degradation rate (mg C l^{-1} h^{-1})	67	17
Bioreactor	Output concentration (mg l^{-1})	17	18
	DOC removed (%)	27	55
	Degradation rate (mg C l^{-1} h^{-1})	28	52
	Overall efficiency (Related to DOC degradation)	93	91

In both coupled systems, 100% of the initial concentration of AMBI and almost 91% of the initial DOC was removed. The residence time of the system without H_2O_2 is 2.5 times higher than for the system with H_2O_2. It is normally accepted that reduction of the cost in wastewater treatment by a combined system typically involves minimization of: (i) the time of pretreatment by AOP and (ii) the use of the chemical additives in order to favour the contribution of biological systems. In our case we can save an expensive chemical reagent, as the H_2O_2, but only extending the phototreatment time. From the practical and economical points of view, more detailed research at higher scale are necessary to asses if the addition of H_2O_2 can be avoided. In this sense, we decided to go further in the investigation carrying out some experiments using the direct solar radiation with the pilot solar CPC reactor described in the experimental section.

4.4   Conclusions

A general strategy to develop combined photochemical and biological systems for biorecalcitrant wastewater treatment was proposed. For the development of this strategy, the following points need to be considered: the biodegradability of the initial pollutant, the chemical and biological characteristics of the phototreated solutions, the definition of the optimal pretreatment time, and the efficiency of the coupled reactor.

Following this strategy, two kinds of combined systems were developed using for the photocatalytic pretreatment $h\nu/Fe^{3+}/O_{2(air)}$ or $h\nu/Fe^{3+}/H_2O_2$ and in both cases immobilized activated sludge culture for the biological step. Both coupled systems were successfully employed for the treatment of AMBI.

The iron photoassisted process was able to remove the initial AMBI concentration and produce biocompatible intermediates. In this sense, a coupled Fe(III) photoassisted-biological system without addition of other electron acceptor than O_2 from air was developed and successfully applied for the mineralization of AMBI.

The coupled reactor was operated in a semi-continuous mode and an optimal pretreatment time of 300 min was found. At this moment the best compromise between the shortest photochemical pretreatment (high cost) and the highest biological (low cost) and overall efficiency was reached. Moreover, the Fe(III) concentration used in the pretreatment (16.8 mg l^{-1}) are low enough for respect the upper limit of iron in an effluent that goes to be discharged to one wastewater treatment plant.

A second coupled reactor using photo-Fenton as a pretreatment was developed. This study demonstrates the utility of the photo-Fenton system as a pretreatment method preceding a biological treatment for the complete mineralization of wastewater containing AMBI. The toxicity and biodegradability analyses of the phototreated solutions show that the solution resulting from the photodegradation of AMBI is biologically compatible and its complete mineralization can be performed by biological means; additionally we observed that the biological mineralization of AMBI wastewater is notably improved by photo-Fenton pretreatment.

The coupled photochemical and biological flow reactor operated in semi-continuous mode seems to be an efficient system for the degradation of AMBI. The primary degradation efficiency, expressed as percentage of AMBI removed, was 100% and the ultimate degradation efficiency (mineralization) was 83.5%.

H_2O_2 and O_2 were compared as electron acceptors in the iron photoassisted pretreatment. For both compared systems the same global efficiency of the coupled reactor was achieved (90% of DOC removed). Nevertheless the $h\nu/Fe(III)/H_2O_2$ was 2.5 times more efficient that the $h\nu/Fe(III)/O_{2(air)}$ system, regarding the phototreatment time. The higher biological efficiency was observed in the system with O_2.

The degradation of AMBI by the $h\nu/Fe^{3+}/O_{2\ (air)}$ - biological system is an important result from the environmental point of view. However, in the tested conditions, this system appears as a not promising alternative for AMBI wastewater, due to the long photo pretreatment time that is needed.

4.5   References

Esplugas S, Ollis D F, Eds. (1993). Process integration development: Reactor kinetic models for sequential and biological oxidation for water treatment. Chemical Oxidation Technologies for the Nineties IV. Lancaster, Technomic Publishing Company.

Mailhot G, Asif A, Bolte M (2000). Degradation of sodium 4-dodecylbenzenesulphonate photoinduced by Fe(III) in aqueous solution. *Chemosphere* **41** (3) 363-370.

Marco A, Esplugas S, Saum G (1997). How and why combine chemical and biological processes for wastewater treatment. *Water Sci. and Technol.* **35** (4) 321-327.

Matthews R W (1993). Photocatalysis in water purification: possibilities, problems and prospects. Photocatalytic Purification and Treatment of Water and Air. Ollis D F, Al-Ekabi H, Ed. Elsevier Science Amsterdam.

OECD (1996). *Guidelines for testing of Chemicals, test 302B.*

Scott J P, Ollis D F (1996). Engineering Models of Combined Chemical and Biological Processes. *J. Environ. Eng.* **122** (12) 1110-1114.

Conseil Féféral Suisse (1998). Ordonnance sur la protection des eaux usées (OEaux) 814.201 du 28 octobre.

COUPLED SOLAR-BIOLOGICAL SYSTEM AT FIELD PILOT SCALE

Chapter 4 described the development of two photochemical-biological systems at lab scale (1 litre); Chapter 5 illustrates the development and optimization, at pilot scale (60 litres), of a coupled system for water treatment. In this chapter a coupled solar-biological system at field pilot scale was designed, erected, and experimental results are presented. The strategy to develop this system implicates, the choice of the most appropriate solar collector and the most efficient AOP, the optimization of AOP, the monitoring of the chemical and biological characteristics of photo-treated solution and the evaluation of the performances of the coupled solar-biological flow system. Experimental results indicate that coupling solar-biological processes at pilot scale is an effective approach to the treatment of real industrial wastewater.

5.1 Introduction

Solar photocatalytic mineralisation of organic pollutants of water employing the interaction between ultraviolet radiation and a catalyst has been widely demonstrated and it represents a strong potential method for the destruction of toxic organics in water [Malato et al. 1996; Malato et al. 1997; Malato et al. 1998; Malato et al. 1999]. Where medium or high solar radiation is available, solar detoxification is useful for treating water contaminants with several hundreds of mg l^{-1} of non-biodegradable contaminants.

Numerous work deal with study of basic factors related to the solar photocatalytic technology and its applications [Alfano et al. 2000]. Previously, Parra [Parra 2001] approached the basic principles related to the solar spectrum and specifically to the solar UV radiation since this part of

the solar spectrum is the most important for driving chemical processes and the application of the solar photocatalysis.

Among different solar photocatalytic degradation systems, several studies have applied the solar photo-Fenton process for the degradation of different organic pollutants: 4-chlorophenol [Krutzler et al. 1999], imidacloprid [Malato et al. 2001], p-nitrotoluene-o-sulfonic acid [Parra et al. 2001] and metobromuron and isoproturon [Parra et al. 2000]. Recently, Mailhot et al. [Mailhot et al. 2002] observed that Fe(III)-solar light induced degradation of diethyl phtalate in aqueous solutions.

At present, it is argued that the use of sunlight instead of artificial light for the photo-Fenton reaction, would dramatically lower the cost of the process and thus provide a major step towards industrial application [Malato et al. 2002]. Nevertheless, according to Scott and Ollis [Scott and Ollis 1997], there could be many scenarios in which, a single-step oxidative treatment could be not economically attractive. Water may contains «scavengers», either as inorganic compounds [Kiwi et al. 2000], natural organic matter [Lindsey and Tarr 2000] or other «non-target» organics [Cavicchioli and Gutz 1997], which compete with the target compound for oxidant, leading to a decrease of efficiency. Even in water containing one predominant target compound, oxidation can quickly lead to the formation of multiple intermediates which can compete for oxidant. Intermediates can also decrease the overall effectiveness of the oxidation process because these more oxidized species generally have lower reactivity toward $^\bullet OH$ radicals. Considering that, coupled photochemical-biological system, in spite of using solar radiation, seems advisable.

In chapters 3 and 4 it was shown that the systems $h\nu/Fe^{3+}/O_{2(air)}$ and $h\nu/Fe^{3+}/H_2O_2$ efficiently removed the initial biorecalcitrant compound (AMBI). Theses systems were also used as a pretreatment step in coupled photocatalytic-biological coupled reactors at lab scale and using artificial radiation. One important factor of the iron photoassisted process is the light sensitivity up to a wavelength of 600 nm (35% of solar irradiation).

This study aims to design, erect and operate on the first coupled solar-biological system at pilot scale. Photo-Fenton system was used in the pretreatment, since this method has shown to be the most effective among different tested AOP and the following biodegradation process was carried in an immobilised activated sludge bioreactor.

In this chapter, the following topics are also studied: (a) the choice of the most appropriate solar collector. This part of the study was carried at the Plataforma Solar de Almeria (PSA) (b) the optimization of Fe^{3+} and H_2O_2 concentrations in the photo degradation process using Response Surface Methodology (RSM), (c) the biodegradability of the phototreated solutions and (d) the performance of the coupled solar-biological flow system.

5.2   Experimental

The analytical methods and chemicals used in this work were identical to that presented in sections "4.2.1" and "4.2.3" .

5.2.1   Coupled solar-biological system at pilot scale

The investigation was carried out using a coupled solar-biological reactor that has been designed, built and operated at EPFL. This system is conformed by a Compound Parabolic Solar Collector (CPC) and a bioreactor as illustrated in Fig. 5.3.

5.2.1.1   Solar reactor

The configuration of the CPC is the same as that at the Plataforma Solar de Almeria (PSA) [Malato et al. 2001]. CPC is a static collector with a reflective surface describing an in-volute around a cylindrical reactor tube. The CPC has 3 modules (total collector surface 3.08 m^2, photoreactor illuminated volume 24 l and total reactor volume 60 l) whereas one module consists of 8 tubes and mounted on a fixed platform 46° tilted (local latitude). The three modules are connected in series with water directly flowing through them at 30 l min^{-1}, leading finally to a recirculation tank connected to a centrifugal pump (Fig. 5.1).

Due to the reflector design of the CPC shown in Fig. 5.2, almost all the UV radiation arriving at the collector aperture area (not only direct, but also diffuse) can be collected and so be available for the process in the reactor. The UV light reflected by the CPC is distributed around the back of the tubular photoreactor and as a result, most of the reactor tube circumference is illuminated.

FIGURE 5.1   *View of the CPC used for the solar driven experiments at the EPFL*
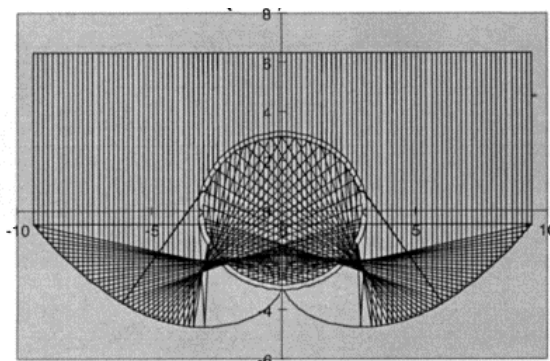
FIGURE 5.2   *Solar reflection on the CPC collector (source: [Robert and Malato 2002]).*

5.2.1.2   Biological reactor

The bioreactor is conformed by 3 modules: a 50-litres conditioning container, a Fixed Bed Reactor (FBR) and a decanter. The conditioning container is equipped with a pH control unit (Liquisys, Endress + Hauser) for pH adjustment using either HCl or NaOH. A 1-l tank was

SOLAR REACTOR
Compound Parabolic Concentrator (CPC)

BIOLOGICAL REACTOR
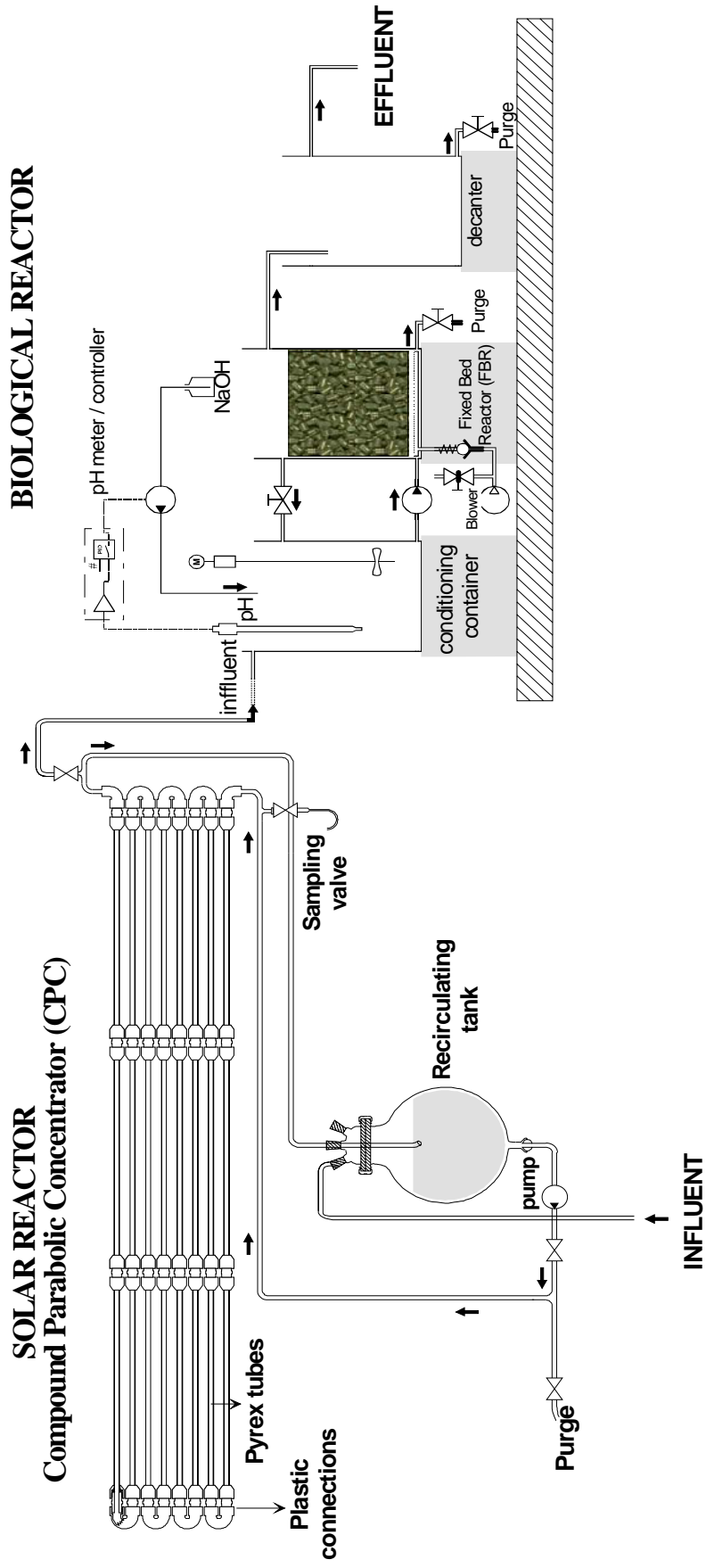
FIGURE 5.3 *Schematic representation of the coupled solar-biological flow reactor*

installed to supply nutrients (N, P, K and microelements) that may be used. The photo-pretreated water is piped across the bottom layer to the FBR by means of a centrifugal pump. The FBR consist of a 43-litre column containing plastic supports (Material: Polypropylene; nominal diameter: 15 mm, density: 80 kg m^{-3}, voluminal surface: 320 m^2 m^{-3}, empty space fraction: 0.91 m^3 m^{-3}) colonized by activated sludge from the municipal wastewater treatment plant of Vidy, Lausanne–Switzerland. The effluent is circulated through the column, which operates as an up-flow reactor. The FBR is equipped with an air blower to supply oxygen (1.15 m^3 min^{-1} of air) to the microorganisms. The recirculation flow rate is 10 l min^{-1}. The top treated water over-flows to a 50-litres decanter, where sludge is extracted. A picture of the pilot system is shown in the Fig. 5.4 and schematic diagram shown in the Fig. 5.3

FIGURE 5.4   *Coupled solar-biological flow reactor at pilot scale installed at EPFL.*

5.2.2   Parabolic-trough concentrator

The Parabolic-Trough Concentrator (PTC), previously described in detail [Minero et al. 1993], consists of a turret with a platform supporting four parabolic trough collectors with focus-

absorber tubes. The platform is moved by two motors controlled by a two-axis (azimuth and elevation) tracking system. The tracking system consists of a photochemical cell keeping the aperture plane perpendicular to the solar rays, which are reflected onto the focus (absorber) through which circulates water to be treated (Fig. 5.5).

FIGURE 5.5   *The Parabolic-Trough Concentrator at the Plataforma Solar de Almeria.*

5.2.3   Solar Ultraviolet radiation

Solar ultraviolet radiation is determined during the experiments by means of a global UV radiometer (KIPP&ZONEN, model CUV3), showed in Fig. 5.6(b), mounted on a 46° fixed-angle platform (the same angle as the CPC). It provides data in terms of global UV solar energy power incident per unit area, W_{UV} m^{-2}. Solar-UV power varies during experiments, especially when clouds are passing by. Data combination from several days and their comparison with other photocatalytic experiments is done by the application of Eq. 5.1.

$$Q_{UV, n} = Q_{UV, n-1} + \Delta t_n \overline{UV}_{G-D, n} \frac{A_{collector}}{V_{TOT}} \qquad \textbf{(5.1)}$$

Where $\Delta t_n = t_n - t_{n-1}$, t_n is the experimental time for each sample, $\overline{UV}_{G,n}$ is the average UV_G (Global UV radiation) during Δt_n, $A_{CPC} = 3.08$ m^2, $V_{TOT} = 39$ l and $Q_{UV,n}$ is the accumulated energy incident on the photoreactor for each sample during the experiment per unit of volume (kJ l^{-1}).

During the experiments performed using the PTC at the PSA, the direct UV radiation has been determined using a direct-UV sensor (international Light-ESD 400), which is mounted on the sun-tracking platform. With Eq. 5.1, the accumulated energy per unit of volume incident on the reactor (Q_{UV}) has been calculated, taking into account that $\overline{UV}_{D,n}$ is the average UV_D (Direct UV radiation) and the PCT dimensions: $A_{PTC} = 29$ m^2 and $V_{TOT} = 260$ l.
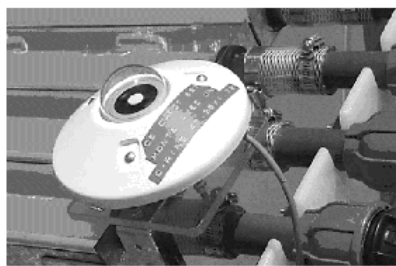
FIGURE 5.6   *View of the solar radiometer.*

5.3   Results

5.3.1   Choice of the solar photoreactor: Comparison between medium and low concentrating solar collectors in hν/Fe^{3+}/O$_2$ degradation of AMBI

This part of the study, carried out at the PSA, focuses on the comparison of performance of two types of solar collectors, in order to find out the more suitable to be used in a pilot coupled solar-biological flow system. A medium concentrating system, two-axis Parabolic Trough Collector (PTC) and a low concentrating system, Compound Parabolic Collector (CPC), were compared. The hν/Fe^{3+}/O$_2$ photocatalytic system was chosen, considering that its performance is only related to the radiation absorbed by the solar reactors.

Fig. 5.7 shows the linear relation between $-\ln(C/Co)$ and Q_{UV} for the AMBI degradation in the reactors. In both cases, the kinetics of AMBI degradation is apparent first order, and its performances are quit similar, with a rate constant (k_{app}) equal to 0.0121 and 0.0112 l x kj^{-1} for the CPC and the PTC reactors, respectively. In order to explain this result, and to choose the best technology, more other factors were taken into account:

- The ability of the CPC to capture both diffuse and direct UV radiation. In contrast, a concentrating design like that of the PTC benefits only the direct UV radiation.

- Statistic analyses carried out at the PSA [Blanco and Malato 1996] revealed that the global radiation is higher than the direct radiation during all the year.

Other advantages of the CPC reactor have been previously reported [Malato et al. 1997; Parra et al. 2001]: low manufacturing, installation, and maintenance cost, and the operational facilities. Considering these observations, the CPC appears as the best technology for a coupled solar-biological wastewater treatment system.
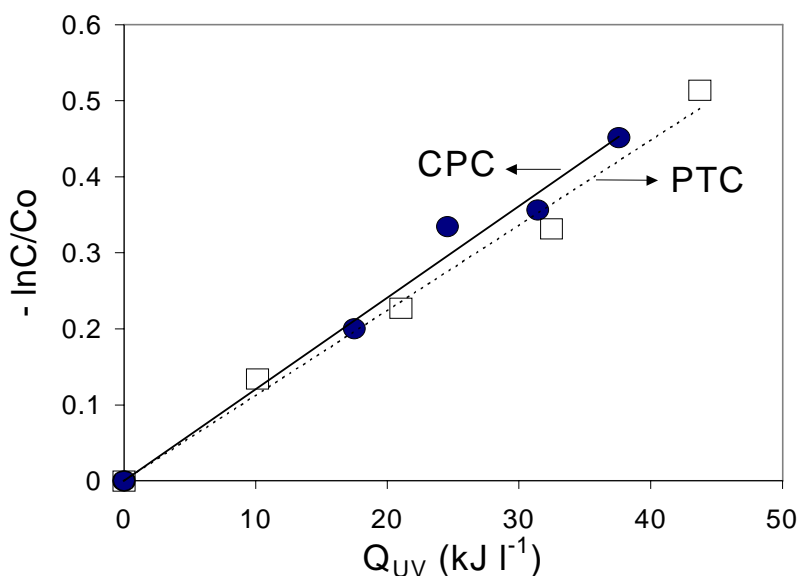
FIGURE 5.7   *Linear transform of kinetic curves of iron-photoassisted degradation of AMBI in a CPC and in a PTC. [AMBI]$_o$ = [Fe^{3+}]$_o$ = 1.0 mmol l^{-1}.*

5.3.2 Comparison of different solar photocatalytic treatments using a CPC

A CPC, described in the experimental section, was erected at EPFL. Various experiments were carried out in order to make an exploratory comparison of the efficiency of some solar photoassisted treatments on the degradation of AMBI.

Fig. 5.8 shows the evolution of AMBI concentration as a function of accumulated energy, when an aqueous solution of AMBI is exposed to $h\nu/TiO_2/O_2$, $h\nu/TiO_2/H_2O_2$, $h\nu/Fe^{3+}/O_2$ and $h\nu/Fe^{3+}/H_2O_2$ systems.
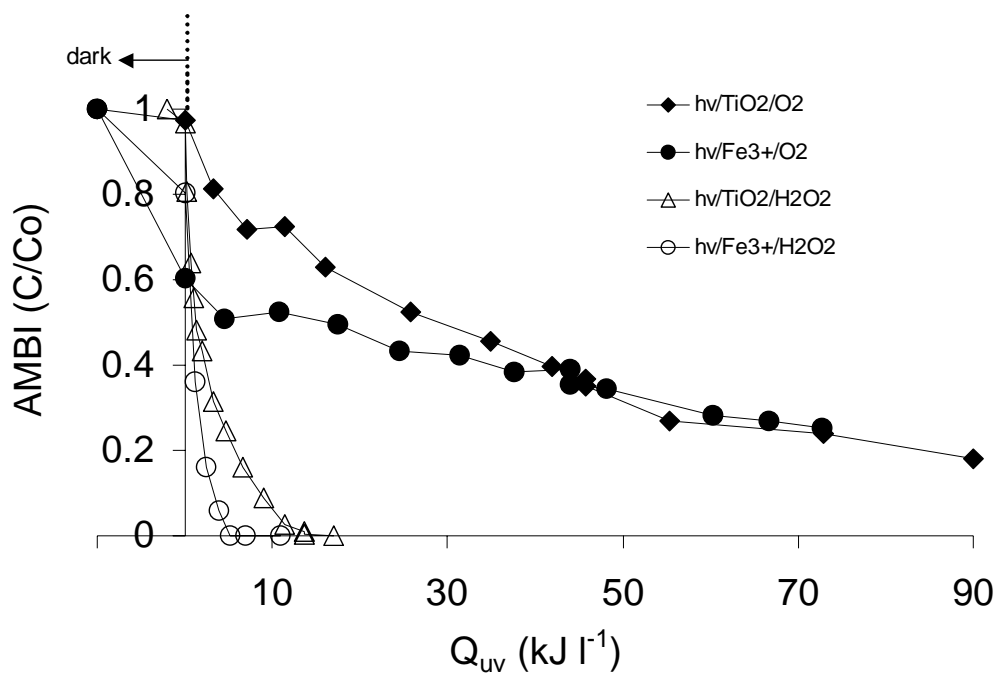
FIGURE 5.8   *Evolution of AMBI concentration as a function of the accumulated solar energy. Study of some photocatalytic systems. AMBI (1.0 mmol l^{-1}), H_2O_2 (25 mmol l^{-1}), TiO_2 (1 g l^{-1}) and Fe^{3+} (1.0 mmol l^{-1}).*

The results presented in Fig. 5.8 clearly demonstrate that both $h\nu/Fe^{3+}/H_2O_2$ and $h\nu/TiO_2/H_2O_2$ systems are effective, from the kinetic point of view. With an accumulated solar energy of 10 and 18 kJ l^{-1}, 100% of the initial AMBI concentration is eliminated from the solution using $h\nu/Fe^{3+}/H_2O_2$ and $h\nu/TiO_2/H_2O_2$ systems, respectively.

It was also observed that the performances of $h\nu/Fe^{3+}/O_2$ system are similar to those of the most common system studied, $h\nu/TiO_2/O_2$. The system $h\nu/Fe^{3+}/O_2$ appears as a new and interesting alternative for the treatment of pollutants in water.

Although the four oxidation systems are effective to the degradation of AMBI, the photo-Fenton process appears to be the most efficient. Moreover, its homogenous character provides with reasonable limitations good engineering conditions for coupling this system with a complementary biological treatment.

5.3.3   Optimization of Fe^{3+} and H_2O_2 concentration on the solar photo-Fenton degradation of AMBI using Response Surface Methodology

Optimization procedures for water treatment, in particular iron-photoassisted systems, is an enormous challenge. To find out the optimal degradation parameters, most studies have focused on a univariate approach [Parra et al. 2000]. In this case, one parameter is varied each time maintaining the others constant during the experiment. An alternative to such approach is the Response Surface Methodology (RSM) [Khuri and Cornell 1987], a statistical tool that allows the simultaneous change of several variables. This methodology has shown to be a valuable tool to model complex process, such as the light-enhanced Fenton reaction and to achieve at minimal cost, optimal experimental parameters [Oliveros et al. 1997; Fernandez et al. 2002]. RSM is a collection of statistical and mathematical techniques useful to develop, improve, and optimize processes performing a minimal number of well-chosen experiments [Myers and Montgomery 1995].

In this section, the effects of the two critical factors, hydrogen peroxide, and ferric ion concentration, on the solar photo-Fenton degradation of AMBI were simulated and evaluated using the RSM. RSM uses an empirical mathematical model (e.g polynomial) to represent the response (y) in the experimental field, which depends on the controllable inputs that are natural variables: ξ_1, $\xi_{2,...}, \xi_{k,}$ (Eq. 5.2).

$$y = f(\xi_1, \xi_2, ...,\xi_k)\varphi \qquad\qquad\qquad (5.2)$$

Since, in this study the two natural variables:

$\xi_1 = Fe^{3+}$ concentration $(g\ l^{-1})$

$\xi_2 = H_2O_2$ pumping rate $(ml\ min^{-1})$,

are expressed in different units and have different limits of variation, their effects can only be compared by the RSM if they are coded.

To each natural variable ξ_i, there is a correspondent dimensionless coded variable x_i as defined in Eq. 5.3

$$x_i = 2\frac{(\xi_i - \xi^*_i)}{d_i} \tag{5.3}$$

Where ξ_i is the actual value in original units, ξ_i^* the arithmetic mean of the high and low levels of i, and d_i the difference between the low and high levels of i.

In terms of the coded variables, the true response function (Eq. 5.4) is now written as:

$$y = f(x_1, x_2, ..., x_k)\varphi \tag{5.4}$$

Because the form of the true response function f is unknown, we approximate. So for, a Doehlert's uniform array was employed allowing modelizing the curve response surface. The associated response function (y) is represented by a quadratic polynomial model of the form:

$$y = b_0 + b_1x_1 + b_2x_2 + b_{12}x_1x_2 + b_{11}x_1^2 + b_{22}x_2^2 \tag{5.5}$$

Where b_0, b_i, b_{ii} and b_{ij} are the regression coefficients of the polynomial function. x_i and x_j, the concentration of Fe^{3+} and H_2O_2, are the coded variables and y is the apparent initial rate constant for the abatement of AMBI.

Table. 5.1 presents the experimental matrix for seven experiments. The experimental points, considering low and high levels for Fe^{3+} $(0.0–0.2\ g\ l^{-1})$ and H_2O_2 $(0.060\text{-}0.112\ ml\ min^{-1})$, are

uniformly distributed in a spherical experimental domain. Experiment 7 was repeated twice more (8 and 9) in order to check the reproducibility.

TABLE 5.1 *Experimental plan design and results obtained for the optimization of Fe^{3+} and H_2O_2 concentration in the photo-Fenton degradation of AMBI wastewater (5 mmol l^{-1}; DOC = 480 mg C l^{-1}) using a CPC reactor.*

Experiment number	Coded variables		Natural variables		Response
	Conc. Fe^{3+}	H_2O_2 pumping rate	Conc. Fe^{3+} (g l^{-1})	H_2O_2 pumping rate (ml min^{-1})	k_{app} (l kJ^{-1})
1	1.00	0.00	0.20	0.06	0.02
2	-1.00	0.00	0.00	0.06	0.01
3	0.50	0.87	0.15	0.11	0.02
4	-0.50	-0.87	0.05	0.01	0.00
5	0.50	-0.87	0.15	0.01	0.00
6	-0.50	0.87	0.05	0.11	0.01
7	0.00	0.00	0.10	0.06	0.01
8	0.00	0.00	0.10	0.06	0.01
9	0.00	0.00	0.10	0.06	0.01

The treatment of experimental responses, the mathematical resolution of the matrix, and the three-dimensional representation of the phenomenon were performed using the NEMROD Software [Mathieu et al. 2000].

The coefficients of the quadratic model in the polynomial expression (Eq. 5.5) calculated by multiple regression analysis, are given in Eq. 5.6. These coefficients represent the weight of each variable, the quadratic effect, and the first order interaction between the coded variables.

$$y = 0.012 + 0.007x_1 + 0.006x_2 + 0.005x_1x_2 + 0.002x_1^2 - 0.007x_2^2 \qquad \textbf{(5.6)}$$

The polynomial equation permits to draw the contour plots and the three-dimensional representation of the phenomenon (Fig. 5.9).
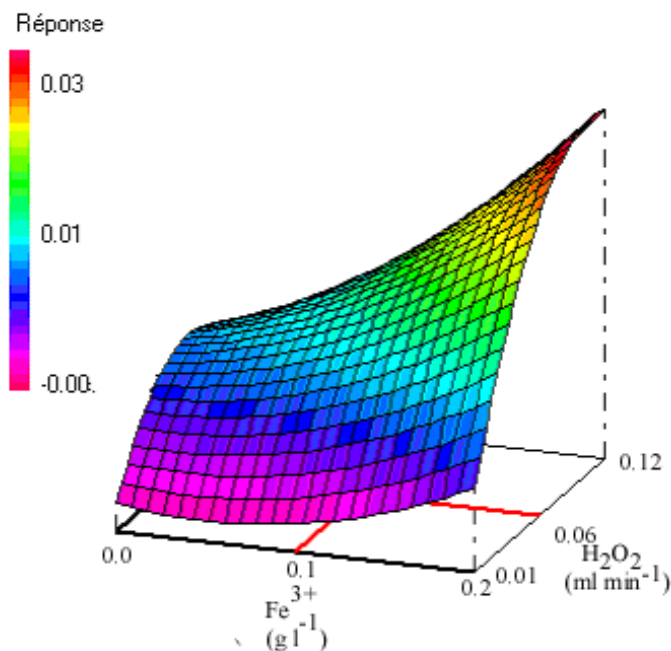
FIGURE 5.9   *Optimization of Fe^{3+} and H_2O_2 concentration for solar photo-Fenton degradation of AMBI using Surface Response Methodology. Three-dimensional representation of the response surface for the apparent initial rate constant (k_{app}).*

Fig. 5.9 shows that, for all iron concentrations, the H_2O_2 concentration has an optimum value in which the k_{app} reaches a maximum. For high H_2O_2 concentrations the AMBI degradation decays. The effect is more clear when the iron concentration is low.

The detrimental effect of higher H_2O_2 concentrations is probably due to both auto-decomposition of H_2O_2 into oxygen and water, and the recombination of $^\bullet OH$ as presented in section "3.3.2.3" .

Maximum degradation rate was predicted in the region of 0.15 to 0.2 g l^{-1} of Fe^{3+} and 0.06 to 0.12 ml l^{-1} of H_2O_2. Taking into account the initial AMBI concentration, it is observed that optimal ratio of AMBI/Fe^{3+}/H_2O_2 of 1/0.1/10 provides optimal performances for AMBI degradation.

5.3.4 Chemical and biological characteristics of photo-treated solutions using hν/Fe^{3+}/H$_2$O$_2$

Considering that the basic objective of this investigation was not to achieve the complete photo-mineralization, but to reach a biocompatible solution that can be conducted towards a biological process, it was necessary to assess the chemical and biological characteristics of the residual DOC contained in the photo-treated solutions.

Several experiments were carried out in order to obtain information concerning the evolution of the biorecalcitrant compound concentration and the AOS, with the aim to define the moment when photo-treatment can be stopped to lead the solution to the biological reactor.

Fig. 5.10 shows the profile of AMBI concentration and the AOS as a function of accumulated amount of energy per unit of volume (kJ l^{-1}). During the first part (dark conditions) almost 10% of the initial DOC concentration is removed. This can be attributed to the complexation of AMBI by Fe(III) as well as the dark Fenton reactions. Upon solar illumination (photo-Fenton reaction) the degradation rate is clearly improved and almost 40% of the initial AMBI is removed when 10 kJ l^{-1} are accumulated in the CPC.
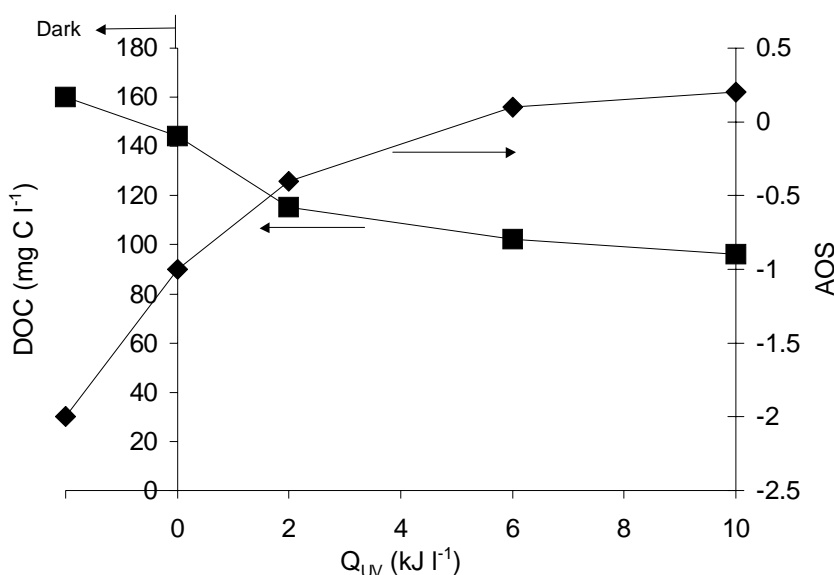
FIGURE 5.10   *AMBI concentration and average oxidation state (AOS) evolution as a function of accumulated energy for the degradation of 60 l of real AMBI wastewater. AMBI (1 mmol l^{-1}), Fe^{3+} (0.1 mmol l^{-1}) and H$_2$O$_2$ (10 mmol l^{-1})*

The AOS, a gross parameter useful to estimate the oxidation degree of mixed solutions, which gives indirect information on its biodegradability, was calculated using the Eq. 2.4 (section "2.3.2.5")

From Fig. 5.10, it is observed that the AOS value increased as a function of the accumulated energy and attained almost a plateau after approximately 8 kJ l^{-1}. This results suggest that more oxidised intermediates are formed in solution and after 8 kJ l^{-1}, the chemical nature of most of them does not vary anymore even if the phototreatment is prolonged. Formation of very oxidised intermediates is an indirect indication of the ability of the solar pretreatment to improve the biodegradability of real AMBI wastewater.

Moreover, as indicated section "4.3.2.1" , according to different biodegradability test using Zahn-Wellens procedures [OECD 1996] as well as on a FBR, the AMBI solution becomes biocompatible after the complete elimination of the initial biorecalcitrant compound (AMBI). This phenomenon is accompanied by the concomitant elimination of 45% of the initial DOC, and the AOS reaches a value around 0.2.

5.3.5 Performances of the coupled solar-biological flow system

The coupled reactor shown in Fig. 5.3 was operated in semi-continuous mode. The photochemical step, using the photo-Fenton reaction, treats the AMBI solution in batch cycles providing phototreated water to the biological reactor. Fig. 5.11. shows the evolution of AMBI during the pretreatment process and the evolution of DOC concentration in both photochemical and biological treatments. From this figure, it is observed that with an accumulated solar energy of 10 kJ l^{-1}, 100% of the initial biorecalcitrant compound (AMBI) was degraded. The pretreated solution flowed to the biological reactor, where the complete mineralization was achieved in 20 h, indicating that the photo-pretreatment is able to produce a biocompatible solution.

The input organic load was increased in the rage of 100 to 800 mg C l^{-1} in order to find out the maximal concentration of AMBI that can be treated by the coupled reactor. Optimal AMBI/ Fe^{3+}/H_2O_2 ratio was utilised in each experiment. The AMBI wastewater is phototreated in

semicontinuous mode, same as in the previous experiments, and when 100% of AMBI degradation is attained, the pretreated solution is then lead into the biological reactor.
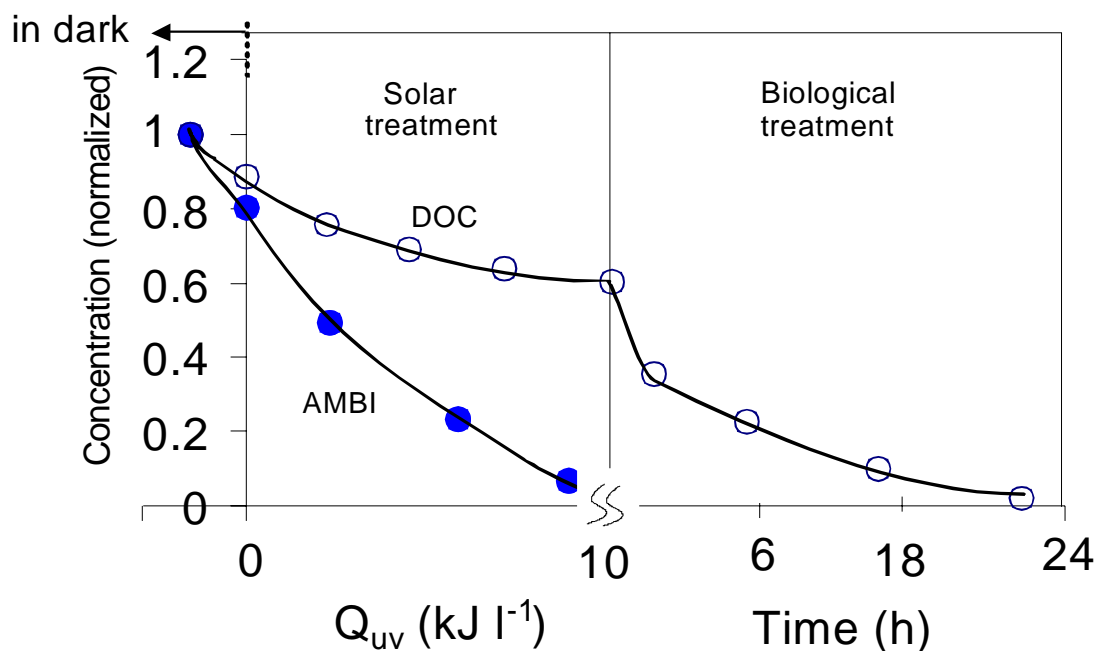
FIGURE 5.11   *Evolution of AMBI and DOC concentration during the solar photo-Fenton and biological treatment. AMBI (1.0 mmol l^{-1}), Fe^{3+} (0.1 mmol l^{-1}) and H_2O_2 (10 mmol l^{-1}).*

Fig. 5.12 shows the percentage of DOC removed in the solar, the biological and the whole coupled reactor as a function of the initial DOC of the solution.

In Fig. 5.12, it is observed that the solar system is able to removed 50% of the initial DOC with an initial load of 160 mg C l^{-1}. However, this efficiency is considerably diminished when the initial organic load increases form 160 to 300 mg C l^{-1}, reaching 30% of efficiency for the same energy accumulated. The DOC removal efficiency of the biological reactor is 60% until 500 mg C l^{-1}, but an important diminution is observed for higher concentrations, probably due to inhibition of the microorganisms. Nevertheless, a whole performance of 80-90% is reached in the range of 300-500 mg C l^{-1}, indicating the plausibility of the coupled approach at pilot scale in the context of the treatment a real industrial wastewater.
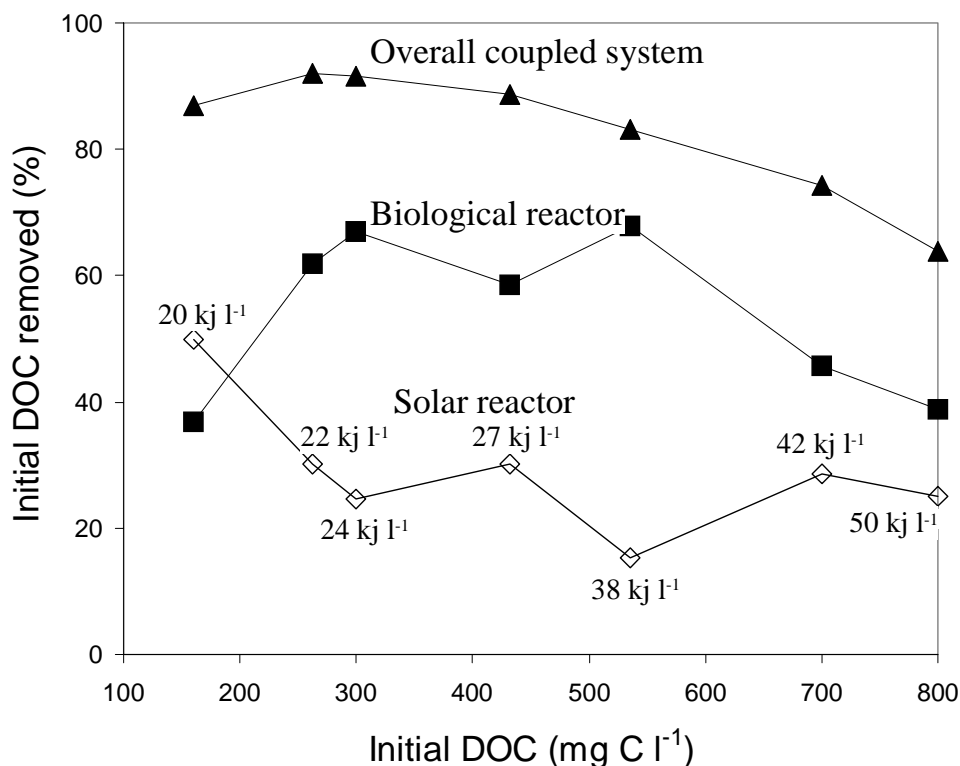
FIGURE 5.12 *DOC degradation by solar, biological and coupled treatment as a function of the initial organic load in the coupled reactor. The insert values represent the solar energy accumulated necessary to attain the complete transformation of AMBI.*

5.3.6 Economical considerations

In most cases the economics of the solar photocatalytic applications will determine the commercial viability of this process [Alfano et al. 2000]. According to Goswami [Goswami 1997, 1997] an economic analysis should include the fixed capital costs, recurring operation and maintenance costs, as well as energy costs.

Based on experimental results, Vidal et al. [1999] reported a treatment cost of US $0.7 per m^{-3} of thiocarbamate pesticides (500 μg l^{-1}). In a review Goswami [Goswami 1997] reported cost calculations for the solar photocatalytic wastewater treatment ranging from US $0.53 m^{-3} all the way to US $27.57 m^{-3} based upon various literature sources. Obviously, the predicted treatment

cost will strongly depend upon the type of wastewater, the desired mode of plant operation (i.e., continuous vs. discontinuous), the location of the projected plant, and a variety of other individual factors. Thus, in each case an individual economic assessment will be based upon reliable experimental data, which have to be obtained under realistic operating conditions to be able to compare the costs with traditional technologies.

It has been shown that the costs of the photocatalytic reactors are contributing the main part to the overall treatment costs [Goswami 1997]. In many cases the cost of the land area required for the installation of a solar water detoxification plant will add a significant portion to the overall costs of the process. Therefore, it is important to calculate the required illuminated reactor area as accurately as possible.

Another very important factor for the economical considerations of a photochemical treatment is the availability of ultraviolet solar radiation.

5.3.6.1 Annual available ultraviolet radiation at EPFL

It is interesting to make a statistic treatment of the data of solar energy flux density (energy coming from the sun by surface unit) to know the available energy in the location where the photoreactor is placed. The data of year 2002 were collected using the radiometer presented in the experimental section, and analysed according to the methodology proposed by Maldonado [Maldonado 2000].

Fig. 5.13 represents the energy flux density ($W\ m^{-2}$) as function of the local time for a typical sunny day of each month. The absence of clouds and proximity to day 15 (about at the middle of each month) were the criteria used to select these sunny days.

From this figure it is clear that the amount of solar radiation varies depending on the time of day and the season. In general, solar radiation is higher during midday than during either the early morning or late afternoon. At midday, the sun is positioned high in the sky and the path of the sun's rays through the earth's atmosphere is shortened. Consequently, less solar radiation is scattered or absorbed, and more solar radiation reaches the photoreactor. As expected, there is more solar energy during the summer than during the winter because there are more daylight hours.

FIGURE 5.13   *Solar UV radiation during a typical sunny day*

July

August

September

October

November

December
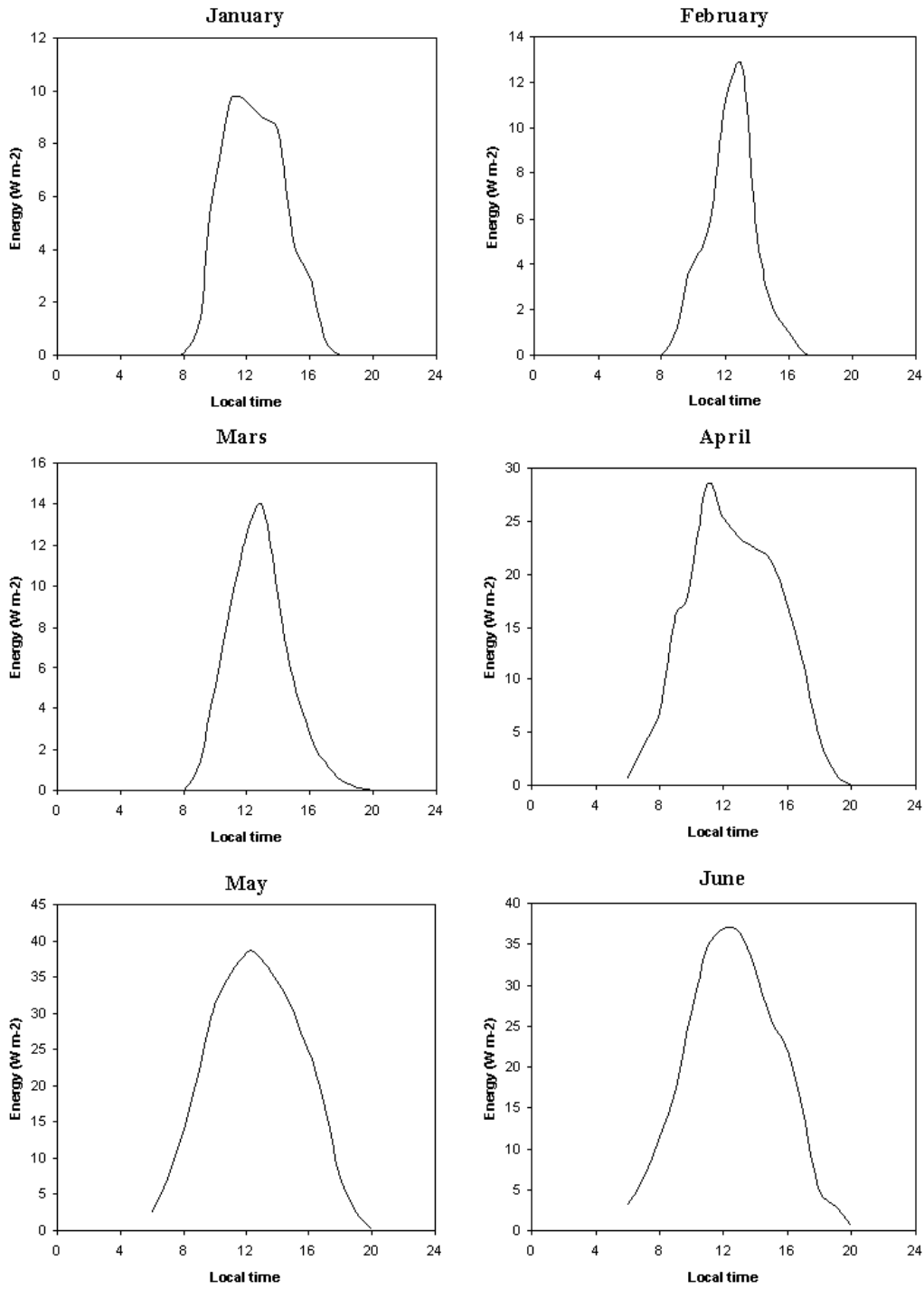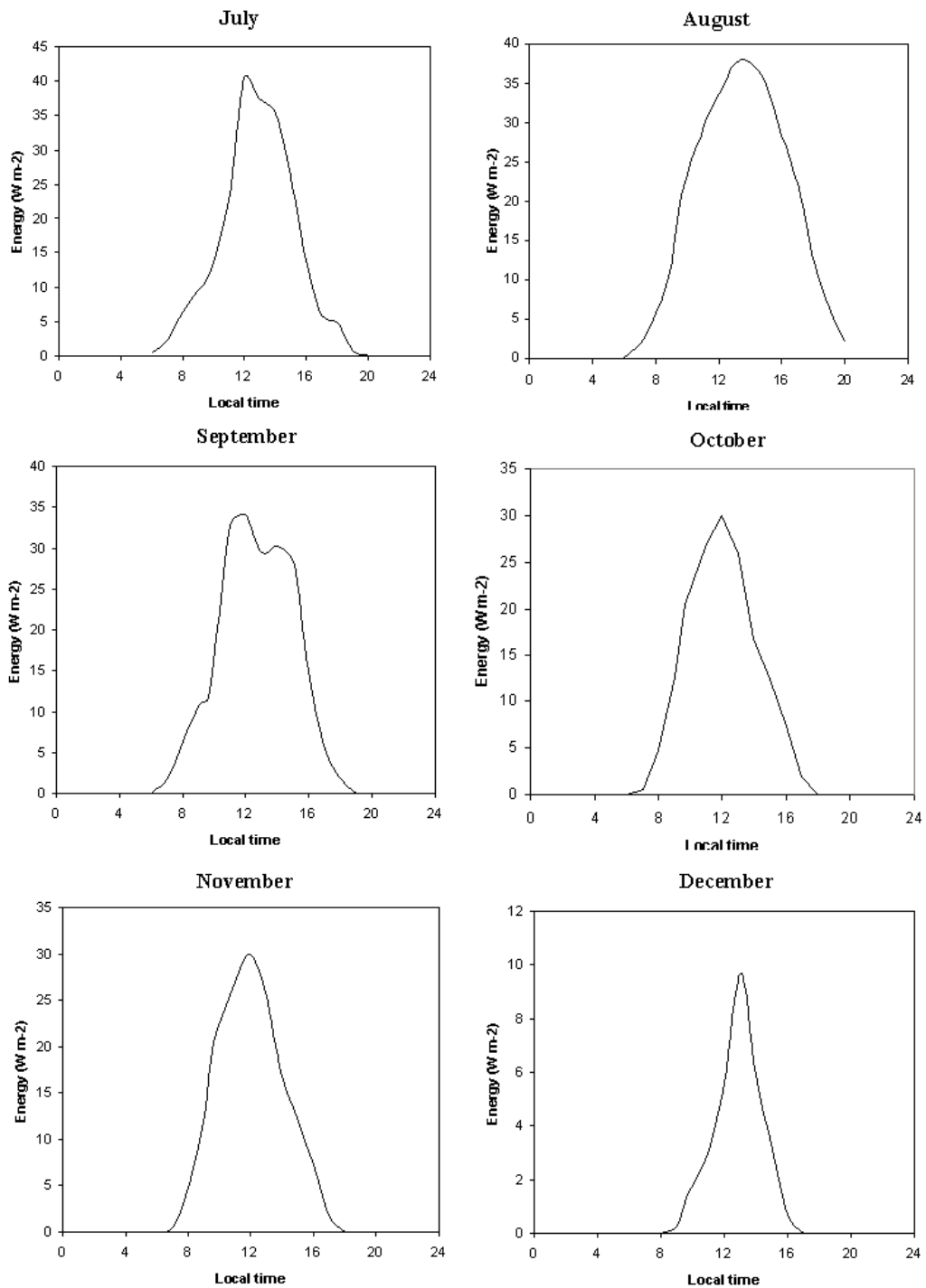
CONTINUATION FIGURE 5.13 *Solar UV radiation during a typical sunny day*

The maximum and the average global UV radiation for each month of year 2002 are presented in Fig. 5.14. These values, without being completely representative, because are based on data of only one year, allow to have an idea of the solar UV radiation at the EPFL. According to these data, it can be considered that the annual energy flux density pondered at EPFL is 11.48 W m^{-2}. A value of 18.6 W m^{-2} was obtained at the PSA using data of 4 years.
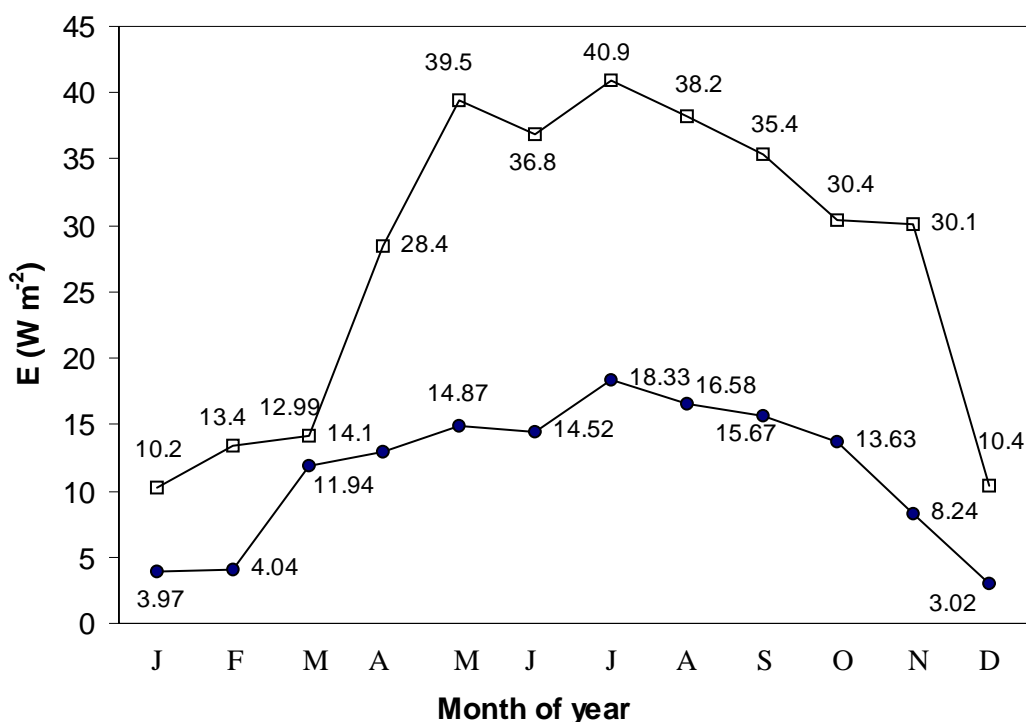
FIGURE 5.14 *Maximum (empty points) and average (full points) global UV radiation for each month at EPFL in 2002.*

5.3.6.2 Assessment of solar treatment cost

To assess a practical application of the solar photo-Fenton reaction as a pretreatment in a coupled system, it is interesting to estimate the treatment cost of this technology using a full-scale commercial system (500 m^2). In this sense we made the following considerations:

- To treat 60 l of real AMBI wastewater, degrading 100% of the initial AMBI concentration (8 mmol l^{-1}), the accumulated energy necessary in the reactor is about 50 kJ l^{-1} (data of Fig. 5.12).

- The UV global radiation average at operating hours, at EPFL is 11.48 W_{uv} m^{-2} and there are about 2336 effective operating hours per year.

- The yearly treatment capacity of real AMBI wastewater using a collector area of 500 m^2 can be calculated using the Eq. 5.7 as follows:

$$V_{TOT} = \frac{A_{CPC} \times \Delta t_n \times \overline{UV}_G}{Q_{UV}} = \frac{500 \times 2336 \times 60 \times 60 \times 11.48}{50 \times 1000 \times 1000} = 965 \text{ m}^3 \qquad \textbf{(5.7)}$$

With 500 m^2 of illuminated CPC reactor, it is possible to treat 965 m^3 of real AMBI wastewater per year. Taking into account this results and by analogy to [Vidal et al. 1999] a cost estimation is effectuated and presented in Table. 5.2.

Total annualised costs were calculated by using an interest rate of 13% over a 15-year period. The land cost that is particularly elevated in Switzerland (200-400 US$ per m^2) has not been considered. The pretreatment cost was estimated to be US$ 32 m^{-3} of AMBI wastewater. After this pretreatment it is possible to send the effluent towards a biological (low cost) system. This result is extremely interesting if we compared with the cost, in Switzerland, of different physicochemical methods applied for the treatment of this kind of industrial wastewater, such as incineration or Wet Air Oxidation, which is about US$ 200 m^{-3}. Nevertheless, using a similar solar collector area a more favourable cost-efficiency of US$ 0.7 m^{-3} has been reached [Vidal et al. 1999]. This value is much smaller than the obtained one by us, since it was achieved for the treatment of diluted solution of lindane (500 mg l^{-1}), in a region with more economical land cost (US$ 1.5 m^{-2}) that was in this case included in the economical evaluation, and under more favourable climatic conditions such 3500 sunny hours per year and a average UV global radiation of 25 W m^{-2}.

TABLE 5.2   *Cost calculations for AMBI wastewater pretreatment with photo-Fenton system*

COMMON INPUT DATA	
Yearly working days (days)	365
Availability factor (%)	80
Average of useful hours (sunny days) (h)	8
Effective yearly operating hours (h)	2336
UV global radiation (average at operating hours) (W_{uv} m^{-2})	11.84
Total collector area (m^2)	500
Cost of $FeCl_3$ (US\$ kg^{-1})	0.3
Cost of H_2O_2 (US\$ kg^{-1})	0.7
Cost of NaOH (US\$ kg^{-1})	0.3
Cost of HCl (US\$ kg^{-1})	0.03
Solar collector cost (US\$ m^{-2})	200
COST ESTIMATION - Treatment capacity $0.8 \, l \, h^{-1} \, m^{-2}$	US\$
Direct cost	
Total collector cost (500 m^{-2} by 200US\$ m^{-2})	100000
Piping and tanks (8% of collectors cost)	8000
Auxiliary equipment and controls (10% of collectors cost)	10000
Others (15% of collectors cost)	15000
Total Direct (TD)	133000
Indirect cost	
Contingencies (12% TD)	15960
Spare parts (1% TD)	1330
Total Capital Required (TCR)	150290
Annual cost	
Capital (13% of the TCR)	19538
Consumables (H_2O_2, NaOH, HCl and $FeCl_3$)	3800
Operation and maintenance (5% TCR) (US\$)	7515
Total annual cost (US\$)	30653
Treatment cost (US\$ m^{-3})	32

5.4   Conclusions

An innovative coupled solar-biological system at field pilot scale was designed, builds, and tested on the degradation of a biorecalcitrant model compound: 5-amino-6-methyl-2-benzimidazolone (AMBI). The strategy follows to develop this system has shown that:

- The Compound Parabolic Collector was the most appropriate to be coupled with a biological reactor;
- Among the tested AOP for the degradation of the AMBI, the photo-Fenton process is the most efficient;
- Using the Surface Response Methodology to optimize the Fe^{3+} and H_2O_2 concentration in the photo-Fenton system, the $AMBI/Fe^{3+}/H_2O_2$ ratio of 1/0.1/10 provides the optimal performance;
- The photo-Fenton pretreatment is able to completely remove the pollutant (AMBI), as well as to improve the Average Oxidation State of the solution, generating a biocompatible effluent;

Using an immobilized-cell aerobic reactor in the biological part of the system, the evaluation of the coupled solar-biological flow system demonstrated that, when operating in semicontinuous mode, it is able to reach a whole performance of 80 - 90% if the pollution load is in the range of 300-500 mg C l^{-1}. This result indicates the efficiency of using the coupled system developed here at pilot scale to treat real industrial wastewater.

5.5   References

Alfano O M, Bahnemann D, Cassano A E, Dillert R, Goslich R (2000). Photocatalysis in water environments using artificial and solar light. *Catal. Today* **58** (2-3) 199-230.

Blanco J, Malato S (1996). Tecnología de fotocatálisis solar: utilización de la radiación solar para el tratamiento de contaminantes industriales. CIEMAT Almeria. 31. p 102.

Cavicchioli A, Gutz I (1997). Effect of scavengers on the photocatalytic digestion of organic matter in water samples assisted by TiO2 in suspension for the voltammetric determination of heavy metals. J. of the brazilian Chem. Soc. **13** (4) 441-448.

Fernandez J, Kiwi J, Lizama C, Freer J, Baeza J, Mansilla H D (2002). Factorial experimental design of Orange II photocatalytic discolouration. *J. Photochem. and Photobio. A.* **151** (1-3) 213-219.

Goswami D Y (1997). A review of engineering developments of aqueous phase solar photocatalytic detoxification and disinfection processes. *J. Solar Energy Eng.* **119** (2) 101.

Goswami D Y (1997). Techno-economic analysis of solar detoxification systems. *J. Solar Energy Eng.* **119** (2) 108-113.

Khuri A I, Cornell J A (1987). *Response Surfaces, Designs and Analyses*. New York, ASQC Quality Press.

Kiwi J, Lopez A, Nadtochenko V (2000). Mechanism and kinetics of the OH-radical intervention during Fenton oxidation in the presence of significant amount of radical scavenger (Cl⁻). *Environ. Sci. Technol.* **34** (11) 2162-2168.

Krutzler T, Fallmann H, Maletzky P, Bauer R, Malato S, Blanco J (1999). Solar driven degradation of 4-chlorophenol. *Catal.Today* **54** (2-3) 321-327.

Lindsey M, Tarr A (2000). Inhibited hydroxy radical degradation of aromatic hydrocarbons in the presence of dissolved fulvic acid. *Wat.Res.* **34** (8) 2385-2389.

Mailhot G, Sarakha M, Lavedrine B, Caceres J, Malato S (2002). Fe(III)-solar light induced degradation of diethyl phthalate (DEP) in aqueous solutions. *Chemosphere* **49** (6) 525-532.

Malato S, Blanco J, Richter C, Braun B, Maldonado M I (1998). Enhancement of the rate of solar photocatalytic mineralization of organic pollutants by inorganic oxidizing species. *Appl. Catal. B.* **17** (4) 347-356.

Malato S, Blanco J, Richter C, Curco D, Gimenez J (1997). Low-concentrating CPC collectors for photocatalytic water detoxification: comparison with a medium concentrating solar collector. *Water Sci. Technol.* **35** (4) 157-164.

Malato S, Blanco J, Richter C, Milow B, Maldonado M I (1999). Solar photocatalytic mineralization of commercial pesticides: methamidophos. *Chemosphere* **38** (5) 1145-1156.

Malato S, Blanco J, Vidal A, Richter C (2002). Photocatalysis with solar energy at a pilot-plant scale: an overview. *Appl. Catal. B.* **37** (1) 1-15.

Malato S, Caceres J, A. Agüera, M. Mezcua, D. Hernando, J. Vidal, Fernández-Alba A R (2001). Degradation of Imidacloprid in Water by Photo-Fenton and TiO2 Photocatalysis at a Solar Pilot Plant: A Comparative Study. *Environ. Sci. Technol.* **35** (21) 4359-4366.

Malato S, Richter C, Blanco J, Vincent M (1996). Photocatalytic Degradation of Industrial Residual Waters. *Solar Energy* **56** (5) 401-410.

Maldonado M I (2000). Descontaminación de aguas de lavado de envases de plaguicidas mediante fotocatálisis solar. Departamento de Ingeniería Química. Almeria, Spain, Universidad de Almeria.

Mathieu D, Nony J, Phan-Tan-Luu R (2000). NEMROD. L.P.R.A.I., Université d'Aix-Marseille, France.

Minero C, Pelizzetti E, Malato S, Blanco J (1993). Large Solar Plant Photocatalytic Water Decontamination - Degradation of Pentachlorophenol. *Chemosphere* **26** (12) 2103-2119.

Myers R H, Montgomery D C (1995). *Response Surface Methodology: Process and Product Optimization Using Designed Experiments*. New York, John Wiley and sons, Inc.

OECD (1996). *Guidelines for testing of Chemicals, test 302B.*

Oliveros E, Legrini O, Hohl M, Muller T, Braun A M (1997). Large scale development of a light-enhanced fenton reaction by optimal experimental design. *Water Sci. and Technol.* **35** (4) 223-230.

Parra S (2001). Doctoral Thesis : Coupling of photocatalytic and biological process as a contribution to the detoxification of water: catalytic and technological aspects. Institute of Environ. Sci. Technol. Lausanne, Swiss Federal Institute of Technology.

Parra S, Malato S, Blanco J, Péringer P, Pulgarin C (2001). Concentrating versus non-concentrating reactors for solar photocatalytic degradation of p-nitrotoluene-o-sulfonic acid. *Water Sci. Technol.* **44** (5) 219-227.

Parra S, Sarria V, Malato S, Peringer P, Pulgarin C (2000). Photochemical versus coupled photochemical-biological flow system for the treatment of two biorecalcitrant herbicides: metobromuron and isoproturon. *Appl. Catal. B.* **27** (3) 153-168.

Robert D, Malato S (2002). Solar photocatalysis: a clean process for water detoxification. *The Science of The Total Environment* **291** (1-3) 85-97.

Scott J P, Ollis D F (1997). Integration of Chemical and Biological Oxidation Processes for Water Treatment: II. Recent illustrations and experiences. *J. Adv. Oxid. Technol.* **2** (3) 374-381.

Vidal A, Diaz A I, El Hraiki A, Romero M, Muguruza I, Senhaji F, Gonzalez J (1999). Solar photocatalysis for detoxification and disinfection of contaminated water: pilot plant studies. *Catal.Today* **54** (2-3) 283-290.

HYBRID PHOTOCATALYTIC-PHOTOVOLTAIC SYSTEM

Simultaneous pollutant photodegradation and solar energy conversion

Chapter 5 described the development, optimization and performances of a coupled photochemical-biological system at pilot scale. In Chapter 6 a Hybrid Photocatalytic-Photovoltaic System (HPPS) was designed, erected, and tests results are presented. HPPS consist of one device with dual operation: The Photocatalytic system uses the UV radiation to promote the degradation of organic pollutants, and retained the IR radiation. The Photovoltaic (PV) system converts the visible radiation into electricity, which is directly used by the recirculation pump or is stored in a battery for other purposes. The suggested design aims to achieve an autonomous and environmental friendly method for the treatment of biorecalcitrant pollutants.

■ **The HPPS system is actually following a patent procedure at the EPFL**

6.1   Introduction

The utility of coupling solar photoassisted oxidation and biological processes for the treatment of biorecalcitrant pollutants in water is clearly evident and by now demonstrated over a model compound (AMBI). Nevertheless, the development of this technology is confronted to a series of limitations include:

- The aqueous stream being treated must provide good transmission of UV light (high turbidity causes interference).
- Costs may be higher than competing technologies because of energy requirements.

It is possible to consider that one of the sectors in which the AOP have more potential application is in the degradation of micro-pollutants, such as endocrine disrupting chemicals

[Kenfack et al. 2002], as well as in the disinfection of drinking water [Rincon et al. 2001; Rincon and Pulgarin 2003]. In both situations water has a great UV light transmission.

Concerning the energy requirements, better exploitation of solar energy could contribute to a considerable economic gain.

The most common applications of solar energy are in the fields of thermal, photovoltaic (PV), and photochemistry. Over the last few years, there has been a growing interest in photovoltaic/thermal collectors [Sorensen and Munro 2000], which can provide both electrical and thermal energy from the same system. Nevertheless there are no reports on photovoltaic/ photocatalytic hybrid systems.

The photovoltaic (PV) process converts sunlight the most abundant energy source on the planet directly into electricity. The basic PV building block is the photovoltaic cell. This cell consists of two types of material, often p-type silicon and n-type silicon (Fig 6.1).
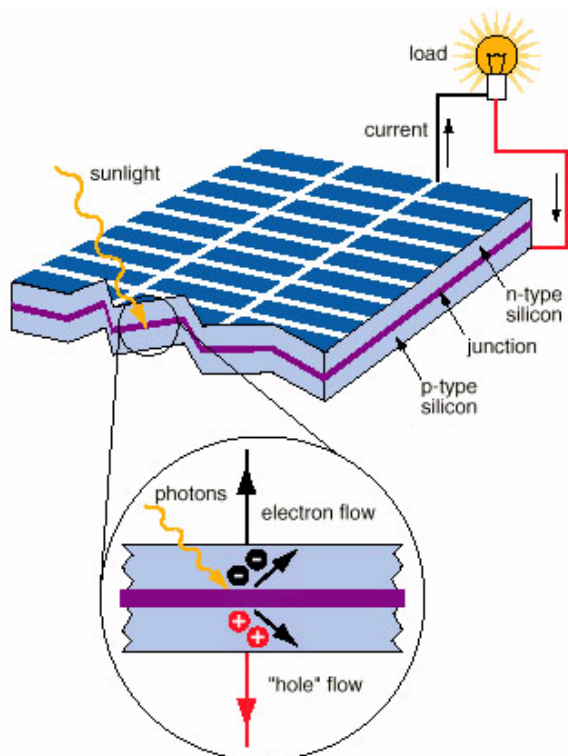

FIGURE 6.1   *Schematic representation of the photovoltaic effect in a PV cell*

Light of wavelengths between 305 and 1200 nm is able to ionise the atoms in the silicon and the internal field produced by the junction separating the positive charges ("holes") from the negative charges (electrons) within the photovoltaic device. The holes are swept into the positive or p-layer and the electrons are swept into the negative or n-layer. Although these opposite charges are attracted each other, most of them can only recombine by passing through an external circuit outside the material because of the internal potential energy barrier. Therefore if a circuit is made as shown in Fig 6.1, power can be produced from the cells under illumination, since the free electrons have to pass through the load to recombine with the positive holes. The electrical output from a single cell is small; so multiple cells are connected together and encapsulated (usually behind glass) to form a module (sometimes referred to as a "panel").

Fig 6.2 [King and Kratochvil 1997] illustrates the spectral response of a typical crystalline silicon (c-Si) photovoltaic module in comparison with the solar spectral irradiance. About 40% of the solar energy incident on a S_i cell passes through because its energy is lower than that of the band gap of S_i. But the sealing and other protective materials used in the module absorb a major part of it. This may increase the temperature of the module to the order of 80°C under hot and humid conditions. The warming up of the PV module can adversely affect its performance due to deterioration of its opto-electronic properties.

Additionally, it is known that the short circuit current (I_{sc}) increases with the increase in temperature whereas the open circuit voltage (V_{oc}) decreases in the same conditions [Custodio et al. 2001]. Generally, the voltage decrement is much more pronounced than the current increment [Radziemska 2003].

From a microscopic point of view, the temperature increment of the PV cell causes a decrease of its lifetime and of the diffusion length of the minority carriers and also a decrease in the mobility of the majority carriers as well. Also, when carriers are being generated in both sides of the union, both Fermi levels move toward the intrinsic level and thus decrease the potential barrier. A potential barrier decrease causes an increase in short circuit current and a decrease in open circuit voltage. Usually, the efficiency falls by 30% when the temperature of the cell increases from 20 to 60°C [Radziemska 2003].
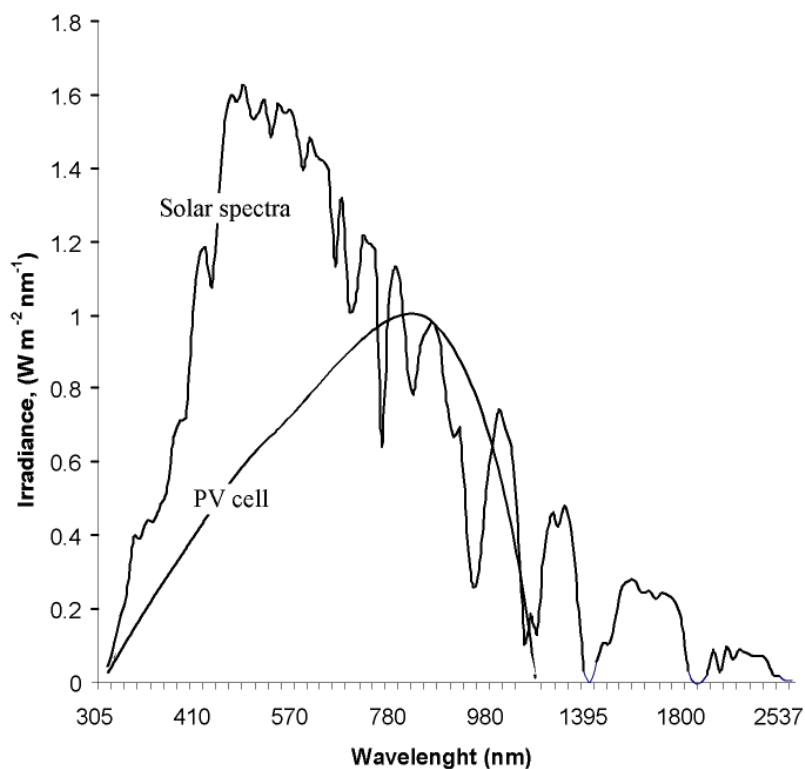
FIGURE 6.2   *Relative spectral response for a typical c-Si module compared to total solar spectral irradiance (source: [King and Kratochvil 1997]).*

Custodio [Custodio et al. 2001] designed an infrared water filter to absorb that part of the solar spectrum, which cannot be exploited by the photovoltaic module and is detrimental for the ideal performance of the module. The infrared filter consisted of a layer of purified water. One important property of water is that it is almost transparent to that part of the solar spectrum (400–800 nm) for which S_i is highly sensitive, whereas water is highly absorbent for wavelengths outside of this spectral range.

Since the silicon PV panel converts principally visible solar radiation into electricity, and since the photocatalytic degradation needs the UV radiation, the approach of simultaneously take advantage of both irradiations, using one engine and not supplementary surface can be advantageous.

To implement this, the aim of this work was to develop a Hybrid Photocatalytic-Photovoltaic System (HPPS). The photocatalytic system uses the UV radiation to promote the degradation of

organic pollutants and retain the IR radiation, so to protect the PV panels and improves its lifecycle. The photovoltaic system converts sunlight into electricity, which can be used for the functioning of the recirculating pump. This energy could also be accumulated, by means of a battery for other purposes. This new concept can represent an autonomous and environmental friendly method for the treatment of biorecalcitrant pollutants.

Herein, we report the construction and results of basic batch experiments employing the HPPS. The photocatalytic degradation of AMBI was performed, and its efficiency was compared to that of a Compound Parabolic Solar Collector.

6.2   Experimental

6.2.1   Hybrid Photocatalytic-Photovoltaic System (HPPS)

A schematic design of the proposed HPPS is presented in Fig 6.3. The ultraviolet (UV), the Visible (Vis) and the infrared (IR) radiation reach the photochemical reactor that uses the UV radiation for the degradation of the organic pollutants. The IR radiation is filtered thanks to the water present in the photocatalytic reactor. Only the visible radiation, useful for the production of electrical energy, reaches the PV panel that is situated below the photocatalytic reactor.

A photo of the HPPS installed at EPFL- Switzerland is presented in Fig 6.4. It is conformed by 4 modules (collector surface, 1.5 m^2, photoreactor volume 7 l, and total reactor volume 25 l) mounted in a fixed platform inclined 46º (local latitude). Each module is a pain of a photocatalytic reactor and a PV panel.
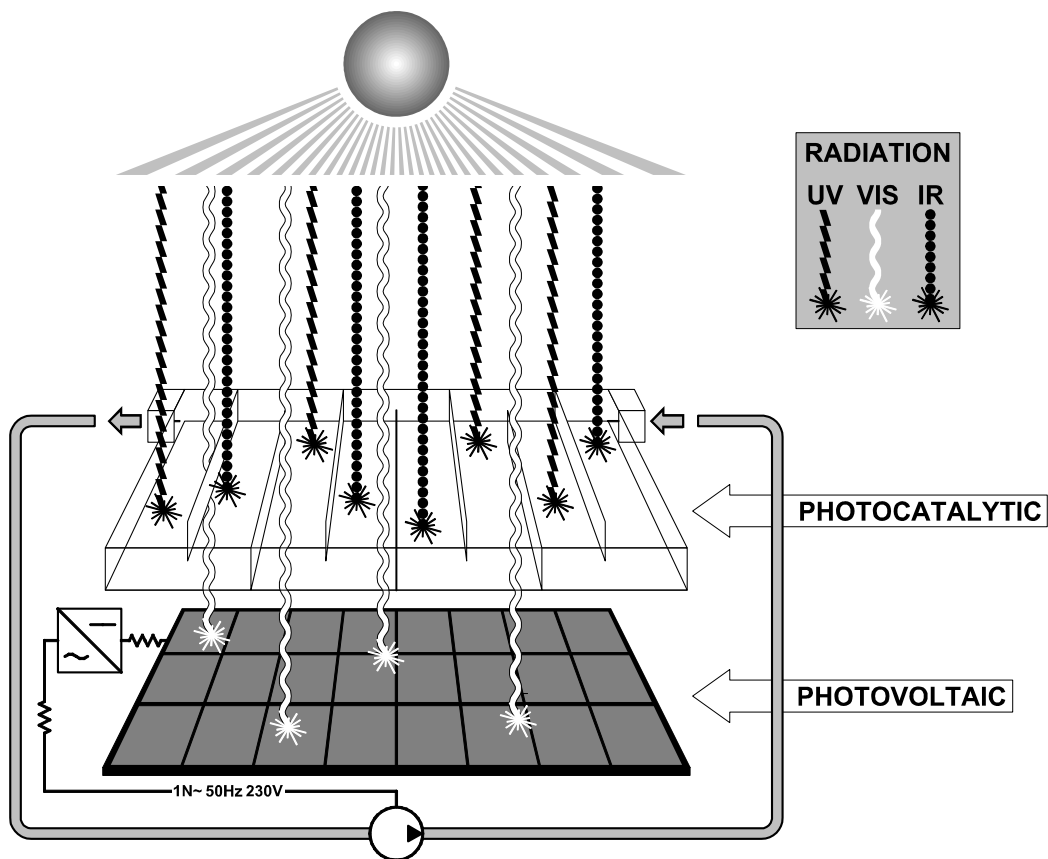
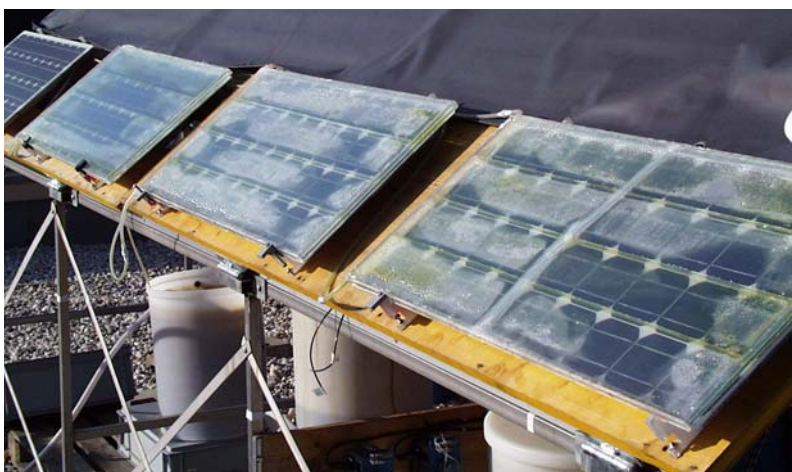**FIGURE 6.3**   *Schematic representation of the HPPS*

FIGURE 6.4   *Picture of the HPPS installed at EPFL - Switzerland*

The photocatalytic system is conformed by 4 rectangular cells of an UV/Vis transparent material through the water to be treated recirculated. These cells, placed in front of the PV panels, are connected in series and the water flows directly from one to another and finally to a tank equipped with a centrifugal recirculation pump.

The Photovoltaic system, constructed in collaboration with the company Solstist SA. is conformed by the following parts:

- 4 PV panels, model BP 270F (50-watt) connected in series
- A sinewave inverter (Studer Joker 400), which is used to convert the low voltage DC to 220 volts of alternative current (AC), as well a to stop the energy accumulation into the battery.
- A battery (12V 105 Ah) to store the energy.
- A Voltmeter to measure the voltage into the battery.
- A charger for the battery, it is not enough the solar energy for a practical application.
- Two energy counters, which allow making the difference between the energy coming form the PV panels and from the local electricity network.
- Two Chronometers, to follow the functioning time of the PV or the local network.
- A three positions commuter (1. automatic, 0. local electricity network, and 2. solar PV panels).

6.2.2   Compound Parabolic Collector

The CPC collector was described in detail in section "5.2.1". For the experiments performed in this section it was used only 4 tubes of each module (collector surface, 1.5 m^2, photoreactor volume 12 l, and total reactor volume 25 l).

Solar ultraviolet radiation (UV) has been determined during the experiments using a global UV radiometer described in section "5.2.1". With Eq. 5.1, combination of data from several days' experiments and their comparison with other photocatalytic experiments is possible.

6.3 Transmittance of different materials suitable for the manufacture of the HPPS

In order to optimize the performance of the HPPS, the photocatalytic reactor must be elaborated using the highly UV-transmitting material. Fig 6.5 presents the UV/Vis spectra of transmittance of different materials. Quartz and Pyrex present the highest UV Transmittance; nevertheless the high cost of these materials makes their usage completely unfeasible for this purpose. Therefore, the usage of commercial glass and Plexiglas appears possible, from the economical point of view. Additionally these materials present interesting specifications of pressure and thermal resistance, as well as keeping its properties during outdoors operation.
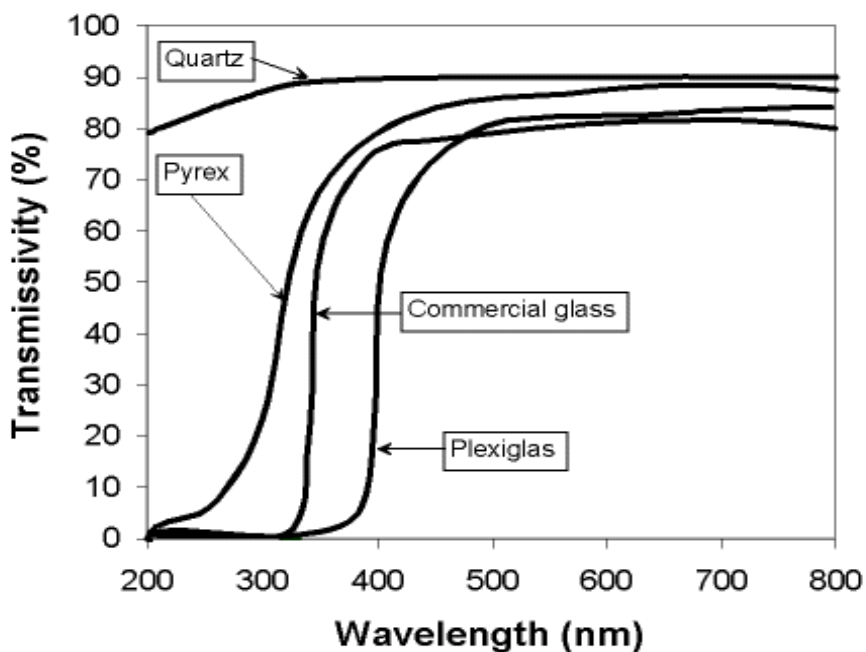
FIGURE 6.5   *Transmittance of different materials suitable for manufacture the HPPS*

For this experiments, we constructed two photocatalytic reactors using commercial glass (HPPS$_G$) and Plexiglas (HPPS$_P$).

6.4   Photovoltaic power

From solar to electrical energy, the conversion parameter to be maximized is the power, which is the product: IV = Current (I) x Voltage (V) measured in a photovoltaic module.

Fig 6.6 shows the photovoltaic power of one PV panel, with and without the glass and the Plexiglas photocatalytic reactors as a function of the local time between 12h00 to 17h00. Power decreases as time increases, it is the expected result taking into account the diminishing of the solar radiation power showed at the right hand side of Fig 6.6. It is observed also that the power is only slight diminished by the photocatalytic reactor: 14% and 22% by the $HPPS_G$ and $HPPS_P$, respectively.
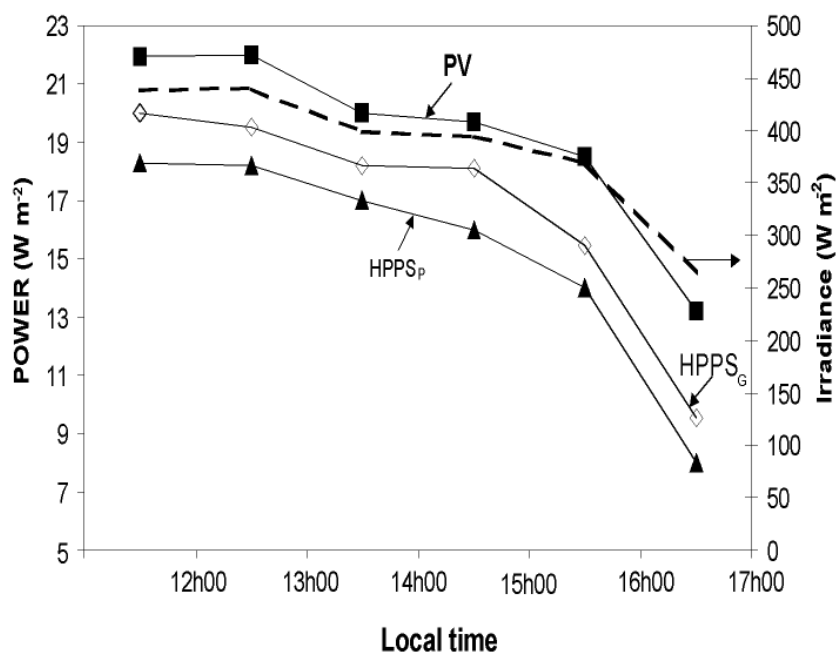
FIGURE 6.6   *Photovoltaic power of the PV panel: (PV) panel alone, (HPPSG) with a commercial glass photoreactor, and (HPPSP) with a Plexiglas photoreactor in the new HPPS system. Comparison with the sunlight irradiance at EPFL-Switzerland, October 7th 2002.*

Another important parameter of the PV panel is the conversion efficiency. The calculated average efficiency for the PV panel is about 5,80% under normal operative conditions (without photoreactor) and about 4,89 and 4,67% for $HPPS_G$ and $HPPS_P$.

The above results illustrate that the energy conversion of the PV panel is not significantly diminished by the installation of a photocatalytic reactor above the PV panel.

6.5 Comparison of a CPC and the HPPS systems for the photo-catalytic degradation of AMBI

In order to appreciate the photocatalytic performance of the new HPPS we simultaneously hold two degradation experiments of AMBI: one in the new HPPS reactor and another in the CPC, which until now is presented as the best solar photocatalytic reactor, for photocatalytic degradation applications [Malato et al. 2002]; and we compared the results.

Iron photoassisted degradation of a diluted solution of AMBI was performed using the CPC, the $HPPS_G$ and the $HPPS_P$ at respectively 0.1 mmol l^{-1} of Fe^{3+} and 0.1 mmol l^{-1} of AMBI. The principal characteristics of the reactors are presented in Table 1. Both, the glass and Plexiglas HPPS reactors have the same dimensions. All the systems have the same surface, and the great difference of them is, the recirculation speed, which is higher in the CPC. Nevertheless, we decide to go further in the exploratory evaluation of the performance of the systems ($30\,l\,min^{-1}$ vs $0.8\,l\,min^{-1}$)..

TABLE 6.1   *Characteristics of CPC and HPPS*

Reactor	Illuminated Area (m^2)	Illuminated Volume (l)	Total volume (l)	Recirculation (l min^{-1})
CPC	1.5	12	25	30
HPPS	1.5	7	25	0.8

Fig 6.7 presents the evolution of the –ln(C/Co) of the AMBI solution as a function of accumulated energy, calculated using the Eq. 5.1, during the photocatalytic degradation experiments using the 3 reactors. C is the concentration during the experiment and Co is the initial concentration of AMBI at the beginning of the experiment.
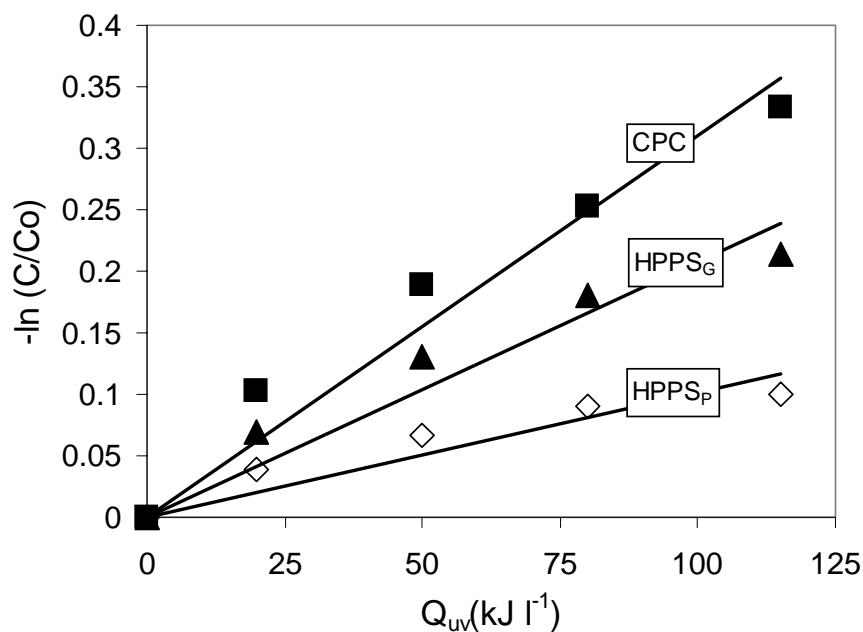
FIGURE 6.7   *Comparison of the CPC and the HPPS system*

According to the results presented in Fig 6.7, it is clear that the CPC is the most efficient. Calculating the slope of the curves of Fig 6.7, we obtain the constant of photodegradation (k_{app}). Table 6.2 illustrates the k_{app} obtained for each reactor. Within the experimented conditions, the CPC is 1.5 and almost 3 times more efficient than the $HPPS_G$ and $HPPS_P$ for the treatment of a diluted solution of AMBI. However, more investigations still to be follow, in order to know if the HPPS efficiency could be improved. Concerned parameters could be: the agitation in the HPPS water circuit, the recirculation speed of water, the utilisation of an immobilized catalyst, and others.

TABLE 6.2   *k_{app} of photocatalytic degradation of AMBI solution*

System	$HPPS_P$	$HPPS_G$	CPC
k_{app} $(l\ kj^{-1})$	0.001	0.0021	0.0031

6.6   Conclusions

A new Hybrid Photocatalytic Photovoltaic System (HPPS) was developed, installed and operated at EPFL in Switzerland. This HPPS use the UV radiation to promote the photocatalytic degradation of organic pollutants, and the visible radiation to generate electricity necessary for the recirculating pump. HPPS represents an autonomous and environmental friendly method for the treatment of biorecalcitrant pollutants.

Commercial glass and Plexiglas, present effective transmittance-cost ratio, and were used to manufacture two prototypes of the HPPS: $HPPS_P$ (Plexiglas) and $HPPS_G$ (commercial glass).

The photovoltaic power of the PV panel was monitored in presence and in absence of two (glass and Plexiglas) photocatalytic reactors. It was observed that the power is only slightly diminished by the presence of the photocatalytic reactors: 14% and 22% for the $HPPS_G$ and $HPPS_P$, respectively.

Moreover, in the HPPS using iron-photoassisted degradation method, it was possible to photodegrade AMBI with performances not so far of those of the CPC solar reactor. Within our experimented conditions, the CPC has shown to be 1.5 and 3 times more efficient than the $HPPS_G$ and $HPPS_P$ respectively.

6.7   References

Custodio E, Acosta L, Sebastian P J, Campos J (2001). A better solar module performance obtained by employing an infrared water filter. *Solar Energy Materials and Solar Cells* **70** (3) 395-399.

Kenfack S, Sarria V, Rincon A G, Becker K, de Alancastro F, Cissé G, Maiga A H, Pulgarin C (2002). Utilisation du rayonnement solaire pour le traitement de la pollution chimique et microbiologique dans l'eau: Etat de l'art et perspectives de recherche en afrique tropicale. Energies renouvelables et cogeneration pour le developement durable en afrique, Yaoundé, Camerun.

King D L, Kratochvil J A (1997). Measuring solar spectral and angle-of-incidence effects on photovoltaic modules and solar irradiance sensors. The 26th IEEE Photovoltaic Specialists Conference, Anaheim, California, Sandia National Laboratories.

Malato S, Blanco J, Vidal A, Richter C (2002). Photocatalysis with solar energy at a pilot-plant scale: an overview. *Appl. Catal. B.* **37** (1) 1-15.

Radziemska E (2003). The effect of temperature on the power drop in crystalline silicon solar cells. *Renewable Energy* **28** (1) 1-12.

Rincon A G, Pulgarin C (2003). Photocatalytical inactivation of E. coli: effect of (continuous-intermittent) light intensity and of (suspended-fixed) TiO2 concentration. *Appl. Catal. B.* **In press.**

Rincon A G, Pulgarin C, Adler N, Peringer P (2001). Interaction between E. coli inactivation and DBP-precursors -- dihydroxybenzene isomers -- in the photocatalytic process of drinking-water disinfection with TiO2. *J. Photochem. and Photobiol. A.* **139** (2-3) 233-241.

Sorensen H, Munro D (2000). Hybrid PV/T collectors. The 2nd World Solar Electric Buildings Conference, Sydney.

GENERAL CONCLUSIONS

General conclusions

The incapability of conventional biological wastewater treatment to remove effectively biorecalcitrant and/or toxic pollutants, as well as the shortage of world water resources have promoted the research of more efficient and ecologically friendly water treatment technologies. In that sense, our goal was to contribute to the development of a new hybrid technology combining advanced oxidation processes (AOP) and biological processes for the treatment of wastewater containing biorecalcitrant and/or toxic pollutants.

Our goal was met in most respects. We have developed and optimize, two kinds of coupled systems at lab scale and one coupled system at pilot scale, which were successfully used for the remediation of biorecalcitrant wastewater. AOP was applied as pretreatment exclusively to modify the structure of the pollutants by transforming them into less toxic and biodegradable intermediates and biological treatment was applied to complete the mineralization.

Main original contributions

This thesis has shown that coupled AOP and biological oxidation processes for water treatment is viable from the economic and environmental point of view, and appears as an alternative to the drastic and/or inefficient single-step processes actually applied in biorecalcitrant pollutant elimination. In this section, I will describe my original contributions to the domain within each chapter.

Chapter 1 introduces AOP and coupled AOP-biological systems for water treatment. An overview of studies which used a combination of photoassisted and biological degradation of organic contaminants in water within the last five years (1998-2002) is presented. This overview confirms the beneficially effects of such two-steps treatment at lab scale and the lack of studies carried out at field scale with the same approach.

In chapter 2 sonochemical, electrochemical and photochemical oxidation processes are explored. The comparison, from the kinetic and economic points of view of these methods to degrade AMBI revealed that the iron photo-assisted process is the most adventageous in the context of coupling with a biological system.

Iron photoassisted process appears as the most convenient since it present several advantages:

- The catalyst is iron, the fourth most abundant element in the earth's crust and it is present naturally in water.

- O_2 or H_2O_2 electron acceptors are ecologically ideal oxidants.

- The homogeneous character of these systems provides, with reasonable limitations, good engineering conditions for coupling them with a complementary biological treatment.

- The photoreactor is simple and can be easily constructed.

- Instead of artificial irradiation source, solar energy could be used, which represent an important economic gain.

Chapter 3 focuses on the degradation of AMBI by means of the $h\nu/Fe(III)/O_{2(air)}$ and $h\nu/Fe(III)/H_2O_2$ systems using an artificial irradiation source. Concerning the application of the system $h\nu/Fe(III)/O_{2(air)}$ for the degradation of AMBI, the main contributions can be pointed out:

The interactions of the mixture of AMBI and Fe(III) in aqueous solution. AMBI exits in two different forms depending on the pH: AMBI and its monoprotonated ($AMBIH^+$) form. A pKa of 4.7 has been measured for the monoprotonation of AMBI. The mixture of AMBI and Fe(III) lead

presumably to the formation of a complex, which have significant absorption in the visible region, with maximums at 284, 440 and 475 nm. This complex is thermally stable, in the case of the ratio $R = [Fe(III)]/[AMBI] < 1$. At higher ratio values ($R \geq 1$), a fast thermal redox process, inside the complex, leading to the decreasing of the maximum at 284 nm and reduction of Fe(III) to Fe(II) was observed.

The study of photodegradation of AMBI by means of Fe(III) photo-assisted system. The illuminated Fe(III) induced the photo-degradation of AMBI. This process is mainly attributed to three simultaneous process: direct photolysis of the $[Fe^{3+}$---AMBI] complex, the attack of the complex by $^{\bullet}OH$ radicals generated by the photolysis of $Fe(OH)^{2+}$, and by the attack of supplementary $^{\bullet}OH$ radicals generated by the Fenton and photo-Fenton like reactions, which are induced by the H_2O_2 that have been formed "in situ". When higher concentrations of H_2O_2 are added to AMBI---Fe(III) solution, Fenton and photo-Fenton reactions are considerably improved.

Concerning the application of the system $h\nu/Fe(III)/H_2O_2$ for the degradation of AMBI, the following contributions can be pointed out:

The optimization of the photo-Fenton degradation of AMBI containing wastewater. The optimal concentrations of AMBI, Fe^{3+} and H_2O_2 are found. Neither Fe^{3+} nor H_2O_2 should be overdosed due to their scavenging effect of hydroxyl radicals. Inhibition of degradation rate was observed at higher concentrations of initial AMBI concentration probably due to the increase of the darkness of the solution, which hinders the absorption of the UV light required for the photo-Fenton process.

Chapter 4 describe the development of two photochemical-biological systems at lab scale. The main contributions in this chapter are:

The proposition of a general strategy to develop combined photochemical and biological systems for biorecalcitrant wastewater treatment. For the development of this strategy, the following points need to be considered: the biodegradability of the initial pollutant, the chemical and biological characteristics of the phototreated solutions, the definition of the optimal pretreatment time, and the efficiency of the coupled reactor.

The development of two coupled processes at lab scale. Two kind of combined systems were developed using for the photocatalytic pretreatment $h\nu/Fe^{3+}/O_{2(air)}$ or $h\nu/Fe^{3+}/H_2O_2$ and in both cases immobilized activated sludge culture for the biological step. Both coupled systems were successfully employed for the treatment of AMBI.

The iron photoassisted process using oxygen was able to remove the initial AMBI concentration and produce biocompatible intermediates. In this sense, a coupled Fe(III) photoassisted-biological system without addition of other electron acceptor than O2 from air was developed and successfully applied for the mineralization of AMBI.

The coupled reactor was operated in a semi-continuous mode and an optimal pretreatment time of 300 min was found when O_2 is used as electron acceptor. At this moment the best compromise between the shortest photochemical pretreatment (high cost) and the highest biological (low cost) and overall efficiency were reached. Moreover, the Fe(III) concentration used in the pretreatment are low enough for respect the upper limit of iron concentration in an effluent that goes to be discharged to one of biological wastewater treatment plant.

A second coupled system using photo-Fenton as a pretreatment was developed and optimal pretreatment time of 120 min was found to be necessary. The toxicity and biodegradability analyses of the phototreated solutions show that the solution resulting from the photodegradation of AMBI is biologically compatible and its complete mineralization can be performed by biological means; additionally we observed that the biological mineralization of AMBI wastewater is notably improved by photo-Fenton pretreatment. The coupled photochemical and biological flow reactor operated in semi-continuous mode seems to be an efficient system for the degradation of AMBI. The primary degradation efficiency, expressed as percentage of AMBI removed, was 100% and the ultimate degradation efficiency (total mineralization) was 83.5%.

H_2O_2 and O_2 were compared as electron acceptors in the iron photoassisted pretreatment. For both compared systems almost the same global efficiency of the coupled reactor was achieved (~85% of DOC removed). Nevertheless the $h\nu/Fe(III)/H_2O_2$ was 2.5 times more efficient that the $h\nu/Fe(III)/O_{2(air)}$ system, regarding the phototreatment time. The higher efficiency in the biological step was observed in the system with O_2.

Chapter 5 describes the development, optimization and performances of a coupled photochemical-biological system applying solar energy at pilot scale. The main contributions are:

The development of an innovative coupled solar-biological system at field pilot scale. This system was designed, build, and tested showing that:

- The Compound Parabolic Collector was the most appropriate to be coupled with a biological reactor.

- Among the tested AOP for the degradation of AMBI, the photo-Fenton process is the most efficient.

- Surface Response Methodology is effectively to optimize the Fe^{3+} and H_2O_2 concentration in the photo-Fenton system.

- The photo-Fenton pretreatment is able to completely remove the pollutant (AMBI), generating a biocompatible effluent.

Using an immobilized-cell aerobic reactor in the biological part of the system, the evaluation of the coupled solar-biological flow system demonstrated, when operating in semicontinuous mode, it is able to reach an overall performance of 80 - 90% if the pollution load is in the range of 300-500 mg C l^{-1}. This result indicates the efficiency of using the coupled system developed here at pilot scale to treat real industrial wastewater.

Another contribution in this chapter is the statistical analysis of the annual ultraviolet radiation for the year 2002 at the EPFL. According to this analysis the annual energy flux density at the EPFL is 11.48 W m^{-2}.

The development, installation and operation of a new Hybrid Photocatalytic Photovoltaic System (HPPS) is the main contribution in chapter 6. This HPPS uses the UV radiation of sun to promote the photocatalytic degradation of organic pollutants in the flat photoreactor, and the visible radiation in the photovoltaic pannel to generate electricity useful for the recirculation pump. HPPS represents an autonomous and environmental friendly approach for the treatment of biorecalcitrant pollutants.

Commercial glass and plexiglas were used to manufacture two prototypes of the flat photoreactors, because both materials present effective transmittance-cost ratio.

Comparing degradation performances of flat photo-reactors constructed here with the effectiveness of CPC solar reactor, it was found that the CPC reactor degrading AMBI was more efficient. However, it was established that the HPPS system is more convenient because it use UV irradiation in photo-reactor to degrade AMBI and simultaneously, visible irradiation for electricity necessary for the recirculation pump.

In general we can conclude that HPPS allows simultaneously decontaminate water and convert solar energy into electricity. This ecological equipment represents an autonomous and environmental friendly system for wastewater remediation.

CURRICULUM VITAE

Victor-Manuel SARRIA MUÑOZ
Avenue du Tir-Fédéral, 12
1022- Chavannes- près- Renens
Phone : +41 21 634 66 73
victor.sarria@epfl.ch
Born on June 28th, 1972 in Cali-Colombia

Education:

1999-2003   **Docteur ès sciences techniques**
Swiss Federal Institute of Technology (EPFL), Lausanne - Switzerland
Thesis: Coupled Advanced oxidation and biological processes for wastewater treatment.

1991-1996   **Chemist**
Universidad del Valle, Cali - Colombia.

Professional experience:

2001-2003   Research assistant at the Laboratory for Environmental Biotechnology, Swiss Federal Institute of Technology (EPFL).

1996-1997   **Chemist in industry** «Analisis Ambiental S.A » Cali - Colombie.

Lenguages:

- Spanish: Mother tongue
- French: Excellent written and spoken knowledge
- English: Good written and spoken knowledge.

Computer skills:

- Word, Excel, Power Point, Designer, FrameMaker, LabView, Photoshop, End-note.

Other activities:

- Vice-President of the colombian association of researchers in Switzerland 2003.

- Reading, cultural trips, football, swimming, cycling, squash.

Referee Papers:

1. Pulgarin C, Invernizzi M, Parra S, Sarria V, Polania R, Péringer P. (**1999**) Strategy for the Coupling of Photochemical and Biological Flow Reactors useful in Mineralization of Biorecalcitrant Industrial Pollutants. Cat. Today, 54, 341-352.

2. Parra S, Sarria V, Malato S, Peringer P, Pulgarin C. (**2000**) Photochemical versus coupled photochemical–biological flow system for the treatment of two biorecalcitrant herbicides: metobromuron and isoproturon. Applied Catalysis B. 27, 153-168.

3. Sarria V, Parra S, Invernizzi M, Péringer P, Pulgarin C. (**2001**) Photochemical-Biological Treatment of a Real Industrial Biorecalcitrant Wastewater Containing 5-amino-6-methyl-2-benzimidazolone. Water Sci. and Technol. 44 (5), 93-101.

4. Rodriguez M, Sarria V, Esplugas S, Pulgarin C. (**2002**) Photo-Fenton treatment of a biorecalcitrant wastewater generated in textile activities: biodegradability of the photo-treated solution. J. Photochem. and Photob., 151, 129-135

5. Sarria V, Parra S, Adler N, Péringer P, Pulgarin C. (**2002**) Recent developments in the coupling of photoassisted and aerobic biological processes for the treatment of biorecalcitrant compounds. Cat. Today, 76 (2-4) 301-315

6. Sarria V, Deront M, Péringer P, Pulgarin C. (**2003**) Degradation of a biorecalcitrant dye precursor present in industrial wastewaters by a new integrated iron(III) photoassisted- biological treatment. Applied Catalysis B, 40, 231-246.

7. Torres R, Sarria V, Peringer P, Pulgarin C. (**2003**) Electrochemical Treatment of industrial wastewater containing 5-amino-6-methyl-2-benzimidazole: Toward an electrochemical-biological coupling. Water Research, 37, 3118-3124.

8. Sarria V, Kenfack S, Guillod O, Pulgarin C. (**2003**) An innovative coupled solar-biological system at field pilot scale for the treatment of biorecalcitrant pollutant. J. Photochem. and Photobiology, 159, 89-99.

9. Sarria V, Péringer P, Cáceres J, Blanco J, Sixto M, Pulgarin C. (**2003**) Solar degradation of 5-amino-6-methyl-2-benzimidazole by TiO_2 and iron(III) catalyst with H_2O_2 and O_2 as electron acceptors. Energy: The International Journal, in press.

Conferences:

10. C. Pulgarin, M. Invernizzi, S. Parra, V. Sarria and P. Peringer. Photochemical treatment vs continuous coupled photophenton-biological process for the degradation of a biorecalcitrant pollutant. Kinetics and economics aspects. AWT98 -Advanced Wastewater Treatment, Recycling and Reuse, Milan, Italia, pp. 919 - 922, Sept. 14-16, **1998**.

11. S. Parra, R. Polania, V. Sarria, P. Peringer and C. Pulgarin. Photoreactivity of phenolic compound in TiO2 suspension. Structure - reactivity relationship observations. AWT98 -Advanced Wastewater Treatment, Recycling and Reuse, Milan, Italia, pp. 923 - 926, Sept. 14-16, **1998**.

12. C. Pulgarin, M. Invernizzi, S. Parra, V. Sarria and P. Peringer. Photochemical Stand-Alone Reactor versus Integrated photophenton-biological flow systems for the mineralization of biorecalcitrant. The 1998 European workshop on Water and Air treatment by Advanced oxidation technologies Lausanne, Switzerland, Oct. 11-14, **1998**.

13. C. Pulgarin, M. Invernizzi, S. Parra, V. Sarria and P. Peringer.. Strategy for the Coupling of Photochemical and Biological Flow Reactors useful in Mineralization of Biorecalcitrant Industrial Pollutants. 2nd Users Workshop of Training and Mobility of Researchers Program at Plataforma Solar de Almeria, Spain, Nov. 10-11, **1998**.

14. V. Sarria and C. Pulgarin. Strategy for the coupling of physicochemical and biological processes for the mineralization of bio-recalcitrant industrial pollutants. 1ères journées: Chimie, soleil, énergie et environnement. Saint-Avold, France. Feb. 3-4, **2000**.

15. S. Parra, V. Sarria, C. Pulgarin, S. Malato and P. Péringer. Photochemical pre-treatment of two herbicides as a way tio improve the biodegradability of their treated solutions. 1ères journées: Chimie, soleil, énergie et environnement. Saint-Avold, France. Feb. 3-4, **2000**.

16. S. Parra, V. Sarria, R. Torres, P. Péringer et C. Pulgarin. Développement de procédées de dégradation de polluants toxiques dans l'eau par un couplage de processus physico-chimiques et biologiques. Forum Développement Durable, EPFL, Lausanne, Suisse. Mar. 28, **2000**.

17. V. Sarria, S. Parra, M. Invernizzi, P. Péringer and C. Pulgarin. Photochemical-biological treatment of a real industrial biorecalcitrant wastewater containing 5-amino-6-methyl-2-benzimidazolone. 2nd International conference on oxidation technologies for water and wastewater treatment. Clausthal-Zellerfeld, Germany. May 28-31, **2000**.

18. S. Parra, V. Sarria, C. Pulgarin and P. Péringer. Photochemical pre-treatment of two herbicides as a way to improve the biodegradability of their treated solutions. 6th international conference on advanced oxidation technologies for waster and air remediation (AOTs-6) and the 5th international conference on TiO2 photocatalytic purification and treatment of water and air (TiO2-5). London, Ontario, Canada. June 25-30, **2000**.

19. S. Parra, V. Sarria, G. Rincon, R. Torres and C. Pulgarin. Electrochemical and Helio-photochemical systems for the treatment of drinking and wastewater. International Conference Water 2000, Cali, Colombie. Oct. 19-21, **2000**.

20. V. Sarria, L. Menkari, S. Parra, N. Adler, P. Peringer, J. Vazquez, J. Blanco, S. Malato and C. Pulgarin. Coupled Photochemical-Biological System Useful in the Complete Mineralization of a Biorecalcitrant Wastewater Pollutant. 3nd Users Workshop of Training and Mobility of Researchers Program at Plataforma Solar de Almeria, Spain, Mars 13-14, **2001**.

21. Sarria, V., Deront, M., Péringer, P., and Pulgarin, C. Iron(III) photoassisted-biological system as an alternative for the treatment of real industrial wastewater, 2o European on: Solar Chemistry an Photocatalysis: Environmental Applications, St Avold, France, May 29-31, **2002**.

22. Sarria, V., Péringer, P., Cáceres, J., Blanco, J., Malato, S. and Pulgarin, C. Solar degradation of 5-amino-6-methyl-2-benzimidazolone by TiO2 and iron(III) catalyst with H2O2 and O2 as electron acceptors, 11th Solar Paces, International Symposium on Concentrated Solar Energy Technologies, Zurich, Switzerland. Sept. 4-6, **2002**.

23. Parra, S., Sarria, V., Péringer, P., and Pulgarin, C. Coupled photocatalytic and biological processes for the treatment of biorecalcitrant compounds, Escuela de fotocalisis heterogenea "uso de materials semiconductores para aplicaciones ambientales". Sevilla, Spain. July 4-7, **2002**

24. Sarria, V., Peringer, P., Pulgarin, C. Key points in the coupling of Fe(III) and TiO2 photoassistedsystems with biological processes, 7th.International Conference on TiO2 Photocatalysis: Fundamentals and Applications, Toronto, Canada, Sept. 17-22, **2002**.

25. Rodriguez, M., Sarria, V., Contreras, S., Jiménez, J., Esplugas, S., Pulgarin, C. Photo-Fenton treatment of a biorecalcitrant wastewater generated in textile activities. Biodegradability of the photo-treated solution, 8th.International Conference on Advanced Oxidation Technologies for Water and Air Remediation, Toronto, Canada, Sept. 17-22. **2002**

26. Sarria, V., Kenfack, S., Peringer, P. and Pulgarin C. Coupling solar and biological processes for the degradation of a dye bio-recalcitrant pollutant, 3rd European Meeting on Environmental Chemistry, Geneva. Dec. 11-14, **2002**.